Dissertation

submitted to the
Combined Faculties for the Natural Sciences and for Mathematics
of the Ruperto-Carola University of Heidelberg, Germany
for the degree of
Doctor of Natural Sciences

presented by

Tamás Szórádi

born in Budapest, Hungary

Oral examination: 05/06/2018

A Stress-Induced Pathway for the Degradation of Misfolded Proteins in *S. cerevisiae*

Faternak (for my Dad)

SUMMARY

The integrity of the proteome is fundamental for cell viability. Proteins can misfold due to genetic mutations or environmental stress. These misfolded proteins have a high tendency to accumulate as toxic protein aggregates which are associated with several well-known pathologies like Alzheimer's, Huntington's or Parkinson's disease. To prevent protein misfolding, cells have evolved several protein quality control mechanisms that monitor and preserve the integrity of the proteome.

In this PhD thesis we have uncovered and characterized a stress-inducible protein degradation pathway in budding yeast (*Saccharomyces cerevisiae*) that targets misfolded but also native proteins in the cytosol and the endoplasmic reticulum (ER) membrane for degradation. We employed an ER membrane-anchored reporter protein harbouring a misfolded cytosolic domain that was selectively degraded by the proteasome under stress conditions. A genetic screen, performed prior to the start of the PhD project, found the ubiquitin E3 ligase Ubr1, the serine protease Ynm3 and an uncharacterized protein (Yjl144W, named Roq1 by us) to be required for the stress-induced degradation of this misfolded model substrate. The three identified proteins act together in novel a linear protein degradation pathway, which we termed Stress-induced Homeostatically Regulated Degradation (SHRED). Mechanistic analysis elucidated that the *ROQ1* gene is transcriptionally upregulated during various stresses. The resulting Roq1 protein is cleaved by Ynm3, which uncovers a positively charged arginine residue on its N-terminus. Subsequently, cleaved Roq1 through its new N-terminus interacts with Ubr1 and modulates its substrate specificity. Modified substrate recognition by Ubr1 enhances the proteasomal degradation of certain cytosolic and ER membrane proteins. Furthermore, a genetic screen and mass spectrometry analysis revealed endogenous candidate substrates of SHRED proposing that this pathway is not only implicated in quality control but also in quantity control of proteins.

II

ZUSAMMENFASSUNG

Die Integrität des Proteoms ist grundlegend für die Lebensfähigkeit von Zellen. Proteine können aufgrund von genetischen Mutationen oder Umweltstress fehlerhaft gefaltet werden. Diese fehlgefalteten Proteine haben eine hohe Tendenz sich als toxische Proteinaggregate anzusammeln, wie sie mit mehreren bekannten Pathologien wie der Alzheimer-, Huntington- oder Parkinson-Krankheit assoziiert sind. Um eine Fehlfaltung von Proteinen zu verhindern haben Zellen mehrere Mechanismen zur Kontrolle der Proteinqualität entwickelt, die die Integrität des Proteoms überwachen und bewahren.

In dieser Doktorarbeit haben wir einen stressinduzierbaren Proteinabbauweg in Backhefe (*Saccharomyces cerevisiae*) entdeckt und charakterisiert, der sowohl fehlgefaltete als auch native Proteine im Cytosol und der Membran des Endoplasmatischen Retikulums (ER) für den Abbau markiert. Wir verwendeten ein in die ER-Membran verankertes Reporterprotein, das eine fehlgefaltete zytosolische Domäne beherbergt und dadurch unter Stressbedingungen selektiv vom Proteasom abgebaut wird. Ein genetischer Screen, der vor Beginn des PhD-Projekts durchgeführt wurde, identifizierte die Ubiquitin-E3-Ligase Ubr1, die Serinprotease Ynm3 und ein nicht charakterisiertes Protein (Yjl144W, von uns Roq1 genannt) als notwendig für den stressinduzierten Abbau dieses fehlgefalteten Modellsubstrats. Diese drei Proteine wirken in einem neuen linearen Proteinabbauweg zusammen, den wir als Stress-induzierte homöostatisch regulierte Degradation (SHRED) bezeichneten. Mechanistische Analysen ergaben, dass das *ROQ1*-Gen während verschiedener Stresssituationen hochreguliert wird. Das resultierende Roq1-Protein wird durch Ynm3 gespalten, was ein positiv geladenes Arginin an seinem N-Terminus freilegt. Anschließend interagiert Roq1 über seinen neuen N-Terminus mit Ubr1 und moduliert dessen Substratspezifität. Die modifizierte Ubr1-Substraterkennung steigert den Abbau bestimmter cytosolischer und ER-Membranproteine durch das Proteasom. Darüber hinaus deckten ein genetischer Screen und eine massenspektrometrische Analyse mögliche endogene Substrate von SHRED auf, was nahelegt, dass dieser Weg nicht nur in der Qualitätskontrolle, sondern auch in der Mengenkontrolle von Proteinen eine Rolle spielt.

TABLE OF CONTENTS

INTRODUCTION

The budding yeast (*Saccharomyces cerevisiae)* genome contains approximately 5800 protein coding genes (Goffeau et al., 1996). In order to maintain the integrity of the proteome, protein synthesis, folding, and degradation have to be in equilibrium. The resulting balanced state of the proteome is called protein homeostasis. Perturbations in protein homeostasis, for example due to accumulation of misfolded proteins, lead to severe consequences, as observed in neurodegenerative diseases such as Alzheimer's, Parkinson's, Huntington's and amyotrophic lateral sclerosis (Hartl, 2017). To maintain proper protein homeostasis, cells have evolved a delicate network of protein quality control (PQC) pathways.

1.1 Protein quality control (PQC)

Proteins can misfold due to stochastic fluctuations, genetic mutations or environmental stress (Hartl and Hayer-Hartl, 2009). Therefore, machineries involved in protein quality control pathways have three main tasks to perform: 1) selective recognition of misfolded proteins, 2) refolding of misfolded proteins and if the latter fails 3) removal of terminally misfolded proteins. Removal is achieved by either sequestration into subcellular protein deposits or degradation by the ubiquitin proteasome system (Chen et al., 2011).

Selective recognition, refolding and sequestration of misfolded proteins is performed by molecular chaperones. Recognition is accomplished by the selective detection of surface exposed hydrophobic stretches, which are normally buried within the core of well-folded proteins (Balchin et al., 2016).

The central players involved in the degradation of misfolded proteins are ubiquitin E3 ligases. By binding misfolded proteins directly or indirectly with the aid of chaperones, they mark their substrates with a polyubiquitin chain for destruction by the proteasome (Zheng and Shabek, 2017).

1.2 Molecular chaperones involved in PQC

Molecular chaperones were originally defined as proteins that promote the folding of newly translated polypeptides but do not get incorporated into the final protein structure

(Ellis and van der Vies, 1991). Most of the molecular chaperones are called heat shock proteins (Hsp) due to their upregulation during elevated temperature. They are broadly categorized by their molecular weight resulting in the chaperone families of Hsp40, Hsp70, Hsp90, Hsp110 and small heat shock proteins. The highly conserved and best studied chaperones involved in PQC belong to the Hsp70 and Hsp90 chaperone family (Balchin et al., 2016; Kampinga and Craig, 2010).

Folding is a highly energy-consuming process: ATP hydrolysis induces a conformational change in Hsp70 that enables substrate binding. Upon replacement of ADP with ATP, enhanced by nucleotide exchange factors, the substrate is released concluding an ATP-dependent folding cycle. Usually multiple folding cycles are required until a substrate protein reaches its final native conformation (Kim et al., 2013).

Hsp70s and Hsp90s can act alone or with the help of different cochaperones. For example, Hsp40 cochaperones can act as substrate adaptors: they selectively recognize un- or misfolded proteins and present them to Hsp70s for (re)folding. A single Hsp70 can interact with multiple different Hsp40s, which enables the recognition of a wide range of substrates. For example, the yeast Hsp70 Ssa1 can interact with either Ydj1 or Sis1 Hsp40 cochaperone. Ssa1 in complex with Ydj1 helps the refolding of misfolded proteins, while Ssa1 bound to Sis1 delivers misfolded proteins to intranuclear protein deposits (Becker et al., 1996; Horton et al., 2001; Miller et al., 2015). Moreover, the interaction with Hsp40 promotes ATP hydrolysis in Hsp70, which further enhances its substrate binding capacity (Kampinga and Craig, 2010).

An important role of molecular chaperones during PQC is triage decision, namely to refold, sequester or degrade misfolded proteins. The interaction of Hsp70 with different cochaperones can also influence triage decision. In mammalian cells the Hsp70 chaperone Hsc70 interacts with different J-domain proteins (Hsp40s) to aid in the folding of un- or misfolded proteins (Kampinga and Craig, 2010). However, upon inefficient refolding the Hsc70 associates with the cochaperone CHIP, which promotes the ubiquitylation and subsequent degradation of the misfolded protein (Connell et al., 2001).

1.3 Removal of misfolded proteins

If refolding of misfolded proteins fails, cells must remove them to avoid severe consequences caused by the aggregation of misfolded proteins. One solution is the active sequestration of misfolded proteins into distinct subcellular protein deposits. The alternative option is the selective degradation of misfolded proteins by the ubiquitin proteasome system (UPS).

1.3.1 Sequestration of misfolded proteins into protein deposits

In yeast several protein deposits for misfolded proteins or aggregates exist: insoluble aggregates and β-sheet-rich amyloids are sequestered into compartments called insoluble protein deposits (IPOD) (Kaganovich et al., 2008). Misfolded and damaged proteins are initially sorted into dynamic Q-bodies prior to their degradation by the UPS (Escusa-Toret et al., 2013). If these misfolded proteins are not degraded immediately by the UPS they are sequestered into the juxtanuclear or intranuclear quality control compartment (JUNQ and INQ respectively) (Bagola and Sommer, 2008; Miller et al., 2015). Additionally, several other protein deposits have been described in yeast including the endoplasmic reticulum (ER)-associated compartments, stress granules, peripheral aggregates and proteasome storage granules (Sontag et al., 2017). Some of the above-mentioned inclusions have overlapping functions and localization suggesting they are the same compartments but differently named (Sontag et al., 2014). Taken together, some protein deposits are terminal destinations for aggregation-prone misfolded proteins, whereas others are formed transiently by misfolded proteins destined for the UPS.

Originally, these inclusions were regarded as an indirect result of defective protein quality control. However, in recent years it has become evident that active sequestration of misfolded proteins and aggregates into distinct deposits is an early step in response to perturbations in protein homeostasis. For example, Q-bodies are proposed to form rapidly upon protein misfolding (Sontag et al., 2017). Hsp70s, together with their relevant cochaperones, serve central roles in delivering misfolded proteins to these deposits. For example, the chaperone Ssa1, together with its cochaperone Sis1, sorts misfolded proteins to INQ (Park et al., 2013). Similarly, the small heat shock protein Hsp42 is implicated in the formation of peripheral aggregates (Specht et al., 2011).

Importantly, sequestration to protein deposits is not necessarily the final destination of misfolded proteins. In yeast the Hsp104 disaggregase removes and unfolds polypeptides from protein aggregates in an ATP-dependent manner. These unfolded proteins are either refolded by downstream chaperones or degraded by the UPS (Glover and Lindquist, 1998). Alternatively, in metazoans protein aggregates have been shown to be removed by a selective autophagic process, called aggrephagy (Mogk et al., 2018; Zhang and Baehrecke, 2015).

1.3.2. The ubiquitin proteasome system

Selective destruction of misfolded proteins is achieved by the UPS. Ubiquitin is a 76 amino acid protein that is found in all eukaryotes (Hershko and Ciechanover, 1998). Covalent modification of a target protein with ubiquitin is catalysed by a canonical cascade of E1, E2 and E3 enzymes. First the E1 enzyme activates ubiquitin in an ATP-dependent manner and transfers it onto an active cysteine residue on the ubiquitin conjugating E2 enzyme. Subsequently, the ubiquitin E3 ligase mediates the formation of an isopeptide bond between a lysine residue on the target protein and the C-terminal glycine residue of ubiquitin (Varshavsky, 2012).

In budding yeast, a single E1 enzyme is responsible for the activation of ubiquitin, while eleven different ubiquitin E2 conjugating enzymes mediate the next step in ubiquitylation. The most diverse and largest group in the ubiquitylation pathway is the family of ubiquitin E3 ligases. Their specific spatial and temporal localization, and selective interaction with target proteins offers the substrate specificity in the ubiquitylation process (Finley et al., 2012).

The E3 enzymes are classified into two major groups: homologous to E6-AP carboxy terminus (HECT) domain E3s and really interesting new gene (RING) domain E3s. The two domains catalyse ubiquitylation in different ways: HECT E3s contain an active cysteine residue, which accepts the ubiquitin from an E2 enzyme before transferring it onto the target substrate (Scheffner et al., 1995). In contrast, RING E3s facilitate ubiquitin transfer by positioning the ubiquitin loaded E2 enzyme in close proximity of the target substrate protein (Metzger et al., 2014). RING domain-containing E3 enzymes are further categorized by whether they bind their substrates directly (single subunit RING E3s) or through specialized substrate receptors and cofactors (multi-subunit RING E3s).

Modification by ubiquitin is heterogenous. Attachment of a single ubiquitin (monoubiquitylation) or multiple single ubiquitin moieties to different acceptor lysine residues on the target protein (multiubiquitylation) mediate subcellular localization, trafficking or activity of target proteins. A polyubiquitin chain is formed by generating ubiquitin-ubiquitin conjugates using one of the seven acceptor lysine residues in ubiquitin. In general, the K48-linked polyubiquitin chain is the signal for proteasomal degradation (Kravtsova-Ivantsiv and Ciechanover, 2012; Yau and Rape, 2016).

The destruction of polyubiquitylated substrates occurs in the proteasome. The proteasome is a multi-subunit macromolecular machine built up from the core particle and the regulatory particle. The core particle provides the proteolytic activity while the regulatory particle is responsible for the binding, deubiquitylation and unfolding of polyubiquitylated proteins. Substrates carrying a polyubiquitin chain are first recognised by ubiquitin receptors. Once the substrates are bound to the proteasome, deubiquitylating enzymes remove the polyubiquitin chain and ATPases unfold and feed the substrates into the catalytic core. After proteolysis the peptides of 5-7 amino acid length are released into the cytosol and further processed by cytosolic peptidases (Finley et al., 2016).

1.4 Ubiquitin E3 ligases involved in PQC

The ubiquitin ligase family comprises the most diverse group of enzymes in the ubiquitylation cascade. There are 60-100 predicted E3 ligases in budding yeast, however only a handful of them function in PQC pathways (Finley et al., 2012). These particular E3 ligases are part of spatially specified PQC pathways: namely the ribosomal, cytosolic, nuclear and ER protein quality control.

1.4.1 E3 enzymes involved in ribosomal protein quality control

Protein quality control at the ribosome involves the monitoring of polypeptides during the process of translation. Protein synthesis can be perturbed by translation from defective mRNAs lacking stop-codons or due to insufficient amount of tRNAs. All these perturbations lead to ribosome stalling. The ribosome-associated protein quality control pathway recognizes stalled ribosomes and initiate the degradation of erroneous nascent chains (Brandman and Hegde, 2016).

Ltn1 (also called Rkr1) is the crucial RING domain E3 ligase involved in the removal of aberrant polypeptides at the ribosome. It was originally identified through a genetic screen for factors involved in chromatin function and transcription (Braun et al., 2007). However, its more prominent role is in the polyubiquitylation of aberrant proteins translated from mRNAs lacking stop codons (Bengtson and Joazeiro, 2010). If translation cannot be terminated, due to the lack of a stop codon, the poly(A) tail on the mRNA is translated into a poly-lysine tract. This generates a highly positively charged sequence that electrostatically interacts with the negatively charged ribosome exit channel leading to ribosome stalling. Polyubiquitylation of aberrant nascent chains occurs while they are still associated with the 40S ribosome (Shao et al., 2013). How does Ltn1 recognize its substrates? One hypothesis is the direct recognition of the poly-lysine tract by Ltn1. Alternatively, translational pausing might induce conformational changes on the ribosome which could recruit Ltn1 directly or indirectly to the stalled ribosome to ubiquitylate nascent chains (Brandman et al., 2012).

Recently it has been shown that degradation of ER-targeted model substrates without stop codons, is also dependent on Ltn1. Intriguingly, degradation of these substrates was not dependent on ER quality control factors Hrd1 and Doa10 (introduced below) (Crowder et al., 2015).

1.4.2 E3 enzymes involved in cytosolic protein quality control

The cytosol contains four known E3s involved in PQC. The RING domain E3 enzyme Ubr1 was the first ubiquitin ligase to be identified (Bartel et al., 1990). It was originally implicated in the N-end rule pathway, which determines the half-life of a protein based on the identity of the very N-terminal residue. In the N-end rule pathway, Ubr1 selectively recognizes, binds to and ubiquitylates target proteins with destabilizing N-terminal residues. Therefore, Ubr1 is also called N-degron (Varshavsky, 2011). However, Ubr1 is also implicated in the removal of cytosolic misfolded proteins. The cytosolic version of misfolded CPY*, a truncated and thus potentially misfolded soluble protein stGnd1 and unfolded cytosolic kinases are all Ubr1 substrates (Eisele and Wolf, 2008; Heck et al., 2010; Nillegoda et al., 2010).

How does Ubr1 recognize misfolded proteins? *In vivo* the cochaperones Sse1 or Sis1 are required for the degradation of cytosolic misfolded proteins by Ubr1 (Heck et al., 2010; Summers et al., 2013). Thus, Sse1 together with an Hsp70 is proposed to mediate PQC by presenting misfolded proteins to Ubr1. On the other hand, Ubr1 can

ubiquitylate denatured luciferase *in vitro* in the absence of chaperones. However, addition of Ssa1 to the reaction enhances the ubiquitylation reaction (Nillegoda et al., 2010). Hence, Ubr1 is able to directly interact with and ubiquitylate misfolded proteins but molecular chaperones can aid ubiquitylation by presenting misfolded substrates to Ubr1.

Intriguingly, Ubr1 is also involved in endoplasmic reticulum-associated degradation (ERAD). In the absence of the canonical ERAD E3 ligases Hrd1 and Doa10, the model ERAD substrate Ste6* is targeted by Ubr1. Moreover, ectopically expressed human cystic fibrosis transmembrane conductance regulator (CFTR), another model ERAD substrate, is also targeted by Ubr1 steady-state (Stolz et al., 2013). Taken together, Ubr1 is responsible for the removal of misfolded proteins from both the cytosol and the ER membrane.

Ubr2 is a paralogue of Ubr1, however it is not involved in the N-end rule pathway (Hochstrasser, 1996). It is responsible for the ubiquitin-mediated degradation of Rpn4, the main transcription factor involved in proteasome biogenesis (Wang et al., 2004). Moreover, Ubr2 is implicated in maintaining the integrity of kinetochores, a large protein assembly formed at the centromeres of chromosomes during mitosis or meiosis (Akiyoshi et al., 2013; Herrero and Thorpe, 2016). Importantly, Ubr2 promotes the degradation of cytosolic misfolded kinases, however the mode of substrate interaction has not been determined (Nillegoda et al., 2010).

Hul5 is one of only five HECT domain E3 ligases in yeast (Wang et al., 1999). Hul5 directly interacts with the proteasome where it extends polyubiquitin chains on target proteins destined for degradation. The extension of the polyubiquitin chain is proposed to stabilize the interaction between proteasome and substrate leading to enhanced degradation of the latter (Crosas et al., 2006; Leggett et al., 2002). In addition, Hul5 is responsible for the degradation of misfolded proteins during heat shock (Fang et al., 2011) and is also implicated in the degradation of ERAD substrates (Kohlmann et al., 2008). However, how Hul5 recognizes misfolded proteins is currently unknown.

Recently, another HECT domain E3 ligase, Rsp5 (Huibregtse et al., 1995) was identified as the main ubiquitin E3 ligase involved in the removal of misfolded proteins during heat shock (Fang et al., 2014). Rsp5 directly recognizes and interacts with PY motifs exposed upon heat shock (Fang et al., 2014). Moreover, Rsp5 is also

responsible for the degradation of many endogenous well-folded substrates involved in diverse biological pathways (Gupta et al., 2007).

1.4.3 E3 enzymes involved in nuclear protein quality control

San1, a RING domain E3 enzyme, is the only known ubiquitin ligase implicated in the removal of misfolded nuclear proteins (Dasgupta et al., 2004; Gardner et al., 2005). San1 directly recognizes short stretches of surface-exposed hydrophobic residues on misfolded proteins, which are prone to form aggregates (Fredrickson et al., 2013, 2011). San1 is not only implicated in nuclear quality control: a genetic screen identified San1 to be important for the removal of misfolded cytosolic proteins as well (Heck et al., 2010). However, San1 is non-functional outside the nucleus. This suggests that the misfolded cytosolic substrates are actively delivered into the nucleus by the cochaperone Sse1 for San1-mediated ubiquitylation and degradation (Gardner et al., 2005; Heck et al., 2010; Prasad et al., 2010).

1.4.4 E3 enzymes involved in ER quality control

Recognition and degradation of misfolded ER luminal or membrane proteins is achieved by the ERAD machinery. In the core of these machines are the ubiquitin E3 ligases, which form a complex with cofactors and substrate adaptors to recognize and ubiquitylate ERAD substrates (Berner et al., 2018). The Hrd1 complex is responsible for misfolded proteins/domains in the lumen or in the membrane-spanning region (ERAD-L and ERAD-M pathway, respectively), while the Doa10 complex recognizes and ubiquitylates proteins with cytosolic misfolded domains (ERAD-C pathway) (Bays et al., 2001; Carvalho et al., 2006; Deng and Hochstrasser, 2006). Recently the Asi1-3 complex has been described in yeast to monitor and degrade misfolded or mislocalized proteins of the inner nuclear membrane (INM), which is an ER subdomain (Foresti et al., 2014; Khmelinskii et al., 2014).

Hrd1 (also called Der3) is a multi-membrane spanning RING domain E3 ligase. It was identified in two independent genetic screens using either Hmg2, a key enzyme in sterol biosynthesis, or luminal CPY* as a model substrate (Bordallo et al., 1998; Hampton et al., 1996; Knop et al., 1996). Further experiments revealed that Hrd1 is part of a complex of at least six subunits (Ruggiano et al., 2014). The entire complex is responsible for the recognition and ubiquitylation of misfolded proteins and for their retrotranslocation from the ER lumen or membrane into the cytosol for proteasomal degradation (Schoebel et al., 2017). Recognition of ERAD-L substrates is

accomplished by the luminal Hsp70 Kar2 and the lectin Yos9. The recognized misfolded proteins are delivered to Hrd1 via a single membrane-spanning protein Hrd3, which interacts simultaneously with both Hrd1 and Kar2 or Yos9 (Denic et al., 2006). Moreover, Der1, another membrane protein in the Hrd1 complex, has been implicated in the recognition of ERAD-L substrates (Knop et al., 1996; Stanley et al., 2011). In contrast to ERAD-L substrates, degradation of ERAD-M substrates is only dependent on Hrd1 and Hrd3 and partially on Usa1, a scaffold protein in the Hrd1 complex (Carvalho et al., 2006; Horn et al., 2009). Hrd1 is proposed to interact directly with ERAD-M substrates through hydrophilic residues in the Hrd1 membrane spanning domains (Sato et al., 2009). Taken together the Hrd1 complex is a huge modular complex that is capable of substrate recognition in a multitude of ways (Kanehara et al., 2010).

Doa10 is a RING domain E3 ligase with multiple membrane spanning domains. It was identified in a genetic screen for the degradation of a soluble transcriptional repressor (Swanson et al., 2001). Intriguingly, it localizes to the INM where it ubiquitylates soluble nuclear proteins for degradation (Deng and Hochstrasser, 2006). However, Doa10 is not only restricted to ERAD-C substrates. Recently it has been implicated in the degradation of an ERAD-M substrate, Sbh2 (Habeck et al., 2015). How does Doa10 recognize its substrates? Similarly to Hrd1, Doa10 also contains hydrophilic residues within its membrane domain suggesting an analogous mode of ERAD-M substrate recognition (Habeck et al., 2015). On the other hand, how Doa10 recognizes ERAD-C substrates is currently unknown. Doa10 does not interact with substrate adaptor proteins like Hrd3 suggesting that Doa10 might directly interact with ERAD-C substrates (Deng and Hochstrasser, 2006).

The Asi1-3 complex contains two RING domain E3 enzymes Asi1/Asi3 and a bridging subunit Asi2. The Asi1-3 complex localizes to the INM and targets misfolded or mislocalized ERAD-M substrates in the nuclear envelope. Asi2 is proposed to function as a substrate adaptor in the complex, however, how the Asi1-3 complex work mechanistically is yet to be investigated (Foresti et al., 2014; Khmelinskii et al., 2014).

In summary, the different subcellular compartments all have their own dedicated E3 ligase(s) for the removal of misfolded or damaged proteins. However, the compartmentalization is not strict, as several E3s regulate quality control mechanisms in multiple subcellular locations.

1.5 Stress response pathways that modulate PQC

During stress, protein folding is compromised and therefore cells trigger adaptive responses to upregulate PQC pathways. For example, protein misfolding in the ER triggers the unfolded protein response (UPR), which upregulates the expression of molecular chaperones and the ERAD components to alleviate ER stress (Walter and Ron, 2011). Similarly, protein misfolding in the cytosol activates the heat shock response (HSR) to induce the expression of cytosolic quality control factors (Labbadia and Morimoto, 2015).

1.5.1 The unfolded protein response (UPR)

All proteins entering the ER obtain their final conformation in the ER membrane and the ER lumen before they are delivered to their final destination along the secretory pathway (Braakman and Hebert, 2013). If folding is delayed or an illegitimate conformation arises, the substrate is either subjected to additional folding cycles or is selected for degradation by ERAD. Collectively, the UPR is responsible for the monitoring of all proteins entering the ER (Ron and Walter, 2007).

In metazoans there are three branches of UPR signalling. The main regulators of each branches are ER-localized membrane proteins namely IRE1, PERK and ATF6. The highly conserved Ire1 branch was the first to be identified and the only UPR signal transducer in budding yeast (Walter and Ron, 2011). Ire1 is a bifunctional enzyme containing both kinase and endoribonuclease activity (Cox et al., 1993; Nikawa and Yamashita, 1992). Upon activation, Ire1 cleaves the mRNA of the UPR transcription factor Hac1 at two specific sites (Sidrauski and Walter, 1997). The cleaved mRNA is subsequently ligated by the tRNA ligase Trl1 (Sidrauski et al., 1996) and translated into the active version of spliced Hac1 (Hac1[s]). Hac1[s] specifically binds to UPR response elements in the promoter region of target genes and activates their transcription (Mori et al., 1996). The main UPR transcriptional targets are involved in protein translocation, folding, modification of nascent chains and degradation of misfolded proteins via ERAD to alleviate ER stress (Travers et al., 2000).

In the absence of protein folding stress Ire1 is in a monomeric "resting" state. Upon accumulation of misfolded proteins in the ER lumen Ire1 forms back-to-back dimers which leads to trans-phosphorylation and formation of higher order oligomers (Korennykh et al., 2009; Lee et al., 2008). In this oligomeric state Ire1 endonuclease

activity is induced resulting in the cleavage of the *HAC1* mRNA. How does Ire1 recognize misfolded proteins? The classical model proposes that steady-state Kar2 interacts with Ire1, which retains Ire1 in an inactive monomeric state. Upon accumulation of misfolded proteins Kar2 dissociates from Ire1 which leads to its activation (Ron and Walter, 2007). However, Ire1 mutants that are unable to bind Kar2 can still induce UPR (Kimata et al., 2004). In the alternative model, direct binding of misfolded proteins to the luminal domain of Ire1 activates the UPR. This model is based on the identification of a peptide binding groove on the luminal domain of Ire1 by crystallography (Credle et al., 2005). The two models are not mutually exclusive, thus in a third hybrid model, activation via both Kar2 dissociation and direct interaction with misfolded proteins is also plausible. Moreover, Ire1 can be activated by aberrant membrane lipid composition as well (Halbleib et al., 2017; Promlek et al., 2011). Therefore, Ire1 is not only sensing unfolded protein stress but also lipid bilayer stress.

1.5.2 The heat shock response (HSR)

As its name suggests, the HSR was initially described as an adaptive response to elevated temperature. The cellular response to heat shock is multifaceted, which involves cell cycle arrest, metabolic reprogramming and alterations in membrane and cell wall dynamics. Moreover, it involves the reprogramming of PQC pathways as a response to increased proteotoxicity caused by the accumulation of misfolded and damaged protein during heat shock (Verghese et al., 2012). Intriguingly, in budding yeast the accumulation of misfolded proteins only occurs upon severe heat shock (45°C or higher), while cells kept at 37°C do not show any hallmarks of protein misfolding even in the absence of Hsp90 (Fang et al., 2011; Nathan et al., 1997). This suggests that during mild heat shock the plasticity of the PQC pathways is capable to efficiently cope with the perturbation in protein homeostasis. Importantly, HSR is not only activated by elevated temperature but also upon accumulation of cytosolic misfolded proteins (Labbadia and Morimoto, 2015).

On the molecular level the initial step in HSR is the upregulation of heat shock proteins which are mostly but not exclusively molecular chaperones (Verghese et al., 2012). In budding yeast, the HSR is regulated by a single essential transcriptional factor Hsf1 (Sorger and Pelham, 1988; Wiederrecht et al., 1988). Hsf1 directly binds to promoter regions with heat shock transcription elements and activates the transcription of the downstream gene. In non-stressed mammalian cells, Hsf1 is kept in an inactive

monomeric state by a constitutively expressed Hsp70 and its cochaperone Hdj1 (Shi et al., 1998). Upon heat shock or accumulation of misfolded proteins in the cytosol, Hsf1 is released, trimerizes and translocates into the nucleus where it upregulates transcription of target genes (Baler et al., 1993). When stress subsides, Hsf1 is acetylated and repressed by molecular chaperones (Raychaudhuri et al., 2014). Besides transcriptional upregulation of the *HSP* genes, the HSR also upregulates the UPS. The latter was deduced from the increased total amount of ubiquitin conjugates and elevated proteasomal degradation upon heat shock (Medicherla and Goldberg, 2008; Parag et al., 1987). The main UPS members involved in the clearance of misfolded or damaged proteins upon heat shock are Rsp5 and Hul5 (Fang et al., 2014).

1.5.3 The environmental stress response (ESR)

Unicellular organisms like budding yeast are exposed to sudden changes in the environment including fluctuations in temperature, osmolarity, acidity or in nutrient availability. In order to cope with these fluctuations, yeast induces a general stress response pathway, called ESR, which reprograms the expression pattern of approximately 900 genes with one third of them being transcriptionally upregulated and two thirds being downregulated (Causton et al., 2001; Gasch et al., 2000). In general, the induced genes are implicated in protein folding, protein degradation, autophagy and DNA-damage repair amongst others (Gasch, 2003). Conversely, downregulated genes are mainly involved in general protein translation including genes involved in ribosome or tRNA synthesis, general transcription and in mRNA processing and export (Gasch, 2003). Importantly, the ESR is not specific to a certain stressor but instead offers a common response to re-establish the cellular homeostasis (Gasch, 2003).

The main transcription factors governing the ESR pathway are Msn2/4 and Hsf1. Msn2/4 is negatively regulated by the protein kinase A, which in yeast is built up from three subunits namely Tpk1/Tpk2/Tpk3 (Toda et al., 1987). The activity of the Tpk complex is regulated by its inhibitor Bcy1. Upon production of cAMP Bcy1 dissociates from the Tpk1 and Tpk2 subunit resulting in the activation of the Tpk complex (Thevelein and De Winde, 1999). The active complex phosphorylates Msn2/4 which blocks their nuclear entry, and therefore prevents them from transcriptional regulation (Görner et al., 1998). Upon Tpk inactivation Msn2/4 relocalizes to the nucleus and binds to stress response elements in promoter regions to upregulate transcription. Importantly, the HSR is a branch of the ESR, which means that nearly all HSR target

genes are upregulated during ESR activation through Hsf1 (Verghese et al., 2012). However, regulation of Hsf1 during ESR induction is not as well established as its regulation during HSR. *In vitro* studies propose that both Yak1 and Rim15 kinase directly phosphorylate Hsf1, which is required for its activation and DNA binding capability during ESR (Lee et al., 2013; P. Lee et al., 2008). However, no clear *in vivo* data is available on the role of Yak1 and Rim15 on Hsf1 activation.

1.6 Aim of the study

Protein quality control pathways in the ER, the cytoplasm or in the nucleus are well-studied fields of molecular biology and biochemistry. However, much less is known about how cells maintain protein homeostasis on the interface of different subcellular compartments. The main aim of this PhD thesis was to investigate how cells recognize and degrade ER membrane proteins with a cytoplasmic misfolded domain during stressful conditions. To achieve this aim, we employed an ER-anchored misfolded reporter protein that is selectively degraded under stress conditions. A genetic screen, performed prior to the start of the PhD project, identified three relevant genes that are required for the stress-induced degradation of this misfolded reporter. The specific aims of the study were the following:

1) Characterization of the stress-induced degradation phenotype of an ER-anchored misfolded reporter protein
2) Mechanistic analysis of the stress-induced protein degradation pathway identified by the genetic screen
3) Determining the substrate spectrum of the stress-induced protein degradation pathway

RESULTS

2.1 Misfolded reporter proteins to follow PQC mechanisms at the ER membrane

2.1.1 Generation and characterization of misfolded ER reporter proteins

In order to follow the fate of ER membrane proteins with cytosolic misfolded domains, three reporter proteins were generated. The reticulon protein Rtn1 was used to anchor the reporter to the ER membrane (Oertle et al., 2003). Rtn1 is inserted into the ER membrane via two reticulon homology domains (RHD) and both the N- and C-terminus face the cytosol (De Craene et al., 2006; Voeltz et al., 2006). The RHD is an approximately 35 amino acid long hydrophobic segment that forms a hairpin inside the membrane without passing the lipid bilayer (Brady et al., 2015). Thus, none of the reporter protein is visible from the lumen of the ER, which allows its uncoupling from any ER luminal quality control pathways (i.e. the UPR). Two mutated proteins CPY* and Pho8* were attached to the C-terminus of Rtn1 to create misfolded cytosolic domains (**Figure 1A**). CPY* is a mutant version of the vacuolar caboxypeptidase yscY (Finger et al., 1993; Wolf and Fink, 1975), which is continuously degraded by the proteasome via the Hrd1-mediated ERAD-L pathway (Bordallo et al., 1998; Hiller et al., 1996). Pho8*, generated by Sebastian Schuck, is a truncated and point mutant version of the vacuolar phosphatase Pho8. When expressed in the ER lumen, it is degraded via Hrd1 (**Figure 1B**). Additionally, expressing Pho8* in the cytosol leads to its constitutive San1-mediated degradation suggesting that it is misfolded (**Figure 1C**). In order to visually follow the turnover of these reporter proteins, GFP was fused to the C-terminus generating the reporter proteins Rtn1CPY*-GFP and Rtn1Pho8*-GFP. Rtn1-GFP, the reporter protein with no misfolded domain, was used as negative control.

A

Rtn1-GFP

Rtn1CPY*-GFP

Rtn1Pho8*-GFP

B

C
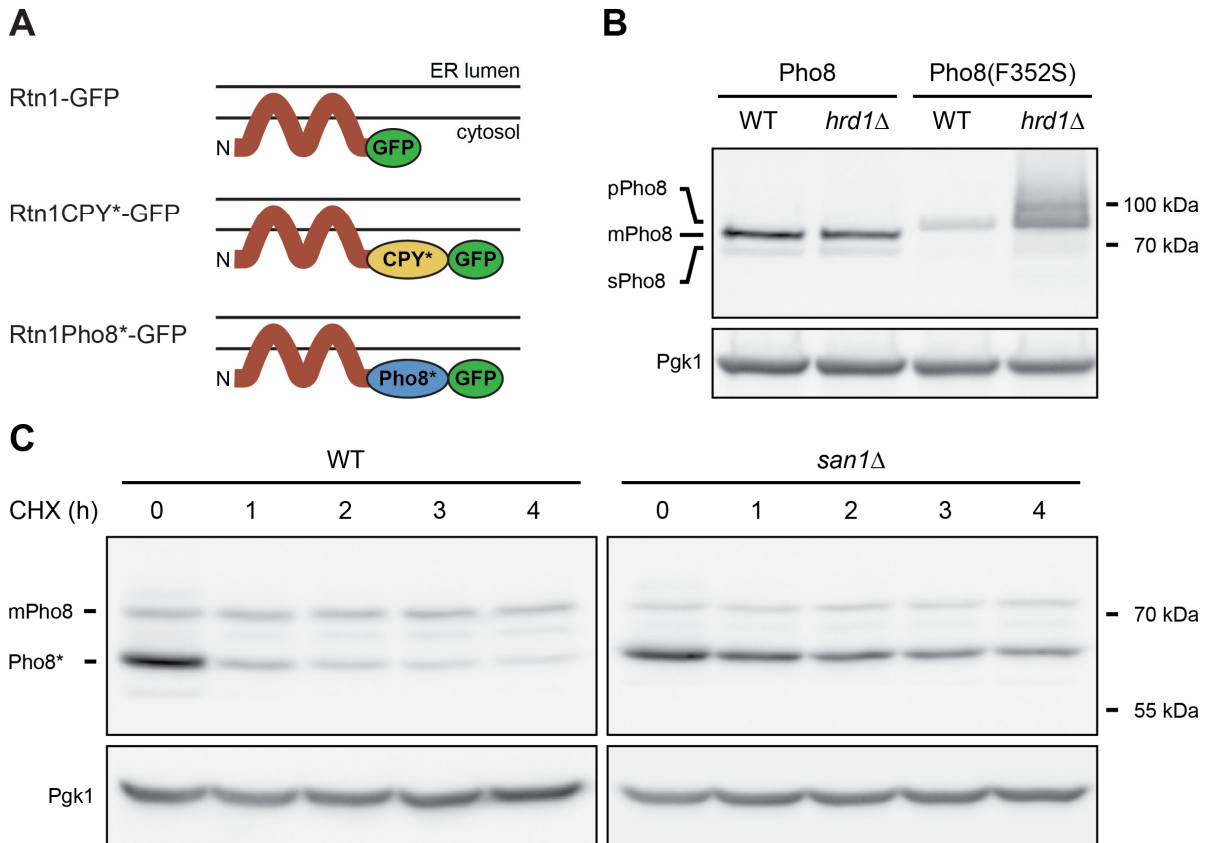
Figure 1. Pho8(F352S) is a misfolded protein
A) Schematic illustration of the reporter proteins used in the thesis. **B)** Western blot of Pho8 and Pgk1 from wild-type (WT) or *hrd1Δ* cells expressing wild-type Pho8 or point mutant Pho8(F352S). Pgk1 served as loading control. pPho8 – enzymatically inactive Pho8 precursor, mPho8 – mature Pho8 in the vacuole membrane, sPho8 – mature soluble Pho8 inside the vacuole. Experiment performed by Katharina Schaeff. **C)** Western blot of Pho8 and Pgk1 after cycloheximide (CHX) treatment of WT or *san1Δ* cells expressing cytosolic Pho8*-GFP. Pgk1 served as loading control. mPho8 – mature endogenous Pho8 in the vacuole membrane. Experiment performed by Katharina Schaeff.

The three reporters were integrated into the genome via homologous recombination and expressed from a constitutive *ADH1* promoter unless noted otherwise. Subcellular fractionation confirmed their proper membrane insertion (**Figure 2A**). Importantly, the reporters overlapped with the general ER membrane marker Sec63-mCherry confirming their ER localization (**Figure 2B**).
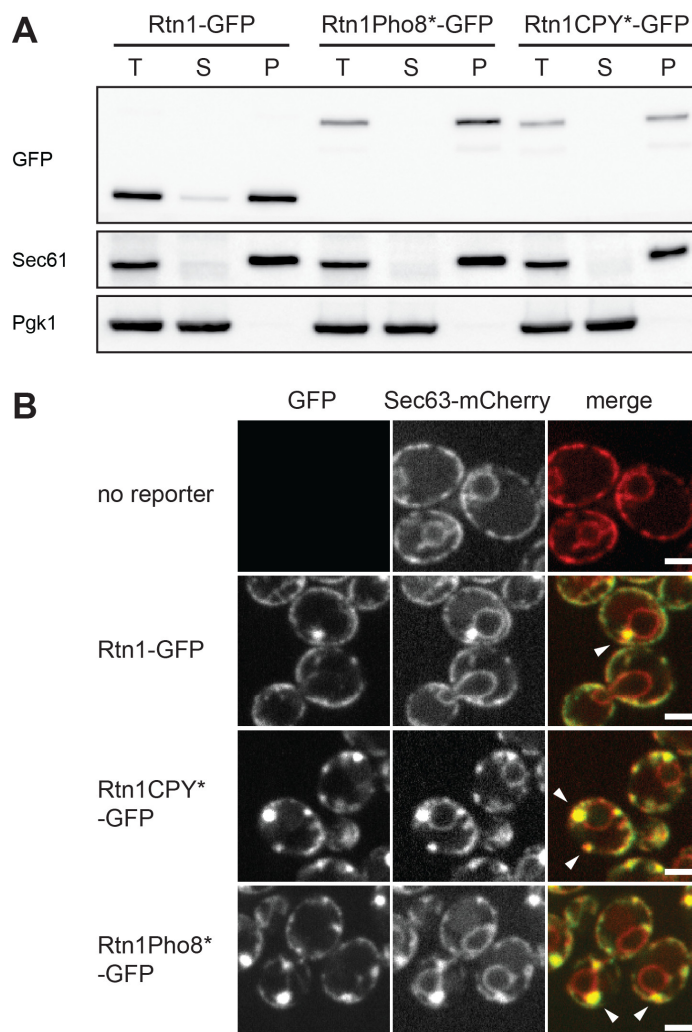
Figure 2. The reporter proteins localize to the ER membrane
A) Western blot of GFP, Sec61 and Pgk1 after subcellular fractionation of wild-type cells expressing Rtn1-GFP, Rtn1CPY*-GFP or Rtn1Pho8*-GFP. Sec61 and Pgk1 served as markers for membrane proteins and soluble proteins, respectively. T – total lysate, S – supernatant fraction, P – pellet fraction. **B)** Fluorescent microscopy images of wild-type cells expressing endogenously tagged Sec63-mCherry and Rtn1-GFP, Rtn1CPY*-GFP or Rtn1Pho8*-GFP. Overexpression of the Rtn1-based reporters induced the formation of bright punctae at the cell periphery (arrowheads). This phenotype is often detected upon Roq1 overexpression and it reflects over-tubulated ER (Voeltz et al., 2006). Scale bar: 2 µm.

2.1.2 Degradation phenotype of Rtn1Pho8*-GFP

In order to determine the stability of the reporters, their steady-state turnover was compared to the turnover of the well-studied ERAD substrate Hmg2 (Hampton and Rine, 1994). Hmg2-GFP was degraded rapidly resulting in a half-life of approximately 30 minutes in a cycloheximide chase experiment (**Figure 3A, B**). As expected, Rtn1-GFP was stable throughout the treatment (Christiano et al., 2014). However, Rtn1CPY*-GFP was continuously degraded with a half-life of roughly two hours. Surprisingly, Rtn1Pho8*-GFP showed the same stability as Rtn1-GFP during four hours of cycloheximide chase despite its misfolded domain (**Figure 3A, B**). This unexpected finding motivated us to further investigate and characterize the degradation phenotype of Rtn1Pho8*-GFP.

A

cycloheximide treatment (h)

0 1 2 3 4

Hmg2-GFP

Rtn1-GFP

Rtn1CPY*-GFP

Rtn1Pho8*-GFP

B
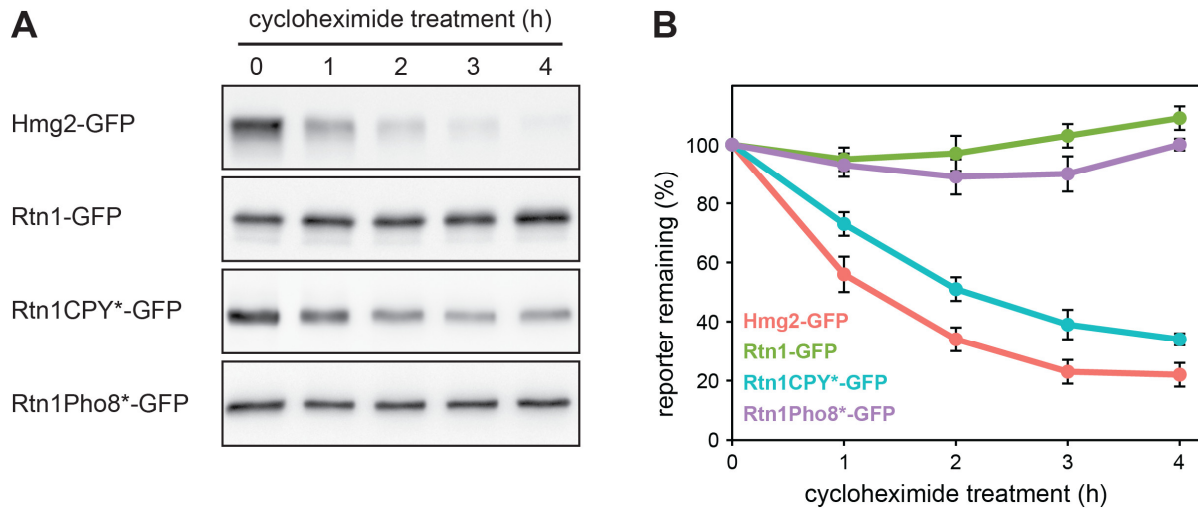
Figure 3. Rtn1Pho8*-GFP is a stable protein steady-state
A) Western blot of GFP or total GFP fluorescence **B)**, measured by flow cytometry, after cycloheximide treatment of wild-type cells expressing Hmg2-GFP, Rtn1-GFP, Rtn1CPY*-GFP or Rtn1Pho8*-GFP. Mean ± SEM, n = 5. The experiment in **(A)** was performed by Katharina Schaeff.

Stress conditions are known to upregulate different quality control pathways (Higuchi-Sanabria et al., 2018). Therefore, the stability of Rtn1Pho8*-GFP was tested under ER-stress conditions. Tunicamycin, an often-used ER-stressor, blocks N-glycosylation in the ER lumen, which leads to protein misfolding and eventually ER-stress (Gerlach et al., 2012). Five hours of tunicamycin treatment caused the selective degradation of Rtn1Pho8*-GFP driven from a constitutive *ADH1* promoter (**Figure 4A, B**). The slight drop in Rtn1-GFP levels during tunicamycin treatment probably reflects the transcriptional downregulation of the *ADH1* promoter upon ER-stress (Pincus et al., 2014). Since both reporters were expressed from the *ADH1* promoter, the excessive drop of Rtn1Pho8*-GFP levels, compared to Rtn1-GFP, is likely to reflect selective protein degradation. In order to confirm this, degradation of the reporter was followed in a chase experiment. Since tunicamycin inhibits N-glycosylation of newly synthesized proteins and thus requires ongoing protein synthesis to be effective, a combination of cycloheximide and tunicamycin treatment is not feasible. To bypass this limitation, the reporters were expressed from an inducible *GAL1* promoter in galactose-containing medium followed by promoter shut-off by diluting the cells back into glucose-containing medium. After promoter shut-off the levels of both reporters remained stable in agreement with the cycloheximide chase. In contrast, Rtn1Pho8*-GFP levels dropped substantially during four hours of tunicamycin treatment while Rtn1-GFP levels showed only a minor drop (**Figure 4C**).
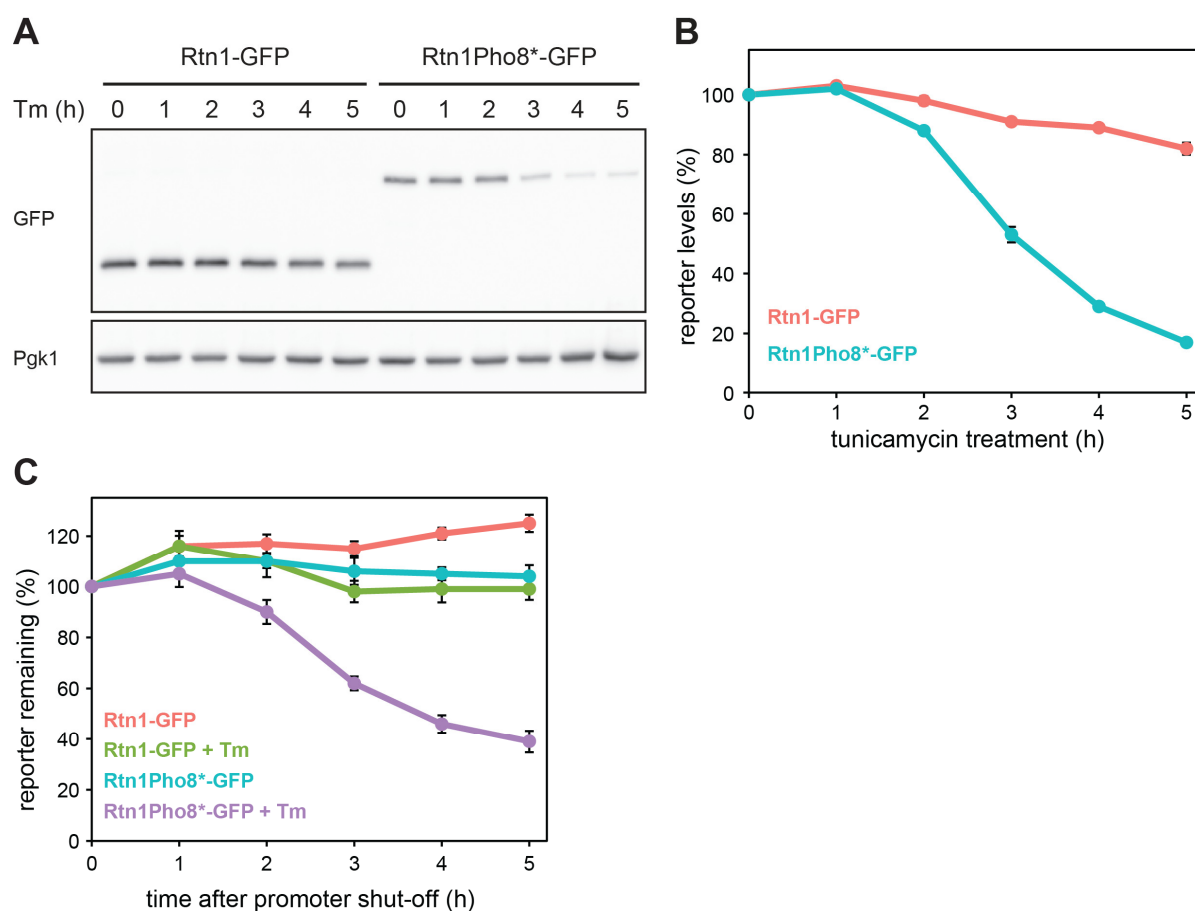
Figure 4. Rtn1Pho8*-GFP is degraded upon ER stress
A) Western blot of GFP and Pgk1 or mean GFP fluorescence **B)**, measured by flow cytometry, after tunicamycin (Tm) treatment of wild-type cells expressing Rtn1-GFP or Rtn1Pho8*-GFP. Pgk1 served as loading control. Mean ± SEM, n = 4. The experiment in **(A)** was performed by Kevin Leiss. **C)** Total GFP fluorescence, measured by flow cytometry, after promoter shut-off and tunicamycin treatment of wild-type cells expressing *GAL1*-driven Rtn1-GFP or Rtn1Pho8*-GFP. Mean ± SEM, n = 4.

Galactose-induced reporters also localized to the ER membranes and subcellular fractionation confirmed their membrane association (**Figure 5A, B**). Thus, ER-stress triggers the selective degradation of pre-existing ER-localized misfolded Rtn1Pho8*-GFP.
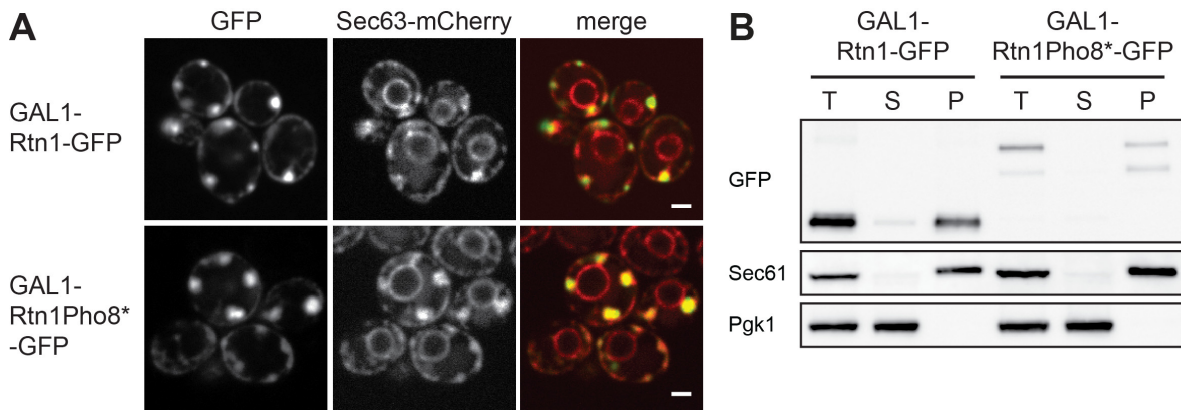
Figure 5. *GAL1*-driven reporters localize to the ER membrane
A) Fluorescent microscopy images of wild-type cells expressing endogenously tagged Sec63-mCherry and *GAL1*-driven Rtn1-GFP or Rtn1Pho8*-GFP. Scale bar: 2 µm. **B)** Western blot of GFP, Sec61 and Pgk1 after subcellular fractionation of wild-type cells expressing *GAL1*-driven Rtn1-GFP or Rtn1Pho8*-GFP. Sec61 and Pgk1 served as markers for membrane proteins and soluble proteins, respectively. T – total lysate, S – supernatant fraction, P – pellet fraction.

2.1.3 Rtn1Pho8*-GFP is degraded by the proteasome

There are two sites of protein degradation in yeast: the vacuole (the equivalent of mammalian lysosomes) and the proteasome. Inhibition of the vacuolar serine proteases by PMSF or the proteasome by MG132 slowed down the tunicamycin-induced degradation of Rtn1Pho8*-GFP (**Figure 6A, B**). This suggested that the reporter is degraded in both compartments. However, combined addition of the drugs resulted only in a minor additive effect. Moreover, deletion of the two major vacuolar proteases Pep4 and Prb1 (Teichert et al., 1989) had no effect on reporter degradation (**Figure 6A, B**). Since PMSF is a non-selective serine protease inhibitor, it most likely inhibited additional serine proteases outside the vacuole that are required for Rtn1Pho8*-GFP degradation. Indeed, addition of PMSF in *pep4Δ prb1Δ* cells led to impaired stress-induced degradation of Rtn1Pho8*-GFP (**Figure 6A, B**). Intriguingly, degradation was also not affected by the deletion of ERAD components Hrd1 and Doa10 (**Figure 6C**). Hence, ER-stress induces the proteasomal degradation of Rtn1Pho8*-GFP independent of Hrd1- or Doa10-mediated ERAD.
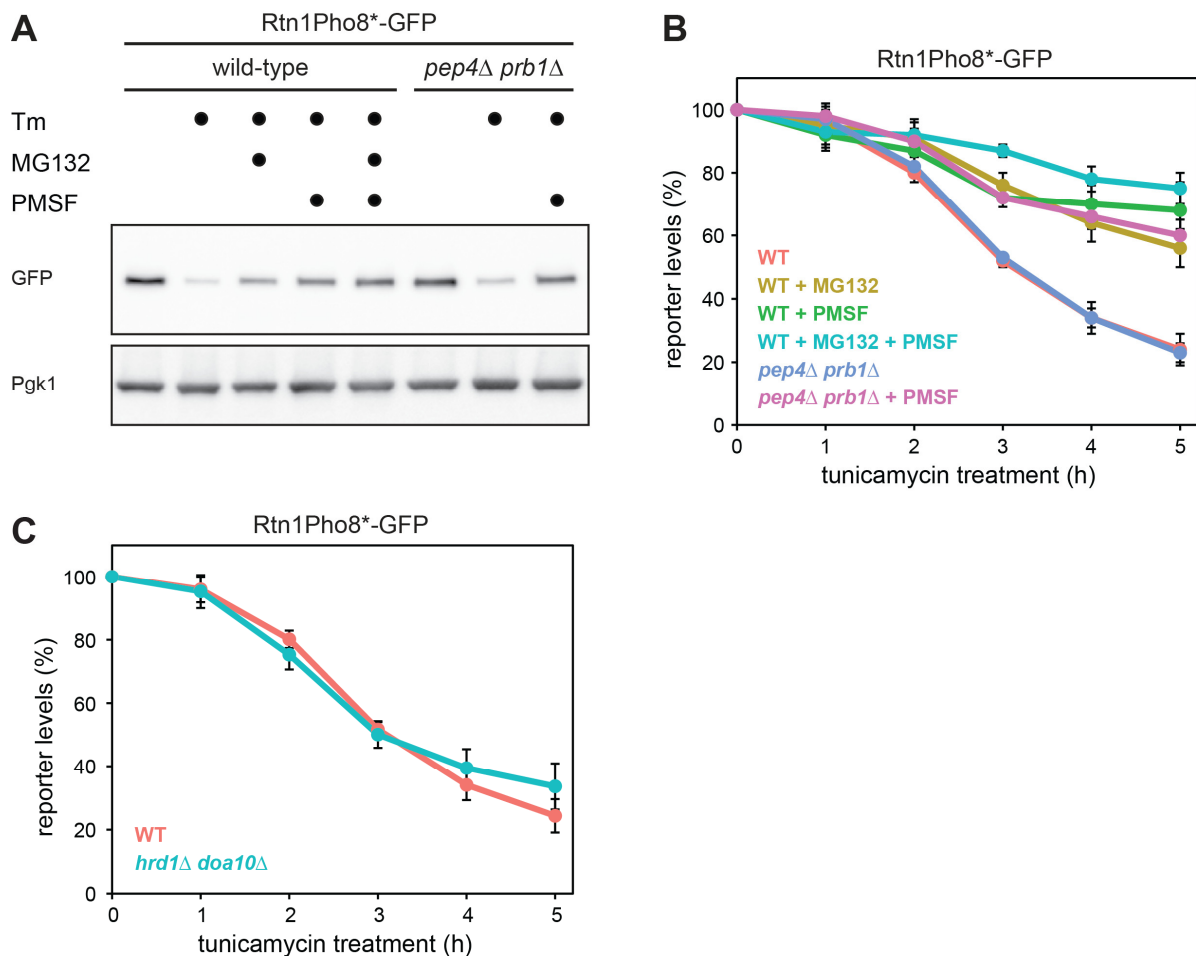
Figure 6. Rtn1Pho8*-GFP is degraded by the proteasome independent of Hrd1/Doa10
A) Western blot of GFP and Pgk1 or mean GFP fluorescence **B)**, measured by flow cytometry, of *pdr5Δ* (wild-type, WT) or *pep4Δ prb1Δ* cells expressing Rtn1Pho8*-GFP after tunicamycin (Tm), MG132 or PMSF treatment where indicated. Pgk1 served as loading control. Mean ± SEM, n = 3.
C) Mean GFP fluorescence, measured by flow cytometry, after tunicamycin treatment of *hrd1Δ doa10Δ* cells expressing Rtn1Pho8*-GFP. Mean ± SEM, n = 3.

2.1.4 A genetic screen to uncover the degradation machinery of Rtn1Pho8*-GFP

These intriguing findings raised the question of which genes/proteins are required for the stress-induced degradation of Rtn1Pho8*-GFP. In order to uncover the degradation machinery Sebastian Schuck, Enrique Garcia-Rivera, Vivian Chen and Dale Muzzey performed a random mutagenesis screen. Briefly, wild-type cells harbouring Rtn1Pho8*-GFP were mutagenized with ethyl methanesulfonate and screened by flow cytometry for mutants that were unable to degrade Rtn1Pho8*-GFP during tunicamycin treatment. Subsequent complementation analysis and whole genome sequencing uncovered mutations in five relevant genes: *PRE2, UMP1, UBR1, YNM3/NMA111* and YJL144W.

PRE2 is an essential gene that encodes the β5 subunit of the 20S proteasome and is responsible for its chymotryptic activity (Heinemeyer et al., 1993). The random mutagenesis screen uncovered a viable but hypomorphic mutant allele coding Pre2(D243N). Ump1 is a short-lived chaperone required for the correct maturation of the 20S proteasome. Upon completion of the assembly Ump1 itself is degraded by the proteasome (Ramos et al., 1998). The requirement for these two factors supports the notion that Rtn1Pho8*-GFP is degraded via the proteasome.

Ubr1 was the first ubiquitin E3 ligase to be identified and it is mainly implicated in the N-end rule pathway (Bartel et al., 1990). Moreover, it has an emerging role in targeting misfolded proteins for degradation (Eisele and Wolf, 2008; Heck et al., 2010; Nillegoda et al., 2010), which is in line with its identification through the screen. Ynm3 is the only budding yeast homologue of the HtrA-like (high-temperature requirement A) serine-protease family (Fahrenkrog et al., 2004), providing an explanation for the sensitivity of reporter degradation to PMSF treatment (Clausen et al., 2011). YJL144W codes for an uncharacterized protein whose plant homologues appear to counteract protein aggregation during desiccation (Garay-Arroyo et al., 2000). Due to its role in protein quality control (see below) we have named this gene R̲egulator o̲f Quality Control (*ROQ1*).

2.1.5 Validation of the random mutagenesis screen

The identification of Ubr1 agrees with its known function in protein quality control. However, its stress-regulation is less established (Stolz et al., 2013). On the other hand, Ynm3 and Roq1 had not been implicated in protein quality control. Hence, throughout the rest of the PhD thesis the function of *UBR1*, *YNM3* and *ROQ1* was investigated in the context of stress-induced protein quality control.

Individual deletion of *UBR1, YNM3* or *ROQ1* did not show any growth defect on agar plates or in liquid culture (**Figure 7A, B**). However, tunicamycin-induced Rtn1Pho8*-GFP degradation was delayed in *ubr1Δ*, *ynm3Δ* and *roq1Δ* strains (**Figure 7C**). The same degradation phenotype was observed when dithiothreitol (DTT), a reducing agent that prevents disulfide bridge formation in the ER lumen, was used as an ER-stressor (**Figure 7D**). The residual drop in the mutant strains might reflect the transcriptional downregulation of the reporter (see above) and/or the involvement of other redundant pathways or proteins. Importantly, degradation of pre-existing galactose-induced Rtn1Pho8*-GFP was also dependent on *UBR1, YNM3* and *ROQ1*

(**Figure 7E**). To note, *UBR1* deletion presented a stronger phenotype on the stress-induced degradation of Rtn1Pho8*-GFP compared to the deletion of *YNM3* and *ROQ1*. This phenotype suggests that during stress, Ubr1 acts in additional quality control pathways as well. Hence, through the random mutagenesis screen we have uncovered a new quality control pathway that degrades proteins with misfolded cytosolic domains at the ER membranes during stress. We termed this pathway <u>S</u>tress-induced <u>H</u>omeostatically <u>R</u>egulated <u>D</u>egradation (SHRED).
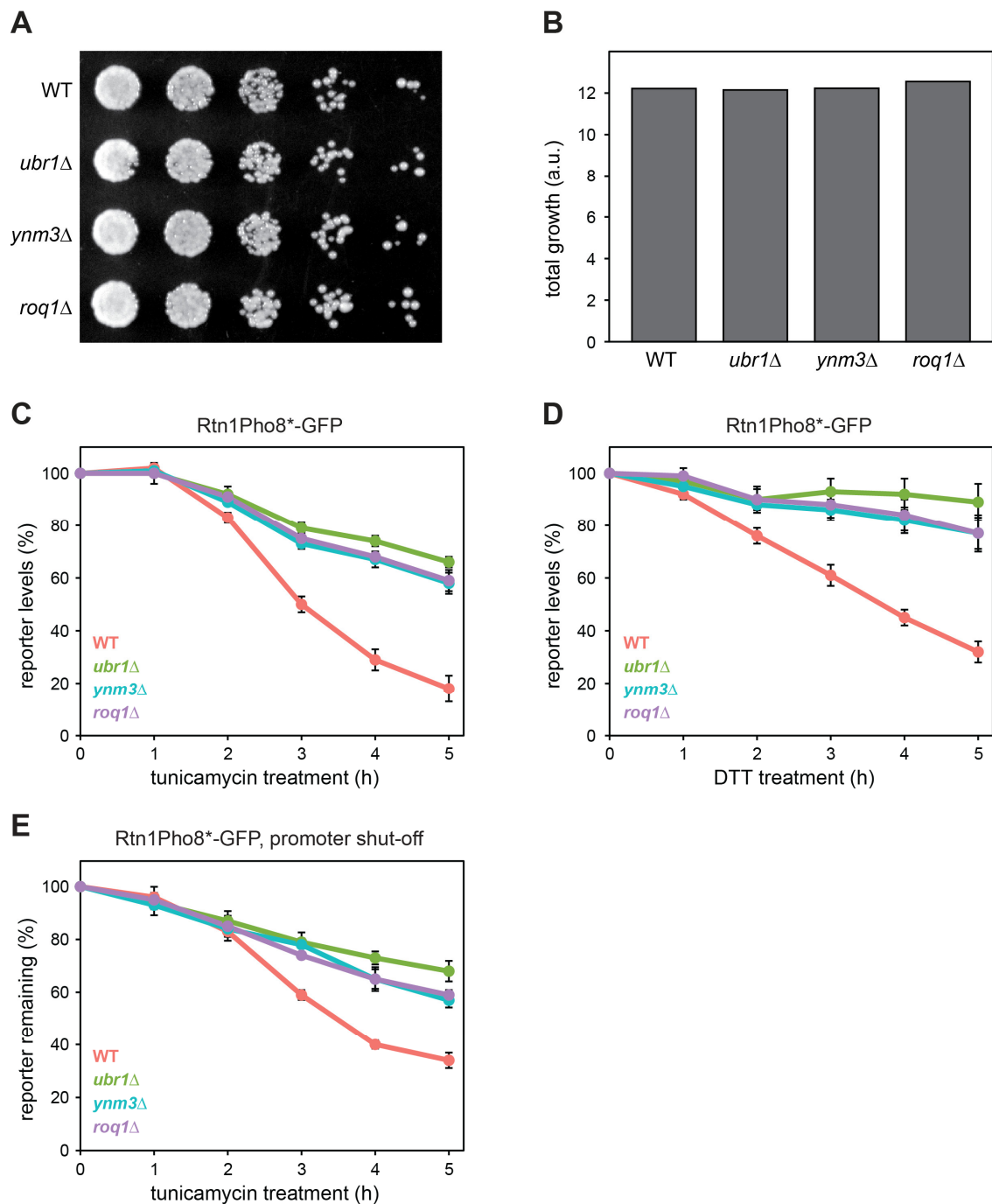
Figure 7. SHRED is required for Rtn1Pho8*-GFP degradation upon ER stress (legend on the following page)

Figure 7. SHRED is required for Rtn1Pho8*-GFP degradation upon ER stress
A) Five-fold dilution steps of wild-type (WT), *ubr1Δ*, *ynm3Δ* and *roq1Δ* cells on YPD agar plates. **B)** Growth of WT, *ubr1Δ*, *ynm3Δ* and *roq1Δ* cells in SC media. Area under a 24-hour growth curve is plotted in arbitrary units. n = 1. **C, D)** Mean GFP fluorescence, measured by flow cytometry, after tunicamycin **(C)** or DTT **(D)** treatment of WT, *ubr1Δ*, *ynm3Δ* and *roq1Δ* cells expressing Rtn1Pho8*-GFP. Mean ± SEM, n = 5. **E)** Total GFP fluorescence, measured by flow cytometry, after promoter shut-off and tunicamycin treatment of WT, *ubr1Δ*, *ynm3Δ* and *roq1Δ* cells expressing *GAL1*-driven Rtn1Pho8*-GFP. Mean ± SEM, n = 5.

2.2 Characterization of SHRED

2.2.1 SHRED is a linear pathway

After confirming the requirement for *UBR1*, *YNM3* and *ROQ1* in SHRED, we tested whether they act in a linear pathway. The deletion of two of these genes in any combination resulted in a similar degradation phenotype as in the single deletion background suggesting that they are epistatic with one another (**Figure 8A, B**). Proteasome inhibition in *ubr1Δ*, *ynm3Δ* or *roq1Δ* background did not show any additional effect indicating that SHRED is the only proteasomal degradation pathway the reporter is subjected to (**Figure 8C**). Furthermore, PMSF treatment in *ynm3Δ* background did not have an additional effect suggesting that the sole serine protease required for SHRED is Ynm3 (**Figure 8D**).
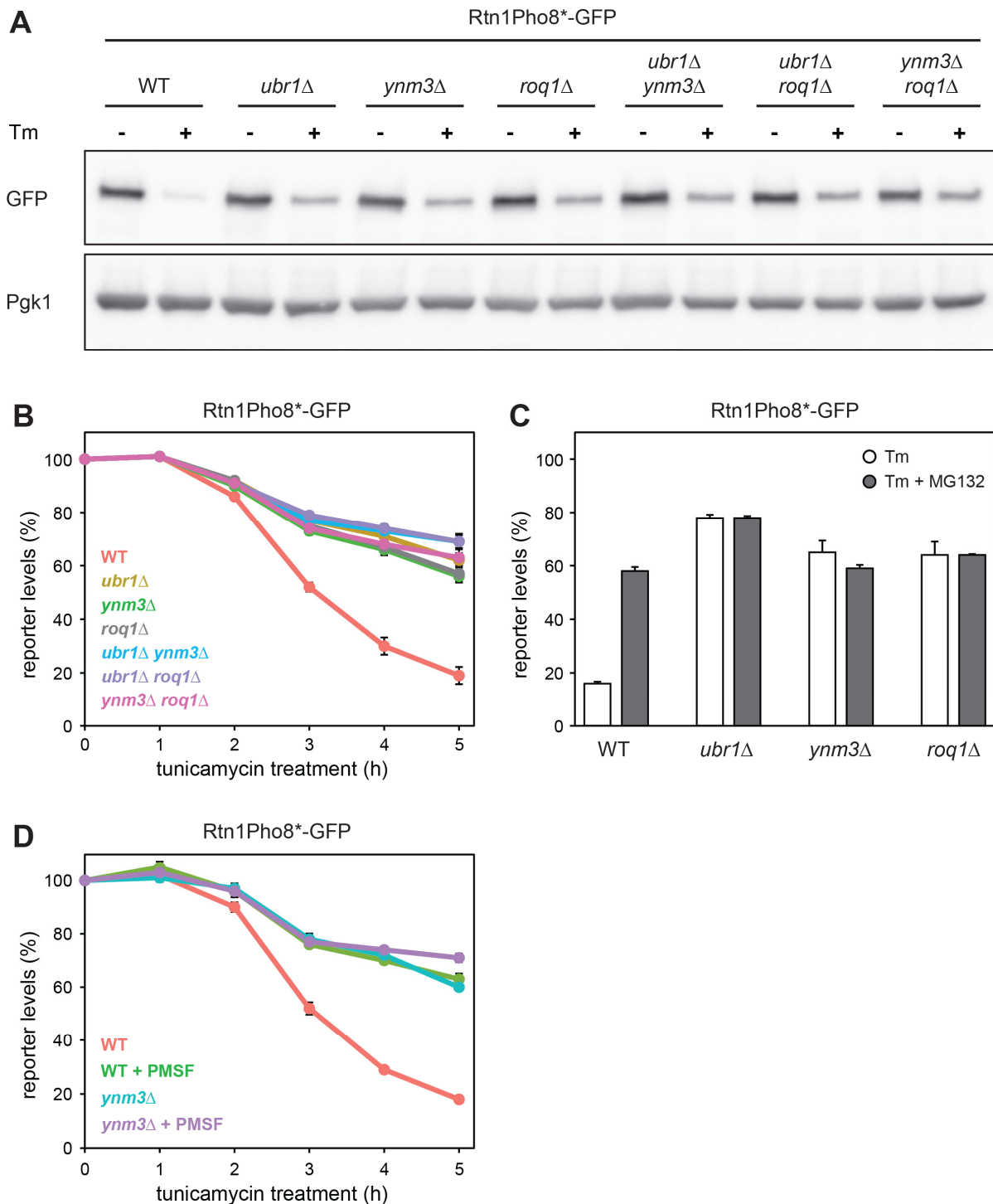
Figure 8. SHRED is a linear pathway
A) Western blot of GFP and Pgk1 from wild-type (WT), *ubr1Δ*, *ynm3Δ*, *roq1Δ*, *ubr1Δ ynm3Δ*, *ubr1Δ roq1Δ* and *ynm3Δ roq1Δ* cells expressing Rtn1Pho8*-GFP after four hours of tunicamycin (Tm) treatment where indicated. Pgk1 served as loading control. **B)** As in **A)** but mean GFP fluorescence of cells, measured by flow cytometry, after tunicamycin treatment. Mean ± SEM, n = 5. **C)** Mean GFP fluorescence, measured by flow cytometry, after tunicamycin or tunicamycin and MG132 treatment of *pdr5Δ* (WT), *pdr5Δ ubr1Δ* (*ubr1Δ*), *pdr5Δ ynm3Δ* (*ynm3Δ*), *pdr5Δ roq1Δ* (*roq1Δ*) cells expressing Rtn1Pho8*-GFP. Mean ± SEM, n = 3. **D)** Mean GFP fluorescence, measured by flow cytometry, after tunicamycin or tunicamycin and PMSF treatment of WT or *ynm3Δ* cells expressing Rtn1Pho8*-GFP. Mean ± SEM, n = 4.

2.2.2 Additional genes required for SHRED

It is known that certain quality control factors act in multiple protein quality pathways (see Introduction) (Prasad et al., 2010; Stolz et al., 2013). Hence, we tested other quality control factors for thier potential role in SHRED. Rad6, the ubiquitin-conjugating E2 enzyme of Ubr1 (Dohmen et al., 1991), was required for the degradation of Rtn1Pho8*-GFP. However, neither the cytosolic ubiquitin E3 ligase Ubr2 (Hochstrasser, 1996; Wang et al., 2004) nor the nuclear E3 ligase San1 (Dasgupta et al., 2004), was required for reporter degradation (**Figure 9A**). The minor effect of *SAN1* deletion on Rtn1Pho8*-GFP degradation is probably indirect since there was no additional effect in the *ubr1Δ san1Δ* strain compared to *ubr1Δ* alone (**Figure 9A**). Since Rtn1Pho8*-GFP is a membrane protein, the AAA-type ATPase Cdc48, a molecular motor implicated in the removal of ERAD substrates from the ER membrane (Ye et al., 2001), was also tested. *CDC48* is an essential gene therefore we employed the temperature sensitive *cdc48-3* mutant allele. Already at semi-permissive temperature (30°C) the tunicamycin induced degradation of galactose-driven Rtn1Pho8*-GFP was impaired in *cdc48-3* cells, indicating that it is involved in the removal of the reporter from the ER membrane (**Figure 9B**).
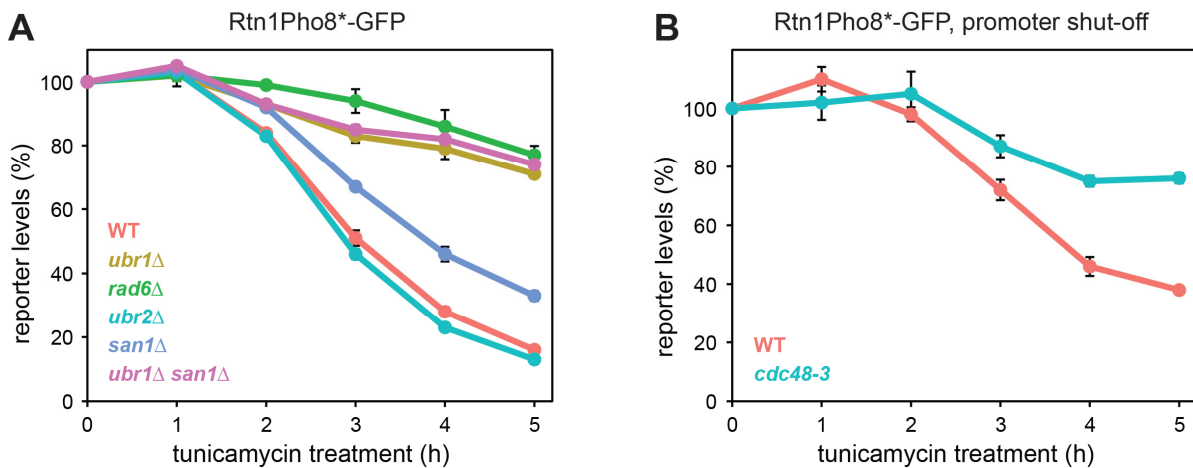
Figure 9. Rad6 and Cdc48 is required for Rtn1Pho8*-GFP degradation
A) Mean GFP fluorescence, measured by flow cytometry, after tunicamycin treatment of wild-type (WT), *ubr1Δ*, *rad6Δ*, *ubr2Δ*, *san1Δ* and *ubr1Δ san1Δ* cells expressing Rtn1Pho8*-GFP. Mean ± SEM, n = 3. **B)** Total GFP fluorescence, measured by flow cytometry, after promoter shut-off and tunicamycin treatment of WT and *cdc48-3* cells expressing *GAL1*-driven Rtn1Pho8*-GFP. Mean ± SEM, n = 3. Experiment performed by Sebastian Schuck.

2.3 Regulation of SHRED

2.3.1 The environmental stress response pathway is the main regulator of SHRED

Thus far it has been elucidated that Ubr1, Ynm3 and Roq1 with the help of Rad6 and Cdc48 act in a linear pathway to degrade the misfolded ER reporter Rtn1Pho8*-GFP by the proteasome during ER-stress. The next major question was how the pathway is regulated. Tunicamycin inhibits glycosylation of luminal ER proteins or ER membrane proteins with luminal domains, however the reporter does not have any domain that is detectable from the luminal side nor is it glycosylated. This suggested that the effect of tunicamycin treatment on reporter degradation is indirect. Therefore, we tested if UPR signalling is required for SHRED. Deletion of UPR sensor *IRE1* or UPR transcription factor *HAC1*, had no effect on the degradation of Rtn1Pho8*-GFP, ruling out UPR as a signalling pathway to regulate SHRED (**Figure 10A**). Persistent ER-stress is known to activate the general or environmental stress response (ESR) (Gasch et al., 2000). ESR initiates a broad remodelling of the proteome including downregulation of general protein synthesis and upregulation of chaperones and quality control factors during a wide variety of stresses (Gasch, 2003). During ideal growth conditions, protein kinase A (PKA), the main regulator of ESR, phosphorylates the transcription factors Msn2/4 and Hsf1, thereby blocking their nuclear entry and thus their regulation of transcription (Görner et al., 1998). To test if ESR regulates SHRED we employed analogue sensitive mutants of the yeast PKA homologues *TPK1/2/3*. The mutations enlarge the ATP binding pocket (Hao and O'Shea, 2012), thus addition of a bulky ATP analogue 1-NMPP-1 outcompetes cellular ATP and pharmacologically inhibits PKA (Bishop et al., 2000). Activation of ESR in *tpk1/2/3* cells via 1-NMPP-1 treatment led to the degradation of Rtn1Pho8*-GFP, which was dependent on SHRED (**Figure 10B**). Hence, SHRED and as a consequence RtnPho8*-GFP degradation can be induced in the absence of any ER stressor via pharmacological inhibition of PKA.
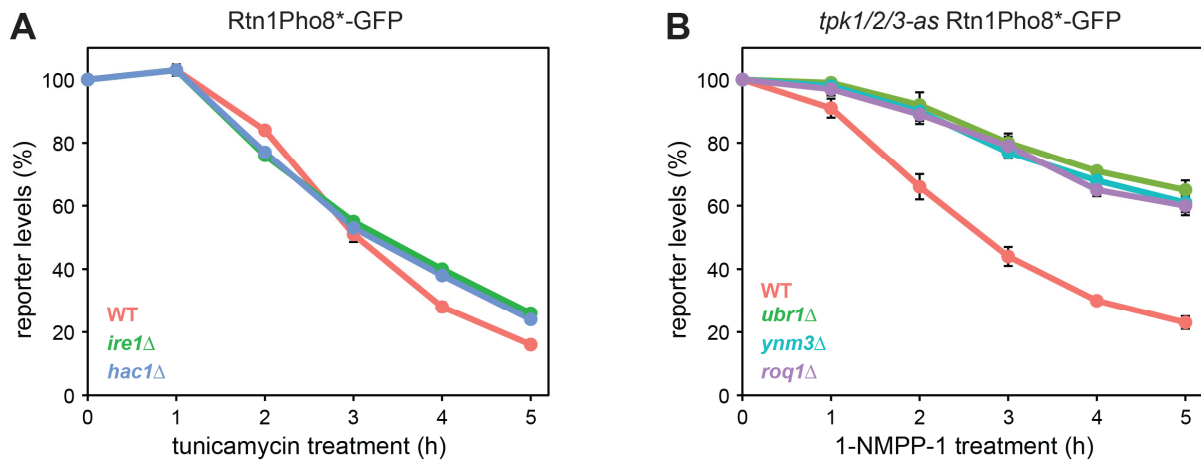
Figure 10. The environmental stress response pathway regulates SHRED
A) Mean GFP fluorescence, measured by flow cytometry, after tunicamycin treatment of wild-type (WT), *ire1Δ* and *hac1Δ* cells expressing Rtn1Pho8*-GFP. Mean ± SEM, n = 3. **B)** Mean GFP fluorescence, measured by flow cytometry, after 1-NMPP-1 treatment of *tpk1/2/3-as* (WT), *tpk1/2/3-as ubr1Δ* (*ubr1Δ*), tpk1/2/3-as *ynm3Δ* (*ynm3Δ*) and *tpk1/2/3-as roq1Δ* (*roq1Δ*) cells expressing Rtn1Pho8*-GFP. Mean ± SEM, n = 3. Experiment performed by Sebastian Schuck.

Since ESR is activated by many stressors (Gasch, 2003) we tested which other conditions could initiate degradation of Rtn1Pho8*-GFP. Treatment with rapamycin, an inhibitor of the main regulator of cell growth *TOR1* (Loewith and Hall, 2011), also led to SHRED-dependent Rtn1Pho8*-GFP degradation (**Figure 11A**). Furthermore, Rtn1Pho8*-GFP was degraded in a SHRED-dependent manner when cells were grown for 24 hours in liquid culture so that they enter post-diauxic phase (**Figure 11B**). Thus, starvation conditions induced by rapamycin treatment or growth into post-diauxic phase, also initiate Rtn1Pho8*-GFP degradation. Hence, ESR emerged as the main regulator of SHRED raising the question which SHRED gene could be the main transcriptional target during stress.

A

Rtn1Pho8*-GFP, rapamycin treatment

B

logarithmic phase
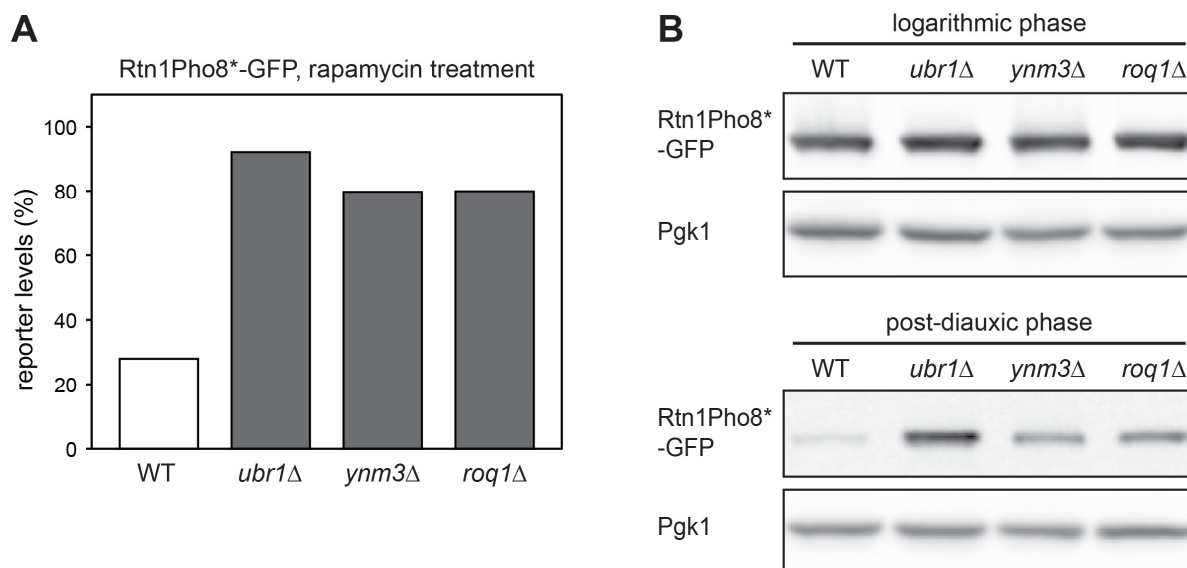
post-diauxic phase

Figure 11. Growth into post-diauxic phase initiates Rtn1Pho8*-GFP degradation
A) Mean GFP fluorescence, measured by flow cytometry, after rapamycin treatment of wild-type (WT), *ubr1Δ*, *ynm3Δ* and *roq1Δ* cells expressing Rtn1Pho8*-GFP. n = 1. **B)** Western blot of GFP and Pgk1 from WT, *ubr1Δ*, *ynm3Δ* and *roq1Δ* cells expressing Rtn1Pho8*-GFP in mid-log phase and in post-diauxic phase. Pgk1 served as loading control.

2.3.2 Regulation of *ROQ1* expression is the initial step in SHRED

The mRNA or protein levels of *UBR1* or *YNM3* do not increase during ER-stress (Pincus et al., 2014; Travers et al., 2000). However, *ROQ1* expression is upregulated during a wide variety of stresses (Gasch et al., 2000). Indeed, qPCR data obtained by Rolf Schmidt showed that mRNA levels of *ROQ1* increased at least 10-fold after tunicamycin treatment or during activation of ESR via 1-NMPP-1 treatment (**Figure 12A**). This result suggests that the initial step in SHRED is the transcriptional upregulation of *ROQ1*. If so, then overexpression of *ROQ1* alone should be able to initiate SHRED. To test this idea an inducible expression system was employed (Pincus et al., 2014). Briefly, the endogenous promoter of *ROQ1* was replaced by a *GAL1* promoter. Additionally, an artificial transcription factor containing the Gal4 DNA binding domain, the Msn2 trans-activating domain and an estrogen receptor domain (abbreviated as GEM), was co-expressed in cells harbouring Rtn1Pho8*-GFP. Addition of β-estradiol induces a conformational change in GEM that enables its binding to and activation of *GAL1*-driven genes (**Figure 12B**). Overexpression of *ROQ1* via the GEM system initiated Rtn1Pho8*-GFP degradation which was strictly dependent on *UBR1* and *YNM3* (**Figure 12C**). Importantly, overproduction of *ROQ1* did not affect the levels of the Rtn1-GFP control (**Figure 12D**) and did not cause any growth defect ruling out that overexpression of *ROQ1* may cause stress that indirectly

upregulates SHRED (**Figure 12E**). Thus, *ROQ1* overexpression alone initiated SHRED-dependent Rtn1Pho8*-GFP degradation. It is noteworthy that *ROQ1* overexpression induced a slower degradation phenotype compared to the tunicamycin-induced reporter degradation. Potentially tunicamycin treatment initiates other secondary effects, besides upregulating *ROQ1* expression, that speed up the degradation of the reporter (see Discussion).
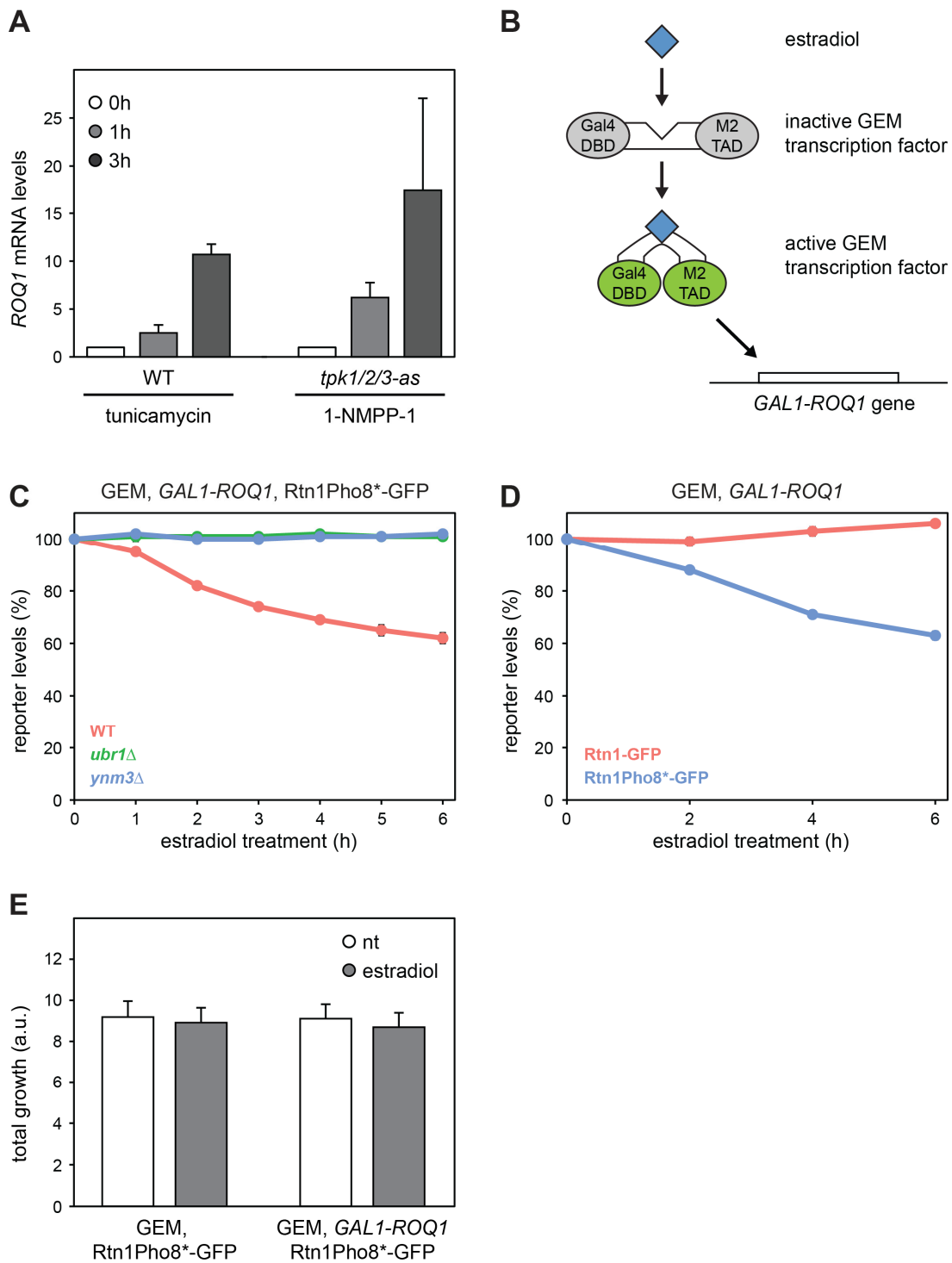
Figure 12. *ROQ1* overexpression initiates SHRED (legend on the following page)

Figure 12. *ROQ1* overexpression initiates SHRED
A) Normalized *ROQ1* mRNA levels, determined by qPCR, after tunicamycin or 1-NMPP-1 treatment of wild-type (WT) and *tpk1/2/3-as* cells. Values were normalized to the mRNA levels of the *TEF10* housekeeping gene. Mean ± SEM, n = 3. Experiment performed by Rolf Schmidt. **B)** Schematic illustration of the GEM expression system (Pincus et al., 2014). **C)** Mean GFP fluorescence, measured by flow cytometry, after estradiol treatment of WT, *ubr1Δ* and *ynm3Δ* cells expressing Rtn1Pho8*-GFP, the GEM transcription factor and *GAL1*-driven endogenous *ROQ1*. Mean ± SEM, n = 3. **D)** Mean GFP fluorescence, measured by flow cytometry, after estradiol treatment of WT cells expressing Rtn1-GFP or Rtn1Pho8*-GFP, the GEM transcription factor and *GAL1*-driven endogenous *ROQ1*. Mean ± SEM, n = 4. Experiments in **(C)** and **(D)** were performed by Sebastian Schuck. **E)** Growth of WT cells expressing Rtn1Pho8*-GFP, the GEM transcription factor and Roq1 from the endogenous *ROQ1* promoter or the *GAL1* promoter, in SC media after estradiol treatment. Area under a 20-hour growth curve is plotted in arbitrary units. Mean ± SEM, n = 3. Experiment performed by Peter Bircham.

2.4 Mechanism of SHRED

2.4.1 Ynm3 cleaves Roq1

After elucidating the initial step in SHRED, the role of *YNM3* was investigated. The catalytically inactive Ynm3(S236A) (Padmanabhan et al., 2009) could not support the stress-induced degradation of Rtn1Pho8*-GFP (**Figure 13A**), indicating that cleavage of a substrate protein by Ynm3 is required for SHRED. Surprisingly, functional Ynm3-GFP localized to the nucleus (**Figure 13B,** Belanger et al., 2009) and ER-stress did not initiate its relocalization to the cytosol (data not shown). Thus, it is unlikely that Ynm3 directly cleaves Rtn1Pho8*-GFP, which is localized at the peripheral ER. Instead, the relevant substrate might localize or has access to the nucleus. Roq1 is a soluble protein with a molecular weight of 12 kDa, which enables its passive diffusion through the nuclear pore complex. This encouraged us to test Roq1 as the proteolytic substrate of Ynm3. The endogenous Roq1 protein displays a very low abundance (Ghaemmaghami et al., 2003), therefore the C-terminally HA-tagged Roq1 was expressed from a strong GPD promoter. In wild-type cells, Roq1-HA appeared as a 15 kDa protein (**Figure 13C**). Intriguingly, addition of proteasome inhibitor led to the detection of a second approximately 2 kDa smaller double band (**Figure 13C arrows**). Whether this double band represents post-translational modification has yet to be determined. Importantly, the smaller molecular weight band was absent in *ynm3Δ* cells indicating that it is a Ynm3-dependent cleavage fragment (**Figure 13C**). The cleavage fragment was only detectable after proteasome inhibition suggesting rapid turnover by the proteasome and low cleavage efficiency. It has been shown that the mammalian Ynm3 homologue Htra2 binds its substrates at the C-terminus (Walsh et al., 2003). Hence, the C-terminal HA-tag on Roq1 might interfere with the binding and cleavage

by Ynm3. Therefore, a Roq1 construct was generated with an internal HA-tag after the 74th amino acid, termed Roq1-HA(74). This position was chosen because it is in a region of Roq1 that is particularly poorly conserved among yeast homologues. Both C-terminally and internally HA-tagged Roq1 constructs were functional in Rtn1Pho8*-GFP degradation (**Figure 13D**). Importantly, the Ynm3-dependent Roq1-HA(74) cleavage fragment was already detectable in the absence of proteasome inhibition (**Figure 13E arrows**).
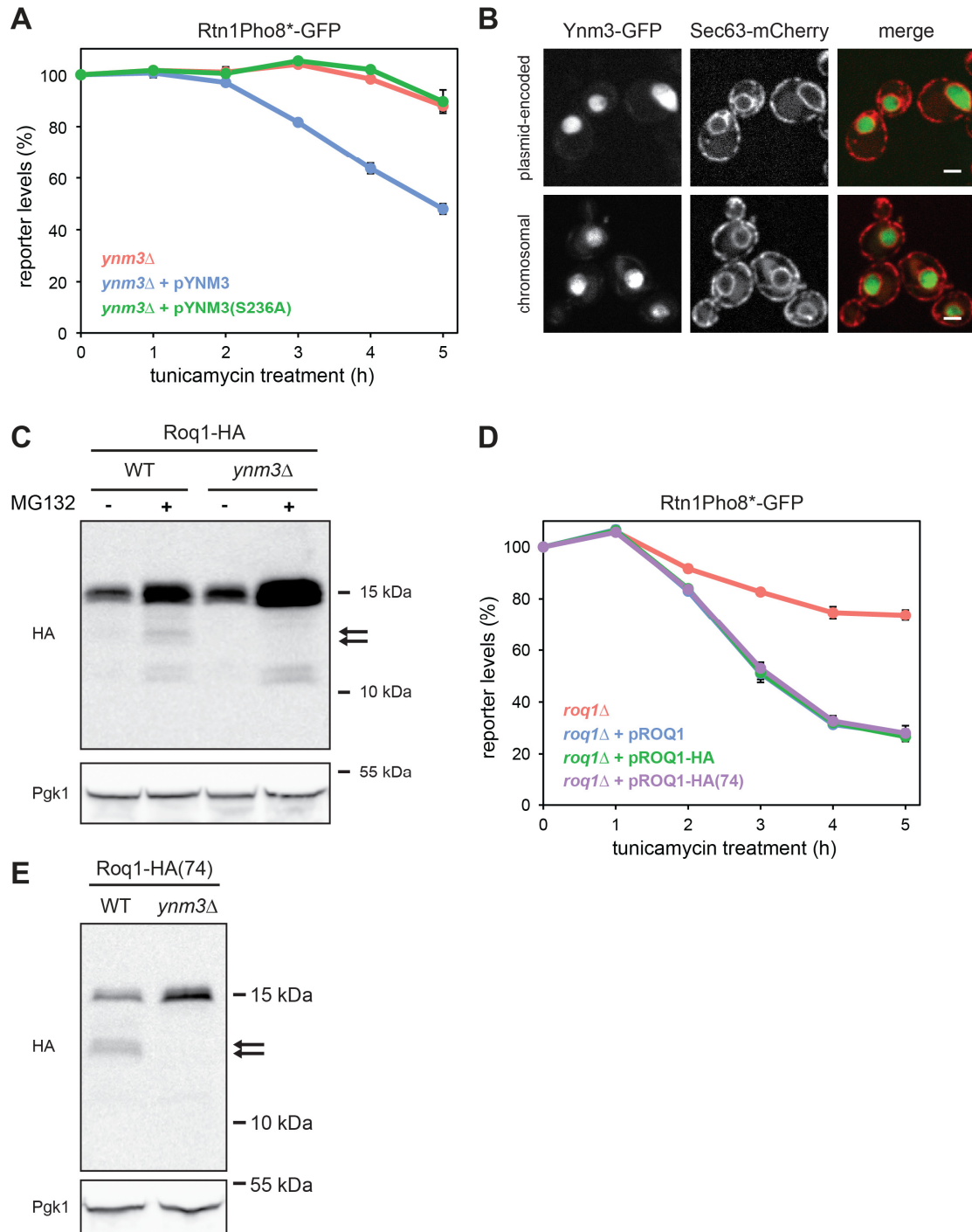
Figure 13. Ynm3 cleaves Roq1 (legend on the following page)

Figure 13. Ynm3 cleaves Roq1
A) Mean GFP fluorescence, measured by flow cytometry, after tunicamycin treatment of *ynm3Δ* cells expressing Rtn1Pho8*-GFP. The cells additionally contained an empty plasmid or different versions of Ynm3 expressed from a plasmid. Mean ± SEM, n = 3. **B)** Fluorescent microscopy images of wild-type cells expressing endogenously tagged Sec63-mCherry and plasmid-encoded (upper panel) or chromosomally GFP-tagged Ynm3 (lower panel). Scale bar: 2 µm. **C)** Western blot of HA and Pgk1 from *pdr5Δ* (wild-type, WT) or *pdr5Δ ynm3Δ* (*ynm3Δ*) cells expressing *GPD*-driven Roq1-HA after MG132 treatment where indicated. The double arrow indicates Roq1 cleavage fragments. Pgk1 served as loading control. **D)** Mean GFP fluorescence, measured by flow cytometry, after tunicamycin treatment of *roq1Δ* cells expressing Rtn1Pho8*-GFP. The cells additionally contained an empty plasmid or different versions of Ynm3 expressed from a plasmid. Mean ± SEM, n = 3. **E)** Western blot of HA and Pgk1 from WT or *ynm3Δ* cells expressing *GPD*-driven Roq1-HA(74). The double arrow indicates Roq1 cleavage fragments. Pgk1 served as loading control.

2.4.2 Cleaved Roq1 with a N-terminal arginine residue is required for SHRED

The detection of the C-terminally HA-tagged Roq1 cleavage fragment indicates the cleavage to be located close to the N-terminus. Using the protein ladder as a reference for molecular weight we predicted the cleavage to occur approximately 20 amino acids (2 kDa) downstream from the N-terminus. To identify the cleavage site, a series of N-terminal truncations were generated where the first 18 to 23 amino acids of Roq1 were removed. The small molecular size of these constructs allowed the comparison of their migration behaviour with the migration of the native Roq1 cleavage fragment on a Tris-Tricine SDS-PAGE gel. To enable translation of the N-terminal truncation constructs, a ubiquitin moiety was fused directly N-terminus, yielding the constructs Ub-Roq1Δ18-HA(74) to Ub-Roq1Δ23-HA(74). After translation ubiquitin is efficiently removed by cellular deubiquitinases, releasing the N-terminally truncated Roq1 constructs (Bachmair et al., 1986). Similar to the native cleavage fragment, the truncated constructs appeared as double bands. Roq1Δ21 showed the most similar migration pattern to the native cleaved Roq1 indicating that Ynm3 cleaves Roq1 after leucine-21 (**Figure 14A**).

If the sole function of Ynm3 in SHRED is to cleave and activate Roq1, then overexpression of cleavage-mimicking Roq1Δ21 fragment should bypass the requirement for Ynm3. Indeed, expression of Roq1Δ21 in *ynm3Δ roq1Δ* cells restored the stress-induced degradation of Rtn1Pho8*-GFP (**Figure 14B, dashed box**). In contrast, expression of Roq1Δ20 or Roq1Δ22, the two closest fragments regarding their electrophoretic mobility, could not bypass the requirement for Ynm3 (**Figure 14B**). Surprisingly, expression of Roq1Δ23 also restored the degradation of Rtn1Pho8*-GFP, despite its clearly distinctive migration behaviour on the Tris-Tricine gel (**Figure 14A**). Therefore, we extended the truncations from Roq1Δ7 through Roq1Δ25. Interestingly,

all truncated constructs that harboured a positively charged N-terminal residue (lysine or arginine) or amino acids that can be turned into these amino acids via deamidylation and arginylation (asparagine, aspartic acid, glutamine, glutamic acid) (Baker and Varshavsky, 1995; Balzi et al., 1990) were capable of bypassing the requirement for Ynm3 (**Figure 14B**). To confirm the requirement for a positively charged residue on the N-terminus of cleaved Roq1, we mutated arginine-22 in the Roq1Δ21 construct. Mutating it to a neutral alanine or leucine residue abolished its function while mutating it to a positively charged lysine residue maintained its function in Rtn1Pho8*-GFP degradation (**Figure 14C**). Thus, a positively charged residue on the Roq1 cleavage fragment is required for SHRED.

In order to confirm that Roq1 is cleaved after leucine-21 mutations were introduced at this position in full-length Roq1-HA(74). The mammalian Ynm3 homologue HtrA2/Omi preferentially cleaves after leucine, isoleucine or valine residue (Vande Walle et al., 2007). In agreement with the latter finding mutating leucine-21 to a structurally similar valine residue had no effect on cleavage while the introduction of a proline mutation abolished cleavage (**Figure 14D**). Accordingly, full-length Roq1(L21P) could not restore Rtn1Pho8*-GFP degradation in *roq1Δ* cells while Roq1(L21V) was still functional (**Figure 14E**). Thus, Ynm3 cleaves Roq1 after leucine-21 and uncovers a positively charged arginine residue on the new N-terminus that is required for SHRED.
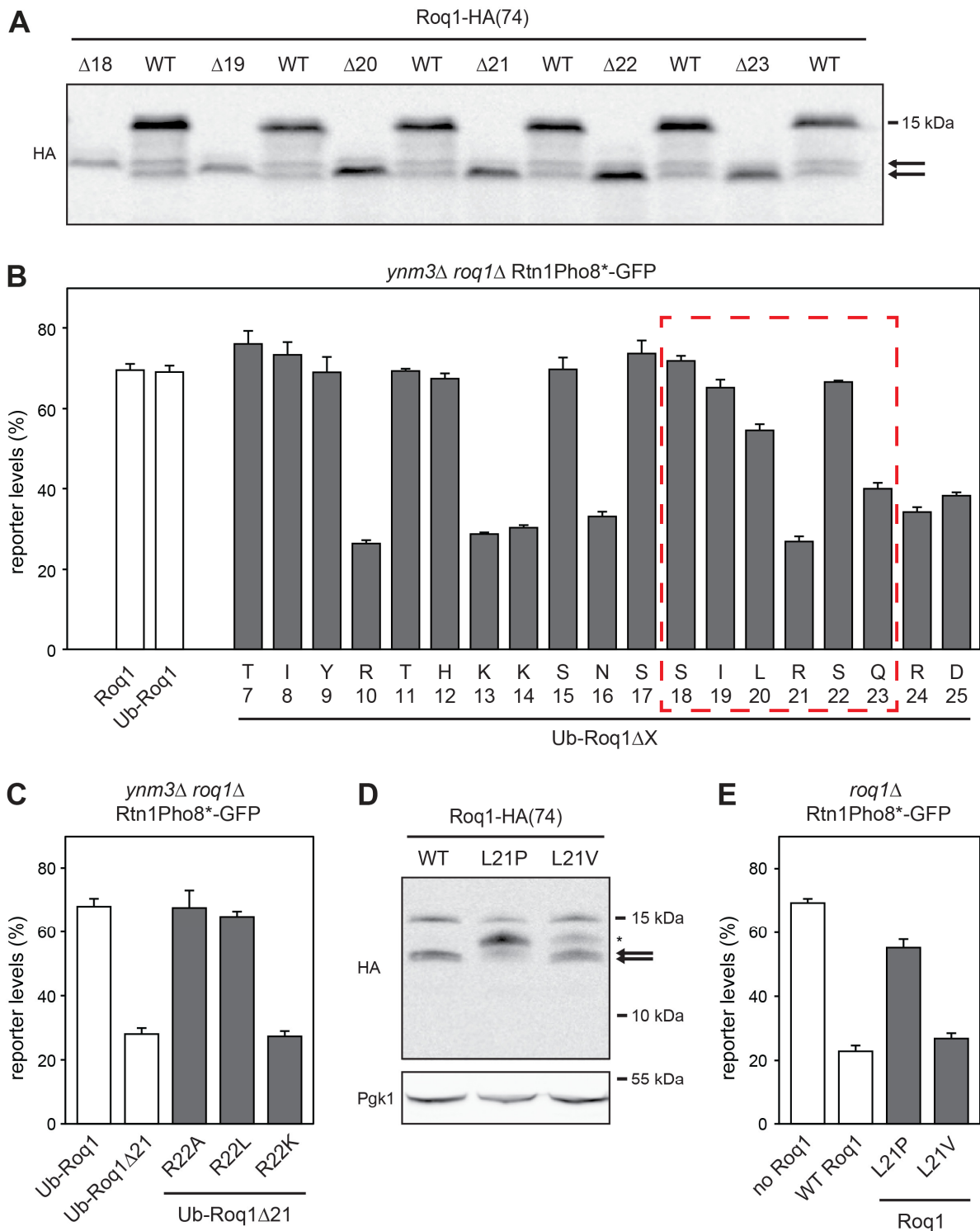
Figure 14. Roq1 is cleaved after leucine-21
A) Western blot of HA from *roq1Δ* cells expressing full-length Roq1 (WT, wild-type) or *ynm3Δ roq1Δ* cells expressing N-terminally truncated Roq1 variants lacking the indicated number of N-terminal residues. The double arrow indicates Roq1 cleavage fragments. **B)** Mean GFP fluorescence, measured by flow cytometry, after five hours of tunicamycin treatment of *ynm3Δ roq1Δ* cells expressing Rtn1Pho8*-GFP and full-length or N-terminally truncated Roq1 variants lacking the indicated number of N-terminal residues. The letters above the numbers indicate the N-terminal residue in the Roq1 cleavage fragment. The red dashed box marks the Roq1 variants used in **(A)**. Mean ± SEM, n = 3. **C)** Mean GFP fluorescence, measured by flow cytometry, after five hours of tunicamycin treatment of *ynm3Δ roq1Δ* cells expressing Rtn1Pho8*-GFP and full-length or N-terminally truncated and mutated versions of Roq1. Mean ± SEM, n = 3. **D)** Western blot of HA and

Pgk1 from *roq1Δ* cells expressing *GPD*-driven wild-type (WT) or point mutant full-length Roq1-HA(74). The double arrow indicates Roq1 cleavage fragments. The asterisk denotes an alternative cleavage product. Pgk1 served as loading control. **E)** Mean GFP fluorescence, measured by flow cytometry, after five hours of tunicamycin treatment of *roq1Δ* cells expressing Rtn1Pho8*-GFP and full-length WT or mutated versions of Roq1 from a plasmid. Mean ± SEM, n = 3.
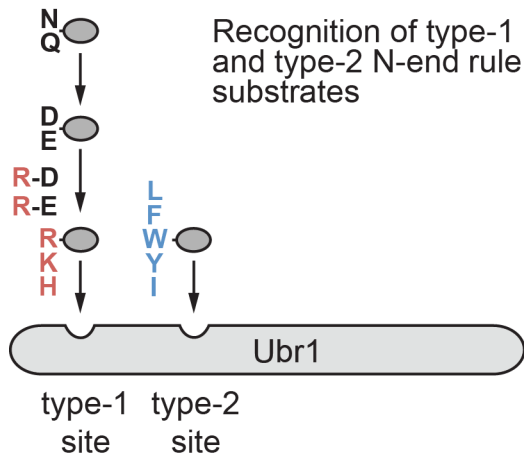
Figure 15. The N-end rule pathway
Schematic illustration of N-end rule substrate recognition by Ubr1.

2.4.3 Roq1 binds to and activates Ubr1 through the type-1 site

Next, we investigated the role of a positively charged N-terminal residue in cleaved Roq1. N-terminal arginines and lysines are type-1 Ubr1 substrates according to the N-end rule that determines the half-life of a protein based on its N-terminal residue (Tasaki et al., 2012; Varshavsky, 2011). Ubr1 harbours two mapped N-end rule substrate-binding sites: the type-1 site binds to positively charged residues while the type-2 site recognizes bulky hydrophobic residues (**Figure 15**) (Xia et al., 2008). To test if any of these sites are required for Rtn1Pho8*-GFP degradation we created site mutant Ubr1 constructs.

While, the type-2 site can be independently mutated, mutation in the type-1 site is known to affect the type-2 site as well (Tasaki et al., 2009; Xia et al., 2008). Thus, we first tested the functionality of the created Ubr1 site mutants. For this purpose, we employed the tandem fluorescent timer (tFT) tagged N-end rule reporter constructs developed in the Knop lab (Khmelinskii et al., 2012). The system is based on the fusion of a fast folding superfolder GFP (sfGFP) and a slower maturing mCherry (Pédelacq et al., 2006; Shaner et al., 2004). Therefore, the mCherry over sfGFP fluorescence intensity ratio indicates the average age of the tFT-tagged protein of interest (Khmelinskii et al., 2012). The N-end rule reporter constructs contained N-terminal ubiquitin fusions of all 20 proteinogenic amino acids with a tFT-tag, termed Ub-X-tFT (X stands for any proteinogenic residue). As expected, constructs with type-1 N-terminal residues (E, K, Q, R, D, N) showed the lowest mCherry over sfGFP ratio indicating a short half-life (**Figure 16A, red bars**). On the other hand, constructs with neutral N-terminal amino acids (T, V, A, G, S, M, C) displayed higher fluorescent ratio, indicating longer half-life (**Figure 16A, grey bars**). The type-2 constructs presented somewhat longer half-lives than the type-1 constructs (**Figure 16A, blue bars**).

In order to test the functionality of different Ubr1 site mutants Ub-R-tFT was selected as a type-1 and Ub-F-tFT as a type-2 model substrate. The stable non-N-end rule substrate Ub-M-tFT served as negative control. These selected N-end rule substrates were expressed in *ubr1Δ* cells in which different versions of Ubr1 were expressed from a plasmid. Expression of wild-type Ubr1 reduced the mCherry/sfGFP ratio in both the Ub-R-tFT and the Ub-F-tFT constructs indicating that they are turned over in a Ubr1-dependent manner (**Figure 16B**). Since Ub-M-tFT is a stable construct (**Figure 16A**) expression of wild-type Ubr1 had no effect on its mCherry/sfGFP ratio (**Figure 16B**). As expected, the type-2 site mutant Ubr1(D318N) was unable to degrade Ub-F-tFT but could still process Ub-R-tFT. On the other hand, the type-1 mutant Ubr1(G173R) was unable to degrade Ub-R-tFT but retained partial activity towards Ub-F-tFT (**Figure 16B**). Thus, in our hands the type-2 site could be mutated independently while mutation to the type-1 site had an effect on type-2 substrates as well.

Using these Ubr1 site mutants, we tested which Ubr1 substrate-binding site is required for Rtn1Pho8*-GFP degradation. The type-2 mutant Ubr1(D318N) could restore degradation of Rtn1Pho8*-GFP in *ubr1Δ* cells comparably to wild-type Ubr1 while type-1 mutant Ubr1(G173R) could not (**Figure 16C**). Hence, the Ubr1 type-1 substrate-binding site is required for SHRED.
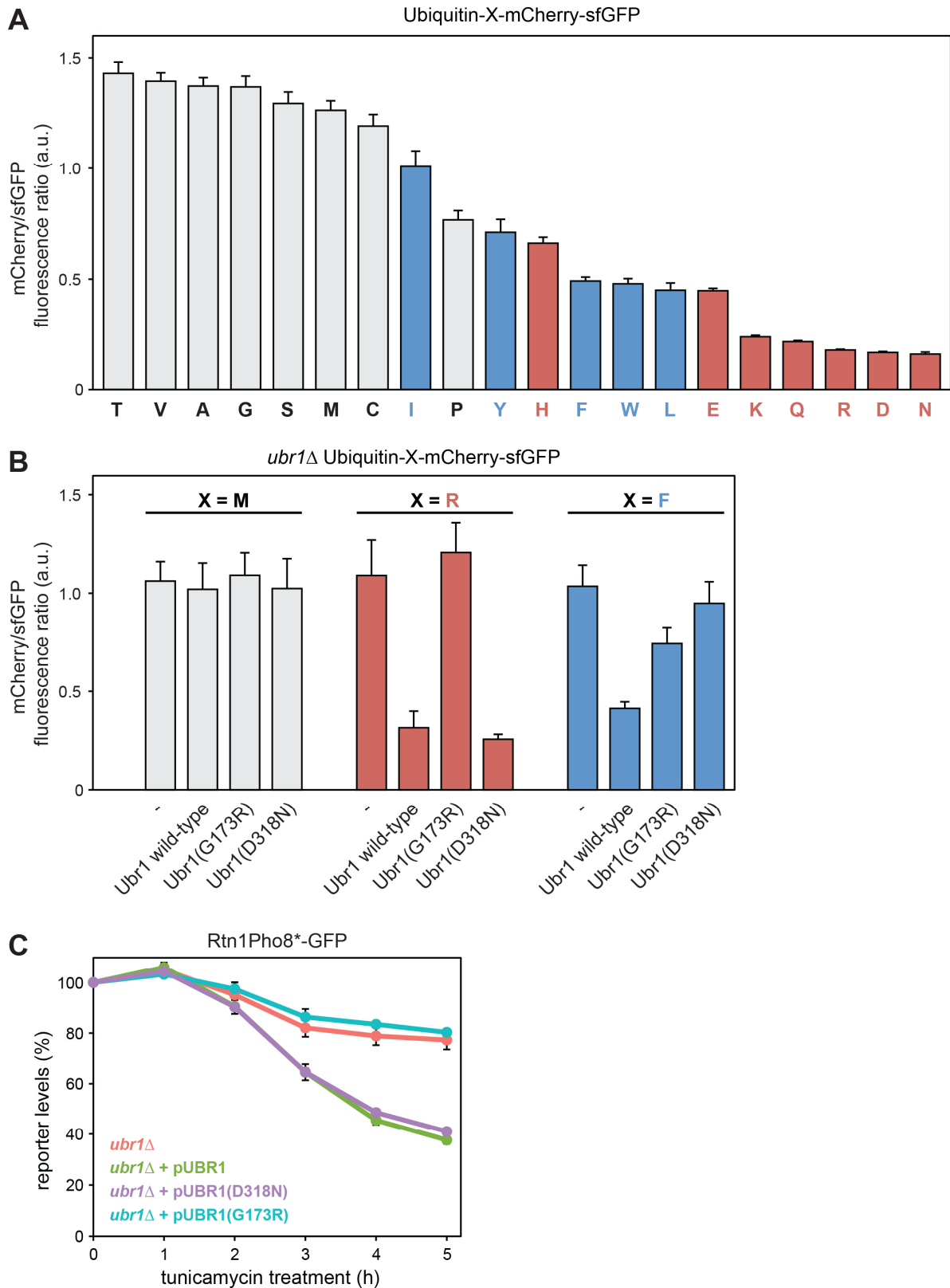
Figure 16. The type-1 substrate-binding site of Ubr1 is required for Rtn1Pho8*-GFP degradation

A) mCherry over sfGFP fluorescence intensity ratio, measured by flow cytometry, from wild-type cells expressing Ubiquitin-X-mCherry-sfGFP (X stands for any proteinogenic amino acid). The letters below each bar indicates the N-terminal residue in the X position after the removal of ubiquitin. Grey bars indicate neutral amino acids, while red and blue bars indicate type-1 or type-2 amino acids, respectively. **B)** mCherry over sfGFP fluorescent intensity ratio, measured by flow cytometry, from

ubr1Δ cells expressing M, R or F-mCherry-sfGFP. The cells additionally contained an empty plasmid or different versions of Ubr1 expressed from a plasmid. **C)** Mean GFP fluorescence, measured by flow cytometry, after tunicamycin treatment of *ubr1Δ* cells expressing Rtn1Pho8*-GFP. The cells additionally contained the plasmids used in **(B)**.

It is unlikely that Rtn1Pho8*-GFP is directly recognised by Ubr1 through the type-1 site, since it does not harbour a type-1 destabilizing residue on the N-terminus (starts with a methionine-serine). Moreover, the stability of Rtn1-GFP, but not of Rtn1Pho8*-GFP, during ER-stress (**Figure 4B**) implies the degron to be localized in the internal Pho8* domain. Besides binding to N-end rule substrates Ubr1 also binds at least one additional substrate through a third internal binding site that is unmapped (Du et al., 2002). Normally an auto-inhibitory domain of Ubr1 blocks the third binding site. However, simultaneous occupancy of the type-1 and type-2 site relieves the inhibition and allows the binding to and degradation of target proteins through the third site (Du et al., 2002). The C-terminal Roq1 cleavage fragment harbours a type-1 arginine N-end rule residue. We therefore hypothesized that the positively charged N-terminus of cleaved Roq1 interacts with and regulates Ubr1 through the type-1 site to promote recognition of misfolded proteins.

In order to test this hypothesis, we performed co-immunoprecipitation experiments between chromosomally integrated Roq1Δ21 variants and plasmid-borne Ubr1 constructs. Immunoprecipitated Roq1Δ21-HA(74) interacted with FLAG-Ubr1 dependent on the N-terminal arginine of cleaved Roq1 (**Figure 17A**). Importantly type-1 site mutant Ubr1(G173R) could not interact with Roq1Δ21-HA(74) (**Figure 17A**), indicating that cleaved Roq1 binds to the Ubr1 type-1 site through its N-terminal arginine.

This model suggests that the Roq1 cleavage fragment would compete with type-1 N-end rule substrates for the type-1 binding site. To test this, we made use of the tFT-tagged N-end rule substrates. Overexpression of full-length Roq1 led to the stabilization of type-1 and destabilization of type-2 substrates, which was strictly dependent on *YNM3* and *UBR1* (**Figure 17B**). This result shows that cleaved Roq1 outcompetes the type-1 substrates at the type-1 binding site. Accordingly, Roq1 overexpression decreased the amount of R-tFT bound to Ubr1 determined by co-immunoprecipitation (**Figure 17C**). Moreover, Roq1 binding enhanced degradation of type-2 substrates suggesting that the binding activates Ubr1 to degrade substrate proteins more efficiently (**Figure 17B**). Accelerated degradation of type-2 substrates

upon occupancy of the type-1 site agrees with the previous findings (Baker and Varshavsky, 1991). Thus, cleaved Roq1 binds to Ubr1 through the type-1 site and changes its substrate specificity leading to decreased degradation of type-1 substrates and enhanced degradation of type-2 substrates and Rtn1Pho8*-GFP.

A

B

GEM, *GAL1-ROQ1* Ubiquitin-X-mCherry-sfGFP

C
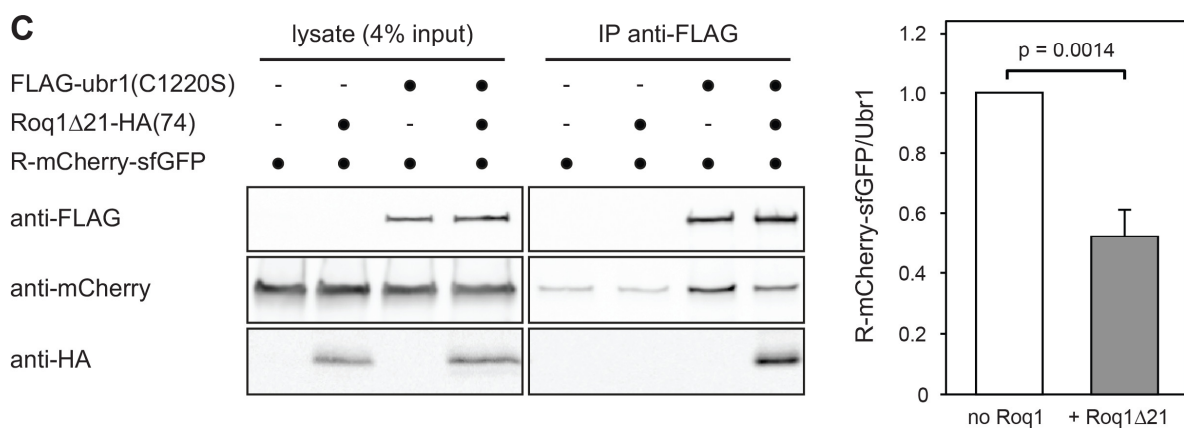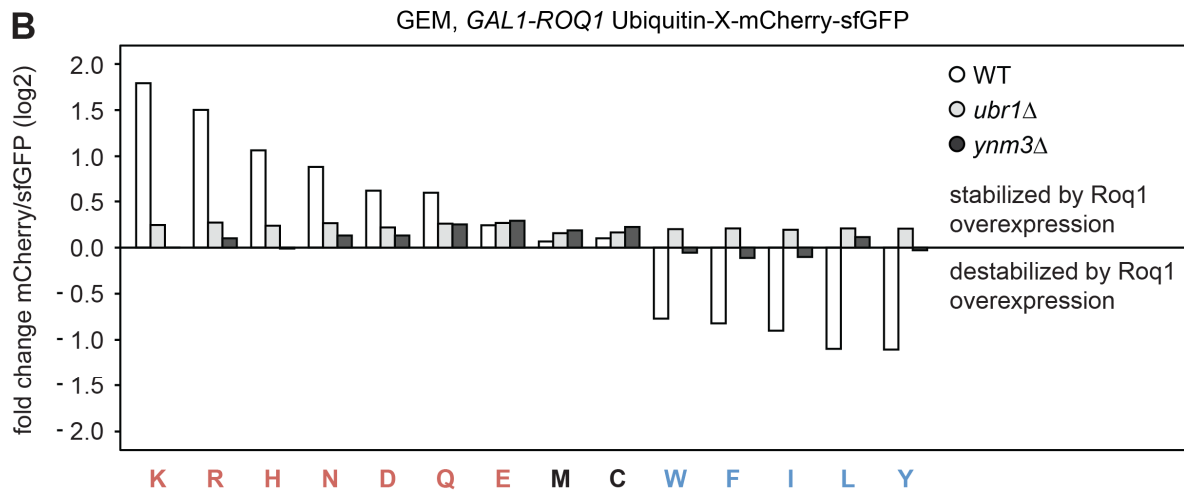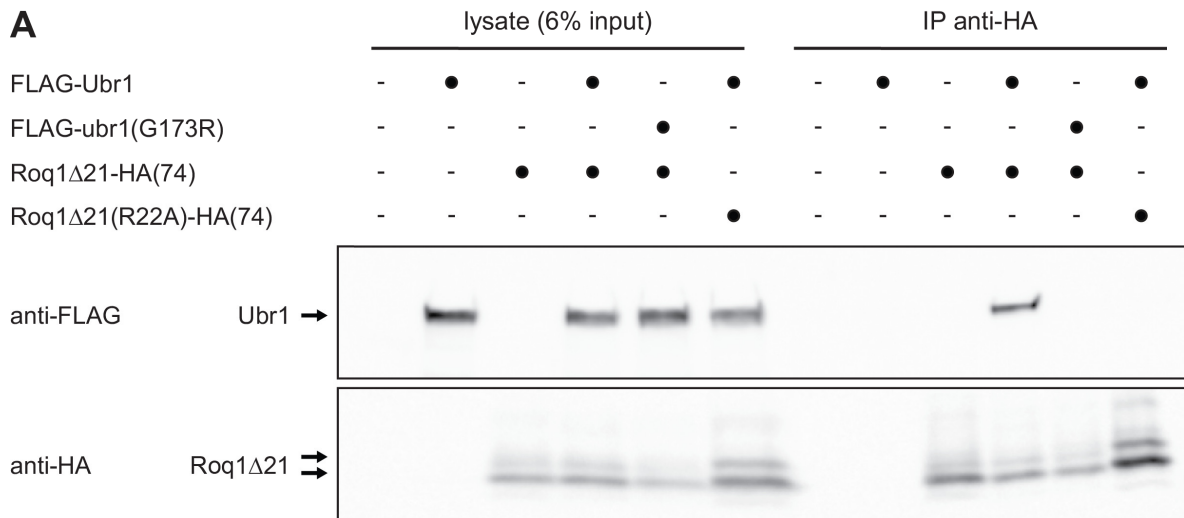
Figure 17. Cleaved Roq1 binds to and activates Ubr1 (legend on the following page)

Figure 17. Cleaved Roq1 binds to and activates Ubr1
A) Western blot of FLAG and HA from cell lysates or anti-HA immunoprecipitates from *roq1Δ ubr1Δ* cells. The cells additionally expressed wild-type or R22A mutant Roq1Δ21-HA(74) from the chromosome and wild-type FLAG-Ubr1 or type-1 site mutant FLAG-ubr1(G173R) from a plasmid where indicated. **B)** mCherry over sfGFP fluorescence, measured by flow cytometry, from wild-type (WT), *ynm3Δ* and *ubr1Δ* cells expressing Ubiquitin-X-mCherry-sfGFP (X stands for any proteinogenic amino acid). The cells additionally expressed the GEM transcription factor and *GAL1*-driven chromosomal Roq1. Plotted on a $\log_2$ scale is the fold change of mCherry/sfGFP fluorescence intensity upon 6 hours of estradiol treatment. The letters below each bar indicate the N-terminal residue in position X after the removal of ubiquitin. Values above 0 indicate stabilization and longer half-life, while values below zero correspond to de-stabilization and shorter-half-life. Mean, n = 2. **C)** Western blot and quantification of FLAG, mCherry and HA from cell lysates or anti-FLAG immunoprecipitates from *roq1Δ ubr1Δ* cells. The cells additionally expressed Roq1Δ21-HA(74) and Ub-R-mCherry-sfGFP from the chromosome and RING mutant FLAG-ubr1(C1220S) from a plasmid where indicated. This Ubr1 mutation was used to stabilize the interaction between Ubr1 and R-mCherry-sfGFP. Quantification shows the ratio of mCherry signal to the corresponding FLAG signal. Mean ± SEM, n = 3.

2.4.4 Roq1 is a short-lived protein

Finally, we wanted to address the shutdown mechanism of the SHRED pathway. Cycloheximide chase experiments revealed that both full-length and cleaved Roq1 are very short lived (**Figure 18A, B**). Thus, the short half-life of the Roq1 protein allows tight regulation of SHRED by rapid turnover of Roq1 protein once expression comes to a halt. Interestingly, *UBR1* deletion had only a minor effect on the steady-state levels of Roq1 (**Figure 18A**), suggesting that the major ubiquitin E3 ligase involved in the turnover of Roq1 is not Ubr1. In conclusion, the mechanistic analyses have revealed that different stressors can transcriptionally upregulate *ROQ1* expression and the resulting Roq1 protein is subsequently cleaved by Ynm3. Cleaved Roq1 then exposes an N-terminal arginine and by this binds to and regulates Ubr1 substrate specificity.

A

Roq1-HA(74)

B
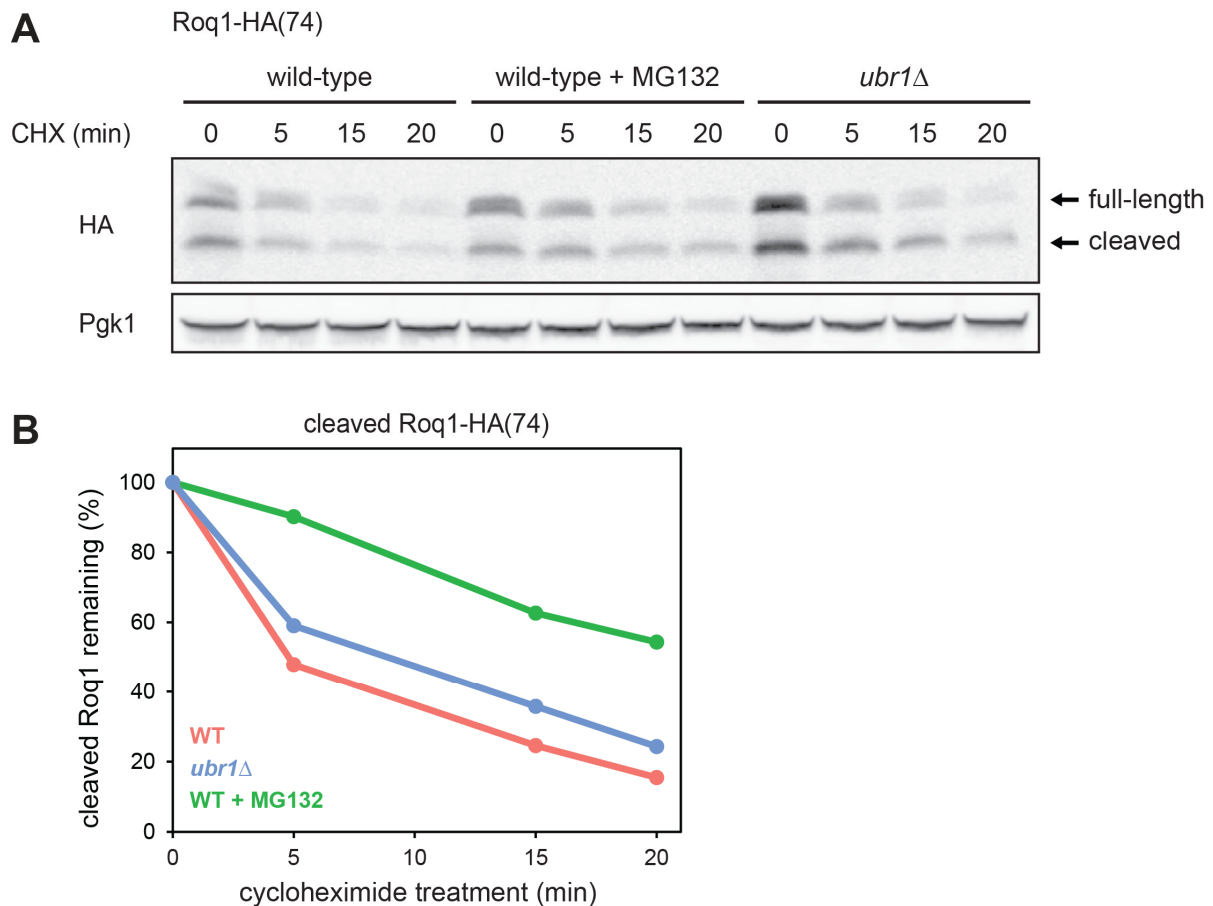
Figure 18. Roq1 is an unstable protein
A) Western blot of HA and Pgk1 from *pdr5Δ* (wild-type) or *ubr1Δ* cells expressing *GPD*-driven Roq1-HA(74) after cycloheximide (CHX) and MG132 treatment where indicated. Marked with arrows are the full-length and cleaved Roq1. Pgk1 served as loading control. **B)** Mean HA levels of cleaved Roq1 from **(A)** relative to Pgk1 and normalized to 0h time point.

2.5 Substrates of SHRED

2.5.1 SHRED degrades misfolded cytosolic and ER membrane proteins

Next, we investigated the substrate spectrum of SHRED by testing different misfolded model proteins. First, the degradation phenotype of Yop1Pho8*-GFP and Rtn1CPY*-GFP was compared to Rtn1Pho8*-GFP. Changing the ER anchor to another reticulon protein Yop1 resulted in a stable protein (**Figure 19A**) but ER-stress induced its degradation, which was dependent on SHRED (**Figure 19B**). As shown before (**Figure 3A, B**), Rtn1CPY*-GFP was continuously degraded and genetic analysis revealed that Hrd1, Doa10 and Ubr1 are required for its steady-state turnover (**Figure 19C**). Importantly, tunicamycin treatment enhanced its degradation, which was dependent on SHRED (**Figure 19B**). This result suggests that under normal growth conditions Rtn1CPY*-GFP is a canonical ERAD and Ubr1 substrate, however, during ER-stress its degradation is accelerated through SHRED. Next we tested cystic fibrosis

transmembrane conductance regulator (CFTR), a well-studied polytopic ERAD and Ubr1 substrate under standard growth conditions (Stolz et al., 2013). Since ER-stress is known to upregulate ERAD components (Travers et al., 2000), we analysed the stress-induced degradation of CFTR in ERAD-deficient *hrd1Δ doa10Δ* cells. As for the Rtn1-based reporters, tunicamycin induced SHRED-dependent degradation of CFTR (**Figure 19D**).
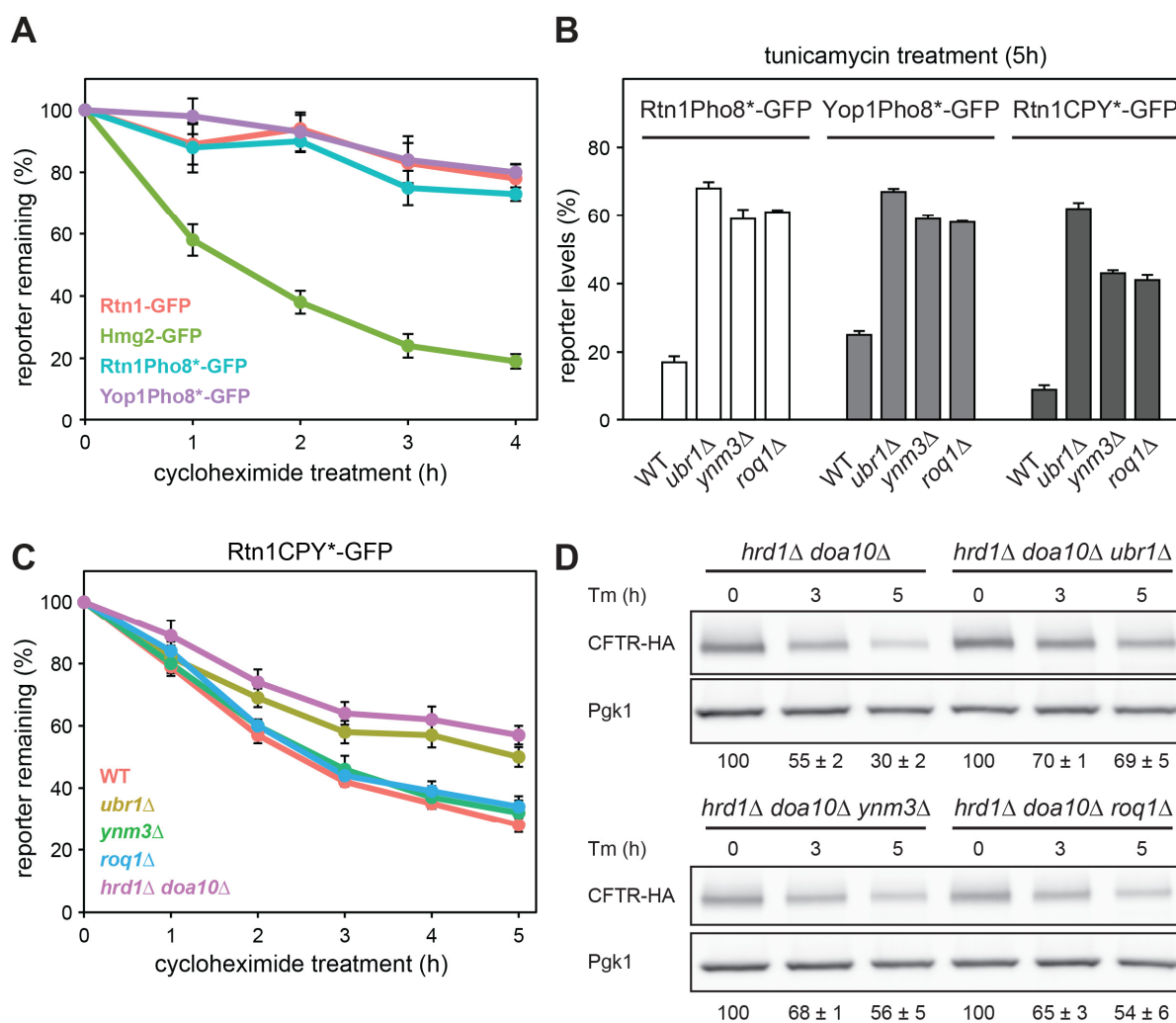
Figure 19. SHRED degrades misfolded ER membrane proteins
A) Total GFP fluorescence, measured by flow cytometry, after cycloheximide treatment of wild-type cells expressing Rtn1-GFP, Hmg2-GFP, Rtn1Pho8*-GFP or Yop1Pho8*-GFP. Mean ± SEM, n = 3. **B)** Mean GFP fluorescence, measured by flow cytometry, after five hours of tunicamycin treatment of wild-type (WT), *ubr1Δ*, *ynm3Δ* and *roq1Δ* cells expressing Rtn1Pho8*-GFP, Yop1Pho8*-GFP or Rtn1CPY*-GFP. Mean ± SEM, n = 3. **C)** Total GFP fluorescence, measured by flow cytometry, after cycloheximide treatment of WT, *ubr1Δ*, *ynm3Δ*, *roq1Δ* and *hrd1Δ doa10Δ* cells expressing Rtn1CPY*-GFP. Mean ± SEM, n = 3. **D)** Western blot of HA and Pgk1 from *hrd1Δ doa10Δ*, *hrd1Δ doa10Δ ubr1Δ*, *hrd1Δ doa10Δ ynm3Δ* and *hrd1Δ doa10Δ roq1Δ* cells expressing CFTR-HA after tunicamycin (Tm) treatment. Numbers under the blots indicate the mean ± SEM HA signal relative to Pgk1 and normalized to 0h time point. Pgk1 served as loading control.

Since all SHRED components are soluble proteins we investigated if the pathway is also responsible for the degradation of cytosolic misfolded proteins. First, degradation of a mutant and misfolded version of firefly luciferase, LuciferaseDM-mCherry was investigated (Gupta et al., 2011). Compared to wild-type Luciferase-mCherry the mutant version was degraded faster (**Figure 20A**) and tunicamycin treatment further enhanced its degradation in a SHRED-dependent manner (**Figure 20B**). *UBR1* deletion showed the strongest effect suggesting a role for Ubr1 acting parallel to SHRED during stress. Importantly, overexpression of *ROQ1* via the GEM expression system induced LuciferaseDM-mCherry but not wild-type Luciferase-mCherry degradation (**Figure 20C**). This is consistent with degradation phenotype of Rtn1Pho8*-GFP, but not of Rtn1-GFP, upon *ROQ1* overexpression (**Figure 12D**). Additionally, the truncated, misfolded and therefore continuously degraded mutant protein stGnd1 (Heck et al., 2010) also degraded upon ER-stress dependent on SHRED (**Figure 20D**). Hence, SHRED emerged as a stress-activated quality control pathway that degrades both misfolded cytosolic and ER membrane proteins.
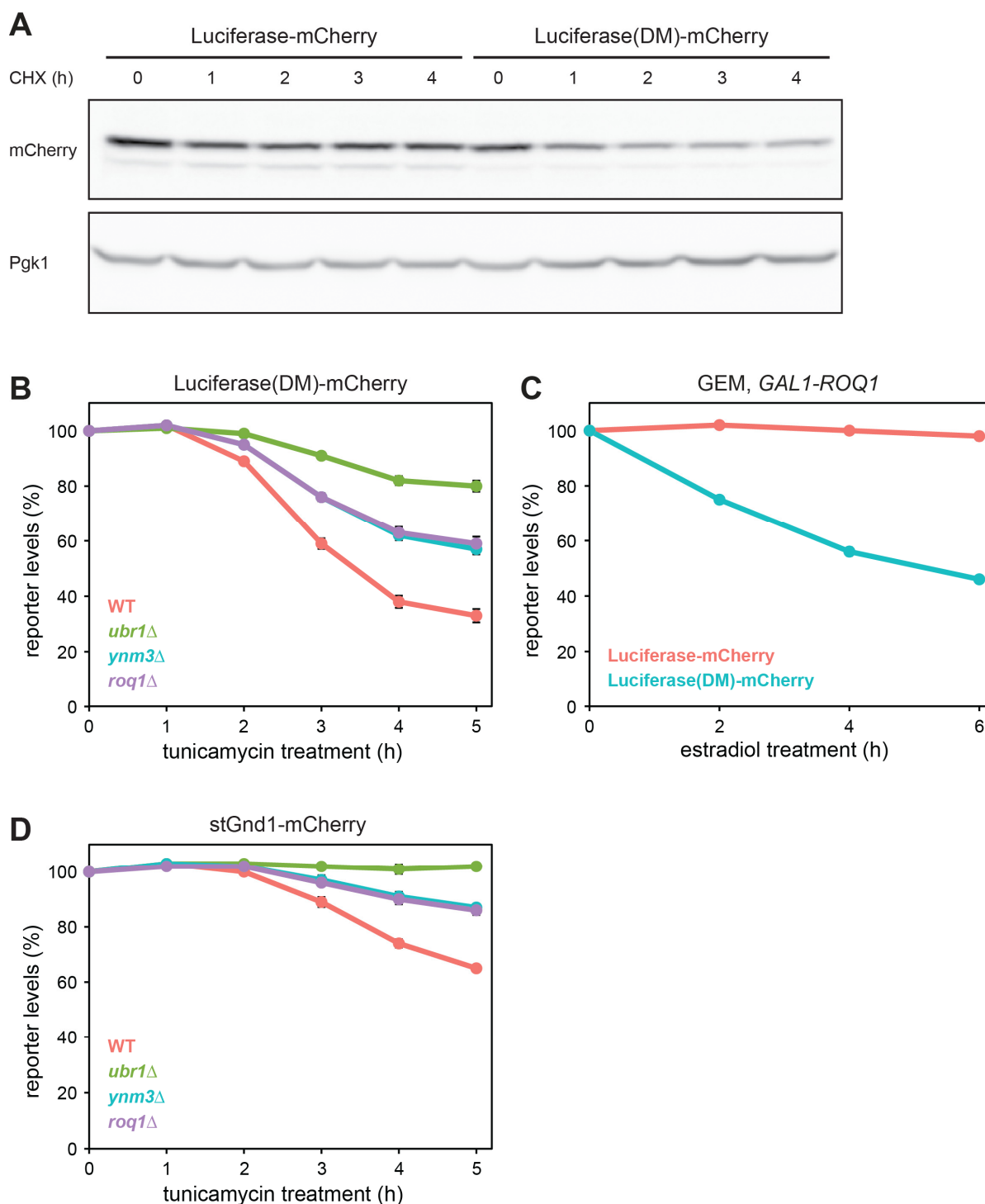
Figure 20. SHRED mediates the degradation of cytoplasmic misfolded proteins
A) Western blot of mCherry and Pgk1 from wild-type cells expressing wild-type Luciferase-mCherry or point mutant Luciferase(DM)-mCherry after cycloheximide (CHX) treatment. Pgk1 served as loading control. Experiment performed by Juan Diaz-Miyar. **B)** Mean mCherry fluorescence, measured by flow cytometry, after tunicamycin treatment of wild-type (WT), *ubr1Δ*, *ynm3Δ* and *roq1Δ* cells expressing Luciferase(DM)-mCherry. Mean ± SEM, n = 3. **C)** Mean mCherry fluorescence, measured by flow cytometry, after estradiol treatment of WT cells expressing the GEM transcription factor, *GAL1*-driven endogenous Roq1 and Luciferase-mCherry or Luciferase(DM)-mCherry. Mean ± SEM, n = 4. Experiment performed by Sebastian Schuck. **D)** Mean mCherry fluorescence, measured by flow cytometry, after tunicamycin treatment of WT, *ubr1Δ*, *ynm3Δ* and *roq1Δ* cells expressing stGnd1-mCherry. Mean ± SEM, n = 3.

2.5.2 Genetic screening to uncover endogenous SHRED substrates

Is SHRED only responsible for degrading misfolded proteins for quality control purposes or does it adjust the levels of well-folded endogenous proteins for regulatory purposes as well? To uncover possible endogenous substrates of SHRED we performed two different genetic screens. In the first approach the tFT-tag genetic library was employed (Khmelinskii et al., 2014). The library contains approximately 70% of all yeast ORFs with a C-terminal tFT-tag. We introduced a *ROQ1* or *URA3* (wild-type control) deletion into the tFT library through mating and sequential selection steps (see Methods for the synthetic genetic array). After the final selection the mCherry and sfGFP fluorescence intensity was measured in haploid colonies after 24 hours of growth on plates using a fluorescence plate reader (**Figure 21A**). On each screening plate, Rtn1-tFT and Rtn1Pho8*-tFT served as negative and positive control, respectively. Growing cells on agar plates (colonies) resulted in a similar Rtn1Pho8*-GFP degradation phenotype as growing cells in liquid culture into stationary phase (**Figure 11C**). Therefore, as expected, Rtn1-tFT showed a nearly identical mCherry/sfGFP fluorescence ratio in *ura3Δ* and *roq1Δ* cells indicating similar turnover in both strains. In contrast, Rtn1Pho8*-tFT showed a higher fluorescence ratio in the *roq1Δ* strain compared to *ura3Δ* indicating a slower turnover (data not shown).

Candidate SHRED substrates were selected based on the fluorescence ratio difference between *roq1Δ* and *ura3Δ* cells (see Materials and Methods for filtering details). Filtering of the hits resulted in a list of approximately 250 potential substrates for SHRED. In order to validate these candidate substrates, we re-screened 152 of those potential substrates in liquid culture measuring the fluorescence with the flow cytometer. Fluorescence intensities of the candidate substrates were measured in logarithmic growth phase and after 24 hours of growth when cells reached post-diauxic phase. As expected, Rtn1-tFT did not show any difference in mCherry/sfGFP ratio between *ura3Δ* and *roq1Δ* strains during both mid-log phase and post-diauxic phase (**Figure 21B, C**). On the other hand, Rtn1Pho8*-tFT displayed the same mCherry/sfGFP ratio in both strain backgrounds during log phase but the mCherry/sfGFP ratio increased after 24 hours of growth in the *roq1Δ* strain (**Figure 21B, C**). Of all the 152 re-screened hits only Cam1-tFT, Tef4-tFT, Sfa1-tFT and Glo1-tFT presented a similar phenotype as Rtn1Pho8*-tFT, meaning identical mCherry/sfGFP ratio in mid-log phase but higher ratio in *roq1Δ* cells compared to *ura3Δ*

after 24 hours of growth (**Figure 21B, C**). The rest of the candidate hits were either not detectable by flow cytometry or did not confirm the phenotype seen in the plate-based screen.

In order to validate the candidate hits as SHRED substrates, we tagged Cam1 and Tef4, the two most prominent hits, endogenously with an HA-tag and followed their protein levels in liquid culture by western blot. We used the small HA-tag to rule out the possibility that the large size of the tFT-tag (52 kDa) perturbs the native folding function of the protein. In agreement with the results from the tFT screen, both Cam1-HA and Tef4-HA protein levels dropped in a SHRED-dependent manner after growing the cells into post-diauxic phase (**Figure 21D, E**). Hence, the tFT screen offered us candidate hits, whose protein levels are regulated by SHRED during post-diauxic phase.
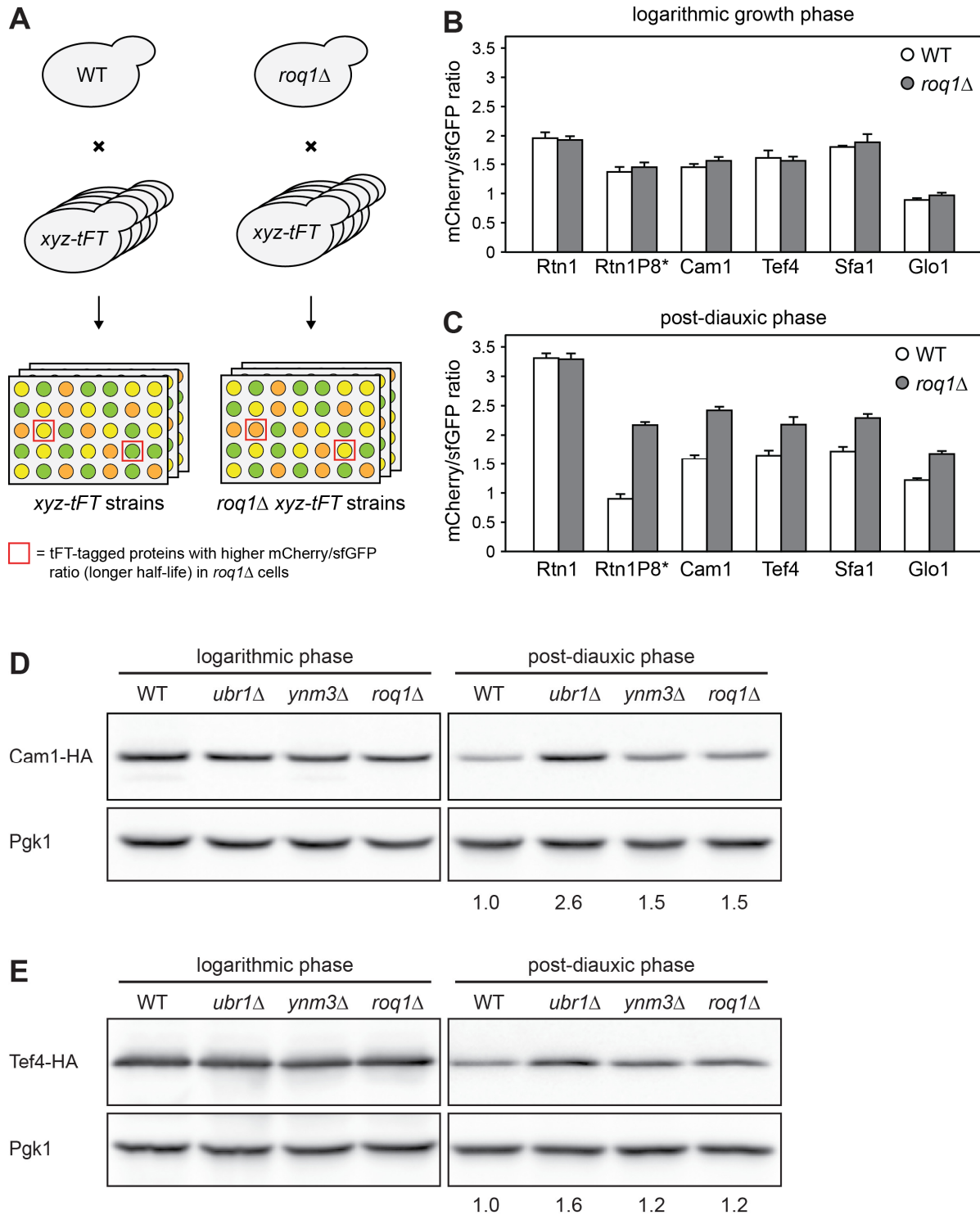
Figure 21. Candidate SHRED substrates discovered via a genetic screen
A) Schematic illustration of the screening strategy to discover endogenous SHRED substrates using the tFT-tag genetic library. Screen was performed jointly with Juan Diaz-Miyar. **B)** mCherry over sfGFP fluorescence intensity ratio, measured by flow cytometry, from wild-type (WT) and *roq1Δ* cells in mid-log phase expressing Rtn1-tFT, Rtn1Pho8*-tFT, Cam1-tFT, Tef4-tFT, Sfa1-tFT and Glo1-tFT. Mean ± SEM, n = 3. **C)** as in **(B)** but cells were grown for 24 hours into post-diauxic phase. Mean ± SEM, n = 3. **D)** Western blot of HA and Pgk1 from WT, *ubr1Δ*, *ynm3Δ* and *roq1Δ* cells expressing endogenously tagged Cam1-HA in logarithmic growth phase or in post-diauxic phase. The numbers below the blots are fold change of the mean HA signal, relative to Pgk1, normalized to the HA signal in WT cells. **E)** As in **(D)** but cells expressed endogenously tagged Tef4-HA.

2.5.3 Search for endogenous SHRED substrates via mass spectrometry

In the second screening approach for endogenous substrates we exploited the fact that overexpression of Roq1 alone activates SHRED and Rtn1Pho8*-GFP degradation (**Figure 12C, D**). In collaboration with Georg Borner (MPI for Biochemistry, Martinsried), we compared the proteome of wild-type and *ubr1Δ* strains after eight hours of Roq1 overexpression using the GEM expression system. For control purposes both strains harboured the Rtn1Pho8*-GFP reporter whose levels dropped by approximately 35% in wild-type but not in *ubr1Δ* cells upon Roq1 overexpression (data not shown). After a series of filtering and statistical analysis, we compiled a list of 18 candidate SHRED substrates, with a false discovery rate of 20%, whose protein levels reduced at least 25% in wild-type but not in *ubr1Δ* cells (**Figure 22A, third column**). Four of the candidate substrates (Caf20, Mmm1, Ncs6, Srp14) showed similar steady-state levels in wild-type and *ubr1Δ* cells (**Figure 22A, fourth column**) reproducing the phenotype of Rtn1Pho8*-GFP. The candidate proteins were either soluble (cytosolic or nuclear) or membrane proteins of the ER, Golgi complex or the mitochondria, suggesting that SHRED could be responsible for the degradation of a wide variety of endogenous proteins from different subcellular compartments.

In contrast to Rtn1Pho8*-GFP, the protein levels of Aap2, Yfr006w, Eaf5 and Agc1 were already reduced in *ubr1Δ* cells steady-state (**Figure 22A, fourth column**). This suggests that Ubr1 degrades them when SHRED is active, however when SHRED is inactive Ubr1 indirectly upregulates them. Further analysis on low abundant proteins revealed that Ptr2 strongly represents this phenotype: Ptr2 protein levels are reduced upon Roq1 overexpression and *UBR1* deletion (**Figure 22B, left and centre panel**), but unaffected by the overexpression of Roq1 in *ubr1Δ* cells (**Figure 22B, right panel**). Ptr2 is a plasma membrane di- and tripeptide transporter (Perry et al., 1994), whose expression is negatively regulated by a transcriptional repressor Cup9, which itself is degraded by Ubr1 upon its allosteric activation by dipeptides (Turner et al., 2000). Therefore, in the absence of Ubr1 high levels of Cup9 repress *PTR2* transcription leading to low Ptr2 protein levels.

In wild-type cells, overexpression of Roq1 resulted in a drop of Ptr2 protein levels (**Figure 22B, left panel**), suggesting that the excessive amount of Roq1 perturbed Ubr1-mediated degradation of Cup9 and thus it repressed *PTR2* expression. Indeed, qPCR data confirmed that Roq1 overexpression decreased *PTR2* mRNA levels in wild-

type cells but had no effect on the already low *PTR2* mRNA levels in *ubr1Δ* cells (**Figure 22C**). This result suggests that Roq1, through the activation of SHRED, reprograms Ubr1 to degrade misfolded and native proteins and at the same time inhibits the degradation of Cup9. Hence, both screening approaches offered candidate endogenous substrates for SHRED.

A

Candidate SHRED substrates

● reduced by >25%   ○ reduced by 10-25%   ● changed by <10%

	FDR (%)	change by Roq1 oe in WT	change by deletion of *UBR1*	localization
GFP	0	●	●	ER (Rtn1Pho8*-GFP)
Pho8	0	●	●	ER (Rtn1Pho8*-GFP)
Caf20	0	●	●	cytoplasm
Mmm1	10	●	●	ER
Ncs6	20	●	●	cytoplasm
Srp14	20	●	●	cytoplasm and ER
Mum2	0	●	○	cytoplasm
Srb7	0	●	○	nucleus
Srb2	10	●	○	nucleus
Rnt1	10	●	○	nucleus
Rsa3	20	●	○	nucleus
Fcy2	20	●	○	plasma membrane
Cog7	20	●	○	Golgi complex
Dap2	20	●	○	vacuole membrane
Hst2	20	●	○	cytoplasm
Ddl1	20	●	○	mitochondria
Aap1	0	●	●	cytoplasm
Yfr006w	0	●	●	cytoplasm
Eaf5	20	●	●	nucleus
Agc1	20	●	●	mitochondria

C

B

Figure 22. Candidate SHRED substrates discovered by mass spectrometry
A) Table of candidate SHRED substrates whose protein levels dropped at least by 25% upon Roq1 overexpression with a maximum false discovery rate (FDR) of 20%. Data analysis performed by Daniel Itzhak and Georg Borner. **B)** The effect of Roq1 overexpression and *UBR1* deletion on protein levels. The X-axis shows the average fold change of expression between two strains; the Y-axis shows the result of a t-test for that difference (two-tailed, n = 4). The 'volcano' lines indicate thresholds of significance (FDR = 5%). Data analysis performed by Daniel Itzhak and Georg Borner. **C)** *PTR2* mRNA levels, determined by qPCR, of wild-type (WT) and *ubr1Δ* cells after Roq1 overexpression where indicated. Values were normalized to the mRNA levels of the *TEF10* housekeeping gene. Mean ± SEM, n = 3.

DISCUSSION

Deteriorating protein quality during stress conditions is an intensively investigated field of molecular biology and biochemistry (Labbadia and Morimoto, 2015). In this PhD thesis, we have uncovered a novel stress-regulated protein quality control pathway that selectively recognizes and degrades misfolded as well as native ER membrane and cytosolic proteins. We named this pathway SHRED for Stress-induced Homeostatically Regulated Degradation. Using yeast genetics and various molecular biology and biochemical assays, we have elucidated how these proteins act in a linear degradation pathway. Specifically, various stressors transcriptionally upregulate the *ROQ1* gene. Subsequently the resulting Roq1 protein is cleaved by Ynm3. Cleaving Roq1 exposes an N-terminal arginine and through this modulates the substrate specificity of the E3 ligase Ubr1 (**Figure 23**). Altered substrate specificity of Ubr1 leads to enhanced proteasomal degradation of SHRED substrates. Furthermore, a genetic screen and mass spectrometry analysis revealed endogenous candidate substrates of SHRED.
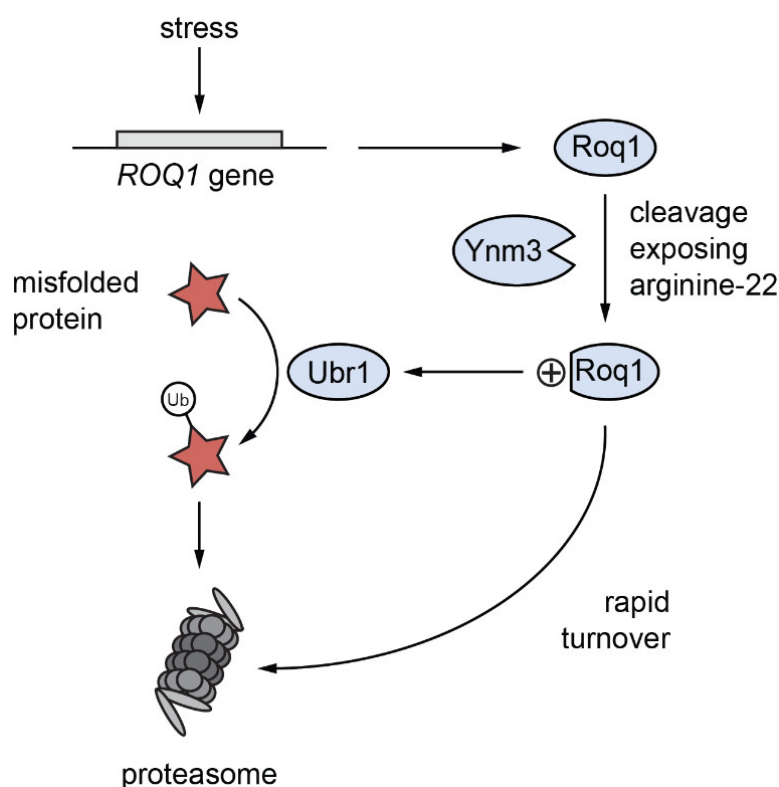
Figure 23. Mechanistic model of SHRED
Stress upregulates *ROQ1* expression and the resulting Roq1 protein is cleaved by the serine protease Ynm3 between leucine-21 and arginine-22. Cleaved Roq1, with an N-terminal arginine residue, directly interacts with Ubr1 and modulates its substrate specificity. Rapid degradation of cleaved Roq1 by the proteasome enables swift downregulation of the pathway as soon as stress subsides.

3.1 Transcriptional regulation of SHRED via Roq1

The initial and key step in SHRED is the transcriptional upregulation of the *ROQ1* gene. Our results confirmed the previous finding (Pincus et al., 2014; Travers et al., 2000) that ER-stress upregulates *ROQ1* transcription. However, *ROQ1* transcription is also upregulated during a wide variety of other stressors including heat shock (Gasch et al., 2000) osmotic shock (O'Rourke and Herskowitz, 2004), oxidative stress (Guan et al., 2012) and nitrogen starvation (Gasch et al., 2000). Moreover, overexpression of ERAD and SHRED substrate CFTR (Buck et al., 2015) or non-translocated and potentially unfolded secretory proteins also upregulate *ROQ1* transcription (Mutka and Walter, 2001). Thus, multiple signals converge on and stimulate *ROQ1* transcription. Besides activating their own response pathway, all these stressors trigger the environmental stress response (ESR) through PKA signalling (Gasch, 2003). In accordance with this, the *ROQ1* promoter contains a stress response element (AGGGG) that is bound by the ESR transcription factors Msn2/4. Indeed, deletion of *MSN2/4* abrogated reporter degradation (data not shown), confirming their importance in the regulation of *ROQ1* transcription. However, the *ROQ1* promoter contains a binding site for the heat shock factor Hsf1 as well (Yamamoto et al., 2005). *HSF1* is activated by many stressors and is also regulated by ESR via PKA (Vihervaara and Sistonen, 2014). Thus, the transcriptional regulation of *ROQ1*/SHRED is likely not controlled by a single transcription factor but rather by a network of regulatory proteins.

3.2 The proteolytic cleavage site within Roq1

After transcriptional upregulation of the *ROQ1* gene the resulting Roq1 protein is cleaved by the serine protease Ynm3 between leucine-21 and arginine-22. Ynm3 belongs to the High temperature requirement A (HtrA) serine protease family whose members are trypsin-type proteases based on their catalytic triad (Clausen et al., 2002). The bacterial homologues DegP/Q and the mammalian counterpart HtrA2 preferentially cleave after aliphatic valine, isoleucine, methionine or leucine residues (Martins et al., 2003; Vande Walle et al., 2007). Thus, the identified cleavage site within Roq1 fits the cleavage site preference of HtrA family members.

Only one Ynm3 substrate is published, the inhibitor-of-apoptosis (IAP) protein Bir1 (Walter et al., 2006; Zhang et al., 2017). Bir1 is the sole known IAP protein in budding

yeast, therefore deletion of *BIR1* leads to increased apoptotic cell death (Walter et al., 2006). The cleavage site within Bir1 is not determined, thus a direct comparison of the two proteolytic sites is not possible. However, it raises the question how Ynm3 distinguishes between its two proteolytic substrates Roq1 and Bir1. Similar to Roq1, Bir1 is a very lowly abundant protein (Ghaemmaghami et al., 2003). However, in contrast to *ROQ1* transcriptional regulation, *BIR1* transcription is essentially not modulated by stressors (Causton et al., 2001; Gasch et al., 2000). Thus, we believe that Roq1 is the main proteolytic target of Ynm3 during stress conditions.

3.3 Substrate recognition by Ynm3

In order to cleave their substrates, proteases have to specifically recognise and bind to their proteolytic substrates. Where does Ynm3 interact with Roq1 to subsequently mediate the cleavage? Tagging Roq1 on the C-terminus rendered the protein partially non-functional and cleavage was less efficient. This observation suggests that Ynm3 might bind Roq1 at or close to the C-terminus. Accordingly, the Ynm3 bacterial homologue DegS binds to its proteolytic substrates at their very C-terminus (Walsh et al., 2003). Intriguingly, the Ynm3 bacterial homologue DegP is a member of the family of "ruler" proteases (Krojer et al., 2008a). In these enzymes the physical distance between the substrate-binding domain and the proteolytic active site acts as a molecular ruler to establish the cleavage site within the substrate protein. Thus, hypothetically the Ynm3 binding site on Roq1 might also influence the location of the cleavage site. Or *vice versa,* since we discovered the cleavage site within Roq1, the Ynm3 binding site could be determined from the proteolytic site.

How does Ynm3 bind to its substrates? The defining features of HtrA proteases are a single trypsin-like protease domain and one or two protein-protein interacting PDZ domains (Clausen et al., 2002). The bacterial homologues DegS/P were shown to bind their substrates via the PDZ domains (Merdanovic et al., 2010). Conversely, the mammalian homologue HtrA1 binds its substrate directly by the protease domain (Truebestein et al., 2011). In contrast to the default domain architecture of HtrA family members, Ynm3 and several other plant or algae homologues, contain two protease domains (a proteolytically active and an inactive one) and four PDZ domains (Schuhmann et al., 2011). This was likely the result of a gene duplication and fusion event from an original DegP-like HtrA protease (Schuhmann et al., 2011). A recent *in*

vitro cryo-electron microscopy (EM) study on the structure of Ynm3 suggests that the first PDZ domain is available for substrate binding, while the conformation of the other three PDZ domains are blocked from substrate engaging (Zhang et al., 2017). Therefore, the first PDZ domain is a good candidate for a role in substrate binding. Additionally, deletion of PDZ1 and 2 *in vivo* rendered Ynm3 unstable, indicating an important role for these PDZ domains in the stability of the entire protein as well (Padmanabhan et al., 2009).

Another intriguing aspect that could influence substrate binding is the oligomerization state of Ynm3. All HtrA family members, including Ynm3, form oligomers, with homo-trimers as their basic building unit (Li et al., 2002; Wilken et al., 2004; Zhang et al., 2017). Intriguingly, the bacterial homologue DegP changes from a "resting" hexamer to a 12 or 24mer upon substrate binding (Krojer et al., 2008b). *In vitro* Ynm3 appeared as a homotrimer forming a cage-like structure with the three protomers arranged in a C3 rotational symmetry (Zhang et al., 2017). Whether the state of Ynm3 oligomerization changes upon substrate binding is yet to be uncovered. However, future *in vitro* structural analysis of Ynm3, in complex with Roq1, would allow us to investigate in detail the binding and cleavage properties of Ynm3.

3.4 Regulation of Ynm3-mediated cleavage of Roq1

Roq1 overexpression initiated a slower reporter degradation compared to reporter degradation upon stress treatments. These findings suggest that the stressors might directly or indirectly activate other processes that speed up SHRED and the degradation of misfolded proteins.

Could Ynm3 processivity be stress-regulated? *In vitro* cryo-EM data proposes that Ynm3 exist in a dynamic equilibrium of open (substrate accepting) and closed (proteolytically non-active) conformational states (Zhang et al., 2017). Hypothetically, stress conditions might change this equilibrium to a more open and enzymatically active state which results in enhanced Roq1 cleavage and as a consequence Ubr1 and SHRED activation. However, we cannot rule out that the stressors caused other secondary, non-SHRED related, effects that resulted in faster reporter degradation.

Another layer of Ynm3 regulation could be achieved by its post-translational modification. The mammalian homologue HtrA2 is phosphorylated in the mitochondrial

inter-membrane space in a PINK1 dependent manner. This modification modulates its proteolytic activity (Plun-Favreau et al., 2007). Ynm3 is proposed to be phosphorylated at serine-993, which influences its function in apoptosis (unpublished results of the Fahrenkrog Lab, Fahrenkrog, 2011). Whether phosphorylation of Ynm3 exists and whether it has an effect on SHRED or Roq1 cleavage is yet to be determined.

3.5 Cleaved Roq1 modulates Ubr1 substrate specificity

The Roq1 cleavage fragment, with an N-terminal arginine residue, binds to and reprograms Ubr1 via the type-1 substrate-binding site. This binding modifies Ubr1 substrate specificity resulting in a slower degradation of Cup9 and type-1 substrates and accelerated degradation of type-2 substrates and misfolded membrane or cytosolic proteins. How does Roq1 modulate Ubr1 substrate specificity? Bound Roq1 might act as an allosteric regulator of Ubr1. Similar, allosteric regulation occurs when dipeptides bind synergistically to the Ubr1 type-1 and -2 site which relieves auto-inhibition and leads to the degradation of Cup9 (Du et al., 2002). In case of SHRED, the activation of Ubr1 occurs strictly through the type-1 site. This raises the possibility that binding of Roq1 to the type-1 site alone initiates a conformational change in Ubr1 that modulates its substrate binding capacity. Indeed, during activation of Ubr1 by dipeptides, the initial occupancy of the type-1 site induces a slight conformational change that increases the accessibility of the type-2 site (Du et al., 2002). Thus, the interaction of cleaved Roq1 with the type-1 site by itself could initiate structural changes within Ubr1, which are relevant for SHRED.

The interaction between Roq1 and Ubr1 was clearly dependent on the N-terminal arginine of Roq1 and the type-1 site of Ubr1. However, it remains to be determined if additional features of Roq1 are also important for Ubr1 activation. Structural information on the yeast and human Ubr1 type-1 site suggests that it is a relatively shallow substrate-binding cleft (Choi et al., 2010; Matta-Camacho et al., 2010). Therefore, Roq1 might physically interact with other regions of Ubr1, which may be important to modulate substrate specificity of Ubr1. Truncations or random mutagenesis analysis of Roq1 would allow us to uncover further important regions or domains of Roq1 besides its N-terminus. Alternatively, Roq1 might act as a substrate adaptor: after its cleavage it interacts with Ubr1 at the type-1 site, which could offer a

new substrate-binding platform on Ubr1. This would enable direct delivery of SHRED substrates to Ubr1 for ubiquitylation and degradation. Further mechanistic experiments will be required to explore the full scope of how Roq1 modulates Ubr1 substrate specificity.

3.6 Substrate recognition by Ubr1

How does Ubr1 recognize misfolded proteins? Cytosolic misfolded proteins are reportedly presented to Ubr1 by the Hsp70 chaperone Ssa1 (Eisele and Wolf, 2008; Heck et al., 2010). However, *in vitro* experiments suggest that Ubr1 can also interact with and ubiquitylate misfolded substrates in the absence of chaperones as well (Nillegoda et al., 2010). If Ubr1 binds misfolded (SHRED) substrates directly, which part of Ubr1 is responsible for the interaction? Cup9 is proposed to bind to a third yet unidentified Ubr1 substrate-binding site (Du et al., 2002). Our mass spectrometry data suggest that Roq1 overexpression inhibits Ubr1-dependent degradation of Cup9 and simultaneously enhances degradation of misfolded proteins. This suggests that either the Cup9 site becomes inaccessible during Ubr1 activation by Roq1 or the SHRED substrates outcompete Cup9 for the same substrate-binding site resulting in its slower turnover. However, we cannot rule out that SHRED substrates may bind to an additional substrate-binding site, which could prevent the binding of Cup9 to Ubr1.

How can the Ubr1 substrate-binding site be identified? Perturbations like point mutations or truncations in Ubr1 often render the entire protein non-functional (see the slight effect of type-1 site mutation on the degradation of type-2 substrates, **Figure 16B**). Hence, mutational analysis of Ubr1 is challenging and might result in secondary indirect effects. An alternative approach could be the structural characterization of Ubr1, potentially in complex with Roq1 and/or misfolded proteins. Up to now, there is no structural information on the entire Ubr1 enzyme. With the current technological advancement in the cryo-EM field, the structural characterization of the entire Ubr1 enzyme, might be possible in the near future.

3.7 Dynamic regulation of SHRED

Dynamic regulation of any given pathway requires that it can be rapidly switched on and off. This can be accomplished by the rapid transcriptional upregulation and quick

turnover of an important regulatory factor in the pathway. In case of SHRED this is achieved through Roq1. As discussed above, *ROQ1* transcription is upregulated several fold during a wide variety of stresses in order to activate SHRED. On the other hand, the very short half-life of Roq1 protein enables rapid inactivation of SHRED as soon as stress subsides. This mode of pathway inactivation is similar to the UPR or the proteasome biogenesis pathway where the short half-life of transcription factors Hac1 and Rpn4 enables swift shut-off as soon as the inducing signal diminishes (Livneh et al., 2016; Walter and Ron, 2011).

Furthermore, the short half-life of Roq1 offers another layer of SHRED regulation. Our results suggest that cleaved Roq1 is degraded by the proteasome but Ubr1 is only partially required for its degradation. This raises the first question: which ubiquitin ligase is required for the degradation of the Roq1 cleavage fragment? Interestingly, cleaved Roq1 does not contain any acceptor lysine that could be marked with a polyubiquitin chain. Thus, cleaved Roq1 has to be processed by a non-canonical ubiquitylation or has to be recognised and degraded by the proteasome without attachment of a polyubiquitin chain (Kravtsova-Ivantsiv and Ciechanover, 2012). It has been reported that cysteine, serine or threonine can be also used as an acceptor residue for polyubiquitin chains (Cadwell and Coscoy, 2005). Additionally, it has been shown that N-termini of target proteins can also obtain polyubiquitin chains (Breitschopf et al., 1998). However, the latter option is unlikely since the N-terminus of Roq1 is buried within type-1 substrate-binding cleft. The identification of the potential ubiquitin ligase of Roq1 and the mode of its degradation will enable us to dissect the post-transcriptional regulation of SHRED

3.8 Stress-regulated protein quality control

The main characteristic of the SHRED pathway is its stress regulation. Stress conditions increase the amount of misfolded proteins therefore, cells mount adaptive responses to re-establish protein homeostasis (Labbadia and Morimoto, 2015). From a metabolic point of view refolding or repairing a misfolded protein is energetically favourable over degradation and re-synthesis (Buchberger et al., 2010). However, during unfavourable conditions chaperone capacity and thus refolding activity might be limiting, therefore protein degradation is inevitable. We propose that SHRED is a

branch of ESR, and together with the UPR and HSR, adjusts protein quality pathways to aid in the removal of the increased amounts of misfolded and damaged proteins. When stress subsides and protein homeostasis is re-established SHRED is inactivated by the swift turnover of its main regulator Roq1.

3.9 Could SHRED be evolutionary conserved?

Roq1 was listed as an uncharacterized protein at the beginning of this PhD project. It belongs to a family of hydrophilin proteins whose defining characteristics are high hydrophobicity and high content of glycine, alanine and serine residues (Battaglia et al., 2008; Dang and Hincha, 2011). Moreover, hydrophilins are intrinsically disordered proteins and they do not share sequence homology between family members (Garay-Arroyo et al., 2000). Most of the hydrophilins are found in the kingdom of Plantae but homologues are also found in Bacteria, Archea and Fungi (Battaglia et al., 2008). A search for Roq1 homologues, based on the amino acid sequence, does not yield any higher eukaryote homologues likely due to the absence of recognisable domain structures and the small molecular size of the Roq1 protein. However, the existence of functional analogues in metazoans cannot be excluded.

As discussed above, Ynm3 has several homologues in the family of HtrA proteases (Clausen et al., 2011). Its bacterial homologues DegS/P function in protein quality control in the periplasm (Spiess et al., 1999) while the mammalian homologue HtrA2 is involved in mitochondrial quality control and apoptosis (Vande Walle et al., 2008). Importantly, the human homologue HtrA2 is further implicated in ERAD (Huttunen et al., 2007).

Ubr1 homologues are also found in many organisms ranging from yeast to humans (Varshavsky, 2011). As mentioned Ubr1 is the main ubiquitin E3 ligase involved in the N-end rule pathway but has emerging roles in cytosolic quality control as well. Importantly, it has been implicated in ERAD in the absence of Hrd1 and Doa10 or during stressful conditions (Heck et al., 2010; Stolz et al., 2013). In summary, although the existence of a higher eukaryote homologue of Roq1 is not obvious, both Ubr1 and Ynm3 are conserved in many organisms raising the possibility that SHRED-like mechanism might exist in metazoans as well.

Are there any biochemical pathways that show a SHRED-like regulatory principle? Human HtrA2 is expressed as a pro-enzyme and delivered to the mitochondria via a mitochondrial localization signal (Martins et al., 2002). In the mitochondrial inter-membrane space, HtrA2 undergoes self-cleavage and upon apoptotic stimulus the C-terminal cleavage fragment is released into the cytosol (Hegde et al., 2002). Intriguingly, the autocatalysis uncovers an N-terminal IAP binding motif that is required for HtrA2 to interact with the inhibitor-of-apoptosis protein XIAP in the cytosol (Martins, 2002). XIAP is a RING domain ubiquitin E3 ligase that inhibits and degrades important caspases in the apoptotic pathway (Silke and Meier, 2013). Binding of cleaved HtrA2 to XIAP inhibits its E3 ligase function (Martins, 2002). This could be considered analogous to SHRED: a proteolytic cleavage uncovers an N-terminal motif that is required for the binding to and reprograming of a ubiquitin E3 ligase. These intriguing observations suggest that SHRED-like mechanistic regulation of ubiquitin E3 ligases might also exist in higher eukaryotes.

3.10 Endogenous substrates of SHRED

Our genetic screen and mass spectrometry analysis revealed that SHRED is not only responsible for the degradation of misfolded proteins but also for the removal of endogenous and potentially well-folded proteins. Both screening approaches offered endogenous candidate substrates for SHRED. However, only Sfa1 was identified as a candidate substrate with both approaches. A likely explanation for the small overlap is the distinct principle of the two screening approaches. The tandem fluorescent timer (tFT) tag approach enables direct analysis of protein half-lives via the mCherry over sfGFP fluorescence intensity ratio. However, the large size of the tFT tag could interfere with folding and the function of the protein of interest. This might introduce false positive hits resulting from misfolding caused by the large bulky tag. In the mass spectrometry approach the candidate substrates were not tagged, thereby bypassing this limitation of the tFT screen. However, the mass spectrometry analysis measures total protein levels from which the half-life of any given protein cannot be calculated. Moreover, Roq1 overexpression induced a weaker reporter degradation: the reporter levels dropped by 35% in the mass spectrometry analysis, compared to the drop by 60% in the tFT screen. Therefore, the dynamic range of this screen was rather small which might conceal weaker hits.

The two most prominent hits from the tFT screen, Cam1 and Tef4, were validated as a candidate substrate of SHRED by western blotting. Both proteins become a SHRED substrate when cells grow into post-diauxic phase. What could be the physiological relevance of this degradation phenotype? The transcriptome and the proteome of budding yeast is remodelled dramatically during growth into post-diauxic phase and to stationary phase (Gasch et al., 2000; Murphy et al., 2015). The transcriptional response involves the upregulation of trehalose and glycogen synthetases and enzymes involved in the tricarboxylic acid and glyoxylate cycle. In contrast, general translation and translation of ribosomal proteins, tRNA synthetases and translation initiation and elongation factors are repressed (DeRisi et al., 1997; Murphy et al., 2015). Both *CAM1* (also called *TEF3*) and *TEF4* encode a subunit of the translation elongation factor eEF1B (Kambouris et al., 1993; Kinzy et al., 1994). These genes are transcriptionally downregulated during post-diauxic phase resulting in a positive feedback loop to inactivate general translation (Gasch et al., 2000). However, after the transcriptional downregulation of a gene the cells still have to remove the translated proteins as well. *ROQ1* transcription is upregulated during post-diauxic phase and entry into stationary phase (Brauer et al., 2005; Segal et al., 2003) suggesting that SHRED is active during post-diauxic phase. Therefore, we propose that SHRED is involved in the remodelling of the proteome during growth into saturation. In summary, SHRED is not only required for protein quality control but also for abundance control of proteins during certain physiological conditions.

MATERIALS AND METHODS

4.1 Materials

Table 1. Plasmids used in the study

Alias	Plasmid name	Source/Reference
pSS077	pFA6a-Pho8Δ60-kanMX6	this study
pSS078	pFA6a-Pho8Δ60(F352S)-kanMX6	this study
pMaM227	pRS303K-TDH3pr-TagBFP	Michael Knop
pMaM245	pRS303H-TDH3pr-TagBFP	Michael Knop
pSS665	pRS305-ADH1pr-Pho8*	this study
pSS421	pRS305-ADH1pr-Rtn1-FLAG-sfGFP	this study
pSS422	pRS305-ADH1pr-Rtn1-Pho8*-FLAG-sfGFP	this study
pSS450	pRS305-ADH1pr-Rtn1-CPY*-FLAG-sfGFP	this study
pSS483	pRS305-ADH1pr-Hmg2-FLAG-sfGFP	this study
pSS170	pRS305-ADH1pr-Rtn1-FLAG-GFP	this study
pSS174	pRS305-ADH1pr-Rtn1-Pho8*-FLAG-GFP	this study
pSS411	pRS305-GAL1pr-Rtn1-FLAG-sfGFP	this study
pSS412	pRS305-GAL1pr-Rtn1-Pho8*-FLAG-sfGFP	this study
pDEP001	pRS306-ADH1pr-GEM(Gal4DBD-EstR-Msn2TAD)	Pincus et al., 2014
pDEP151	pNH605-ADH1pr-GEM(Gal4DBD-EstR-Msn2TAD)	David Pincus
pSS252	pRS316-CYCter	this study
pSS255	pRS316-YNM3pr-Ynm3	this study
pSS257	pRS316-YNM3pr-ynm3(S236A)	this study
pSS352	pRS316-YNM3pr-Ynm3-GFP	this study
pSS254	pRS316-ROQ1pr-Roq1	this study
pSS629	pRS316-ROQ1pr-Roq1-HA	this study
pSS776	pRS316-ROQ1pr-Roq1-HA(74)	this study
pSS634	pRS416-TDH3pr-Roq1-HA	this study
pSS649	pRS416-TDH3pr-Roq1-HA(74)	this study
pSS784	pRS416-TDH3pr-Ub-Roq1Δ18-HA(74)	this study
pSS762	pRS416-TDH3pr-Ub-Roq1Δ19-HA(74)	this study
pSS763	pRS416-TDH3pr-Ub-Roq1Δ20-HA(74)	this study
pSS764	pRS416-TDH3pr-Ub-Roq1Δ21-HA(74)	this study
pSS927	pRS416-TDH3pr-Ub-roq1Δ21(R22A)-HA(74)	this study
pSS765	pRS416-TDH3pr-Ub-Roq1Δ22-HA(74)	this study
pSS766	pRS416-TDH3pr-Ub-Roq1Δ23-HA(74)	this study
pSS734	pRS316-ROQ1pr-Ub-Roq1	this study
pSS804	pRS316-ROQ1pr-Ub-Roq1Δ7	this study
pSS805	pRS316-ROQ1pr-Ub-Roq1Δ8	this study
pSS806	pRS316-ROQ1pr-Ub-Roq1Δ9	this study
pSS745	pRS316-ROQ1pr-Ub-Roq1Δ10	this study
pSS746	pRS316-ROQ1pr-Ub-Roq1Δ11	this study
pSS747	pRS316-ROQ1pr-Ub-Roq1Δ12	this study
pSS748	pRS316-ROQ1pr-Ub-Roq1Δ13	this study
pSS749	pRS316-ROQ1pr-Ub-Roq1Δ14	this study
pSS750	pRS316-ROQ1pr-Ub-Roq1Δ15	this study

Alias	Plasmid name	Source/Reference
pSS751	pRS316-ROQ1pr-Ub-Roq1Δ16	this study
pSS752	pRS316-ROQ1pr-Ub-Roq1Δ17	this study
pSS753	pRS316-ROQ1pr-Ub-Roq1Δ18	this study
pSS754	pRS316-ROQ1pr-Ub-Roq1Δ19	this study
pSS755	pRS316-ROQ1pr-Ub-Roq1Δ20	this study
pSS756	pRS316-ROQ1pr-Ub-Roq1Δ21	this study
pSS757	pRS316-ROQ1pr-Ub-Roq1Δ22	this study
pSS771	pRS316-ROQ1pr-Ub-Roq1Δ23	this study
pSS772	pRS316-ROQ1pr-Ub-Roq1Δ24	this study
pSS773	pRS316-ROQ1pr-Ub-Roq1Δ25	this study
pSS827	pRS316-ROQ1pr-Ub-roq1Δ21(R22A)	this study
pSS830	pRS316-ROQ1pr-Ub-roq1Δ21(R22L)	this study
pSS829	pRS316-ROQ1pr-Ub-roq1Δ21(R22K)	this study
pSS834	pRS316-ROQ1pr-roq1(L21P)-HA(74)	this study
pSS845	pRS316-ROQ1pr-roq1(L21V)-HA(74)	this study
pSS796	pRS316-TDH3pr-roq1(L21P)-HA(74)	this study
pSS797	pRS316-TDH3pr-roq1(L21V)-HA(74)	this study
pSS256	pRS316-UBR1pr-Ubr1	this study
pSS617	pRS316-UBR1pr-ubr1(G173R)	this study
pSS374	pRS316-UBR1pr-ubr1(D318N)	this study
pSS930	pRS415-ADH1pr-FLAG-Ubr1	this study
pSS935	pRS415-ADH1pr-FLAG-ubr1(G173R)	this study
pSS938	pRS415-ADH1pr-FLAG-ubr1(C1220S)	this study
pSS669	pFA6a-kanMX6-GEM,GAL1pr	this study
pAK146	pRS306K-TDH3pr-Ub-A-mCherry-sfGFP	Khmelinskii et al., 2012
pAK147	pRS306K-TDH3pr-Ub-C-mCherry-sfGFP	Khmelinskii et al. 2012
pAK148	pRS306K-TDH3pr-Ub-D-mCherry-sfGFP	Khmelinskii et al. 2012
pAK149	pRS306K-TDH3pr-Ub-E-mCherry-sfGFP	Khmelinskii et al. 2012
pMaM48	pRS306K-TDH3pr-Ub-F-mCherry-sfGFP	Khmelinskii et al. 2012
pAK150	pRS306K-TDH3pr-Ub-G-mCherry-sfGFP	Khmelinskii et al. 2012
pAK151	pRS306K-TDH3pr-Ub-H-mCherry-sfGFP	Khmelinskii et al. 2012
pMaM47	pRS306K-TDH3pr-Ub-I-mCherry-sfGFP	Khmelinskii et al. 2012
pAK152	pRS306K-TDH3pr-Ub-K-mCherry-sfGFP	Khmelinskii et al. 2012
pAK153	pRS306K-TDH3pr-Ub-L-mCherry-sfGFP	Khmelinskii et al. 2012
pMaM46	pRS306K-TDH3pr-Ub-M-mCherry-sfGFP	Khmelinskii et al. 2012
pAK154	pRS306K-TDH3pr-Ub-N-mCherry-sfGFP	Khmelinskii et al. 2012
pAK155	pRS306K-TDH3pr-Ub-P-mCherry-sfGFP	Khmelinskii et al. 2012
pAK156	pRS306K-TDH3pr-Ub-Q-mCherry-sfGFP	Khmelinskii et al. 2012
pMaM66	pRS306K-TDH3pr-Ub-R-mCherry-sfGFP	Khmelinskii et al. 2012
pAK157	pRS306K-TDH3pr-Ub-S-mCherry-sfGFP	Khmelinskii et al. 2012
pAK158	pRS306K-TDH3pr-Ub-T-mCherry-sfGFP	Khmelinskii et al. 2012
pAK159	pRS306K-TDH3pr-Ub-V-mCherry-sfGFP	Khmelinskii et al. 2012
pAK160	pRS306K-TDH3pr-Ub-W-mCherry-sfGFP	Khmelinskii et al. 2012
pMaM67	pRS306K-TDH3pr-Ub-Y-mCherry-sfGFP	Khmelinskii et al. 2012
pSS666	pRS305-ADH1pr-Yop1-Pho8*-FLAG-sfGFP	this study
pSS608	pRS305-ADH1pr-Yop1-Pho8*-FLAG-GFP	this study
pSS607	pRS305-ADH1pr-Rtn1-CPY*-FLAG-GFP	this study

Alias	Plasmid name	Source/Reference
pSM1152	pRS426-PGK1pr-CFTR-HA	Zhang et al., 2001
SSY664	pRS306N-TEF1pr-NES-Luciferase-mCherry	this study
SSY637	pRS306N-TEF1pr-NES-Luciferase(DM)-mCherry	this study
SSY653	pRS306N-TEF1pr-stGnd1-mCherry	this study

Table 2. Yeast strains used in the study
For strains containing centromeric or 2μ plasmids only the genotype of the parent strains are listed. The chromosomally integrated different Ub-X-mCherry-sfGFP substrates are generated in strain SSY1856 (WT), SSY1857 (*ubr1Δ*) and SSY1858 (*ynm3Δ*).

Alias	Genotype	Source
SSY122	*MATa ADE2 leu2-3,112 trp1-1 ura3-1 his3-11,15 (W303)*	lab collection
SSY765	*MATa his3Δ1 leu2Δ0 met15Δ0 ura3Δ0 (BY4741)*	lab collection
SSY2353	*MATα his3Δ1 leu2Δ0 met15Δ0 ura3Δ0 (BY4742)*	lab collection
YJLM11-1	*BY4741 can1Δ::STE2pr-SpHIS5 lyp1Δ::STE3pr-LEU2 URA3*	Knop Lab
YMaM330	*BY4742 can1Δ::STE2pr-SpHIS5 lyp1Δ::STE3pr-LEU2 leu2Δ::GAL1pr-I-SCEI-natR*	Knop Lab
SSY689	*pho13Δ::HIS3 PHO8::kanR*	this study
SSY690	*pho13Δ::HIS3 pho8(F352S)::kanR*	this study
SSY995	*pho13Δ::HIS3 PHO8::kanR hrd1Δ::natR*	this study
SSY996	*pho13Δ::HIS3 pho8(F352S)::kanR hrd1Δ::natR*	this study
SSY1624	*HIS3::TDH3pr-BFP-hphR LEU2::ADH1pr-Pho8**	this study
SSY1632	*HIS3::TDH3pr-BFP-hphR san1Δ::kanR LEU2::ADH1pr-Pho8**	this study
SSY954	*HIS3::TDH3pr-BFP-hphR Sec63-mCherry::HIS3*	this study
SSY1189	*HIS3::TDH3pr-BFP-hphR Sec63-mCherry::HIS3 LEU2::ADH1pr-Rtn1-sfGFP*	this study
SSY1191	*HIS3::TDH3pr-BFP-hphR Sec63-mCherry::HIS3 LEU2::ADH1pr-Rtn1CPY*-sfGFP*	this study
SSY1190	*HIS3::TDH3pr-BFP-hphR Sec63-mCherry::HIS3 LEU2::ADH1pr-Rtn1Pho8*-sfGFP*	this study
SSY1160	*HIS3::TDH3pr-BFP-hphR LEU2::ADH1pr-Hmg2-sfGFP*	this study
SSY1020	*HIS3::TDH3pr-BFP-hphR LEU2::ADH1pr-Rtn1-sfGFP*	this study
SSY1143	*HIS3::TDH3pr-BFP-hphR LEU2::ADH1pr-Rtn1CPY*-sfGFP*	this study
SSY1022	*HIS3::TDH3pr-BFP-hphR LEU2::ADH1pr-Rtn1Pho8*-sfGFP*	this study
SSY829	*HIS3::TDH3pr-BFP-hphR LEU2::ADH1pr-Rtn1-GFP*	this study
SSY831	*HIS3::TDH3pr-BFP-hphR LEU2::ADH1pr-Rtn1Pho8*-GFP*	this study
SSY965	*HIS3::TDH3pr-BFP-hphR LEU2::GAL1pr-Rtn1-sfGFP*	this study
SSY967	*HIS3::TDH3pr-BFP-hphR LEU2::GAL1pr-Rtn1Pho8*-sfGFP*	this study
SSY2354	*HIS3::TDH3pr-BFP-hphR LEU2::GAL1pr-Rtn1-sfGFP Sec63-mCherry::HIS3*	this study
SSY2355	*HIS3::TDH3pr-BFP-hphR LEU2::GAL1pr-Rtn1Pho8*-sfGFP Sec63-mCherry::HIS3*	this study
SSY1084	*HIS3::TDH3pr-BFP-hphR LEU2::GAL1pr-Rtn1-sfGFP Rtn1-mCherry::HIS3*	this study
SSY1086	*HIS3::TDH3pr-BFP-hphR LEU2::GAL1pr-Rtn1Pho8*-sfGFP Rtn1-mCherry::HIS3*	this study
SSY822	*HIS3::TDH3pr-BFP-hphR pdr5Δ::HIS3 LEU2::ADH1pr-Rtn1Pho8*-GFP*	this study
SSY843	*HIS3::TDH3pr-BFP-hphR pep4Δ::TRP1 prb1Δ::HIS3 LEU2::ADH1pr-Rtn1Pho8*-GFP*	this study
SSY901	*HIS3::TDH3pr-BFP-hphR hrd1Δ::HIS3 doa10Δ::TRP1 pdr5Δ::kanR LEU2::ADH1pr-Rtn1Pho8*-GFP*	this study
SSY875	*his3Δ::HIS3*	this study
SSY1782	*ubr1Δ::HIS3*	this study
SSY772	*ynm3Δ::HIS3*	this study
SSY1729	*roq1Δ::HIS3*	this study

Alias	Genotype	Source
SSY644	*MATα atg7Δ::TRP1 LEU2::ADH1pr-Rtn1Pho8*-GFP*	this study
SSY833	*HIS3::TDH3pr-BFP-hphR ubr1Δ::natR LEU2::ADH1pr-Rtn1Pho8*-GFP*	this study
SSY834	*HIS3::TDH3pr-BFP-hphR ynm3Δ::HIS3 LEU2::ADH1pr-Rtn1Pho8*-GFP*	this study
SSY835	*HIS3::TDH3pr-BFP-hphR roq1Δ::kanR LEU2::ADH1pr-Rtn1Pho8*-GFP*	this study
SSY970	*HIS3::TDH3pr-BFP-hphR ubr1Δ::natR LEU2::GAL1pr-Rtn1Pho8*-sfGFP*	this study
SSY969	*HIS3::TDH3pr-BFP-hphR ynm3Δ::HIS3 LEU2::GAL1pr-Rtn1Pho8*-sfGFP*	this study
SSY971	*HIS3::TDH3pr-BFP-hphR roq1Δ::kanR LEU2::GAL1pr-Rtn1Pho8*-sfGFP*	this study
SSY836	*HIS3::TDH3pr-BFP-hphR ubr1Δ::natR ynm3Δ::HIS3 LEU2::ADH1pr-Rtn1Pho8*-GFP*	this study
SSY837	*HIS3::TDH3pr-BFP-hphR ubr1Δ::natR roq1Δ::HIS3 LEU2::ADH1pr-Rtn1Pho8*-GFP*	this study
SSY838	*HIS3::TDH3pr-BFP-hphR ynm3Δ::HIS3 roq1Δ::kanR LEU2::ADH1pr-Rtn1Pho8*-GFP*	this study
SSY839	*HIS3::TDH3pr-BFP-hphR pdr5Δ::HIS3 ubr1Δ::natR LEU2::ADH1pr-Rtn1Pho8*-GFP*	this study
SSY840	*HIS3::TDH3pr-BFP-hphR pdr5Δ::kanR ynm3Δ::HIS3 LEU2::ADH1pr-Rtn1Pho8*-GFP*	this study
SSY841	*HIS3::TDH3pr-BFP-hphR pdr5Δ::HIS3 roq1Δ::kanR LEU2::ADH1pr-Rtn1Pho8*-GFP*	this study
SSY1202	*HIS3::TDH3pr-BFP-kanR rad6Δ::natR LEU2::ADH1pr-Rtn1Pho8*-GFP*	this study
SSY1248	*HIS3::TDH3pr-BFP-hphR ubr2Δ::kanR LEU2::ADH1pr-Rtn1Pho8*-GFP*	this study
SSY1250	*HIS3::TDH3pr-BFP-hphR san1Δ::kanR LEU2::ADH1pr-Rtn1Pho8*-GFP*	this study
SSY1251	*HIS3::TDH3pr-BFP-hphR ubr1Δ::natR san1Δ::kanR LEU2::ADH1pr-Rtn1Pho8*-GFP*	this study
SSY1012	*BY4741 cdc48-3::kanR*	Charles Boone
SSY1278	*BY4741 HIS3::TDH3pr-BFP-hphR ura3Δ::GAL1pr-Rtn1Pho8*-sfGFP-LEU2*	this study
SSY1279	*BY4741 cdc48-3::kanR HIS3::TDH3pr-BFP-hphR ura3Δ::GAL1pr-Rtn1Pho8*-sfGFP-LEU2*	this study
SSY1239	*HIS3::TDH3pr-BFP-hphR ire1Δ::kanR LEU2::ADH1pr-Rtn1Pho8*-GFP*	this study
SSY1240	*HIS3::TDH3pr-BFP-hphR hac1Δ::HIS3 LEU2::ADH1pr-Rtn1Pho8*-GFP*	this study
SSY1482	*tpk1/2/3-as*	Hao and O'Shea, 2012
SSY1484	*tpk1/2/3-as HIS3::TDH3pr-BFP-hphR*	this study
SSY1551	*tpk1/2/3-as HIS3::TDH3pr-BFP-hphR LEU2::ADH1pr-Rtn1Pho8*-GFP*	this study
SSY1552	*tpk1/2/3-as HIS3::TDH3pr-BFP-hphR ubr1Δ::hphR LEU2::ADH1pr-Rtn1Pho8*-GFP*	this study
SSY1553	*tpk1/2/3-as HIS3::TDH3pr-BFP-hphR ynm3Δ::hphR LEU2::ADH1pr-Rtn1Pho8*-GFP*	this study
SSY1554	*tpk1/2/3-as HIS3::TDH3pr-BFP-hphR roq1Δ::hphR LEU2::ADH1pr-Rtn1Pho8*-GFP*	this study
SSY920	*HIS3::TDH3pr-BFP-hphR URA3::GEM*	this study
SSY1488	*HIS3::TDH3pr-BFP-hphR LEU2::ADH1pr-Rtn1Pho8*-GFP URA3::GEM*	this study
SSY2143	*HIS3::TDH3pr-BFP-hphR LEU2::ADH1pr-Rtn1Pho8*-GFP URA3::GEM ubr1Δ::natR*	this study
SSY1559	*HIS3::TDH3pr-BFP-hphR LEU2::ADH1pr-Rtn1Pho8*-GFP URA3::GEM kanR::GAL1pr-ROQ1*	this study
SSY1561	*HIS3::TDH3pr-BFP-hphR LEU2::ADH1pr-Rtn1Pho8*-GFP URA3::GEM kanR::GAL1pr-ROQ1 ubr1Δ::natR*	this study
SSY1560	*HIS3::TDH3pr-BFP-hphR LEU2::ADH1pr-Rtn1Pho8*-GFP URA3::GEM kanR::GAL1pr-ROQ1 ynm3Δ::natR*	this study
SSY1762	*HIS3::TDH3pr-BFP-hphR LEU2::ADH1pr-Rtn1-GFP URA3::GEM*	this study
SSY2030	*HIS3::TDH3pr-BFP-hphR LEU2::ADH1pr-Rtn1-GFP URA3::GEM kanR::GAL1pr-ROQ1*	this study
SSY1490	*Ynm3-GFP::HIS3 Sec63-mCherry::kanR*	this study
SSY760	*pdr5Δ::HIS3*	this study
SSY791	*ynm3Δ::HIS3 pdr5Δ::kanR*	this study
SSY838	*HIS3::TDH3pr-BFP-hphR ynm3Δ::HIS3 roq1Δ::kanR LEU2::ADH1pr-Rtn1Pho8*-GFP*	this study
SSY792	*ubr1Δ::natR roq1Δ::HIS3*	this study
SSY2323	*ubr1Δ::natR roq1Δ::HIS3 ura3Δ::TDH3pr-Ub-roq1Δ21-HA(74)-URA3*	this study
SSY2324	*ubr1Δ::natR roq1Δ::HIS3 ura3Δ::TDH3pr-Ub-roq1(R22A)Δ21-HA(74)-URA3*	this study
SSY1856	*HIS3::TDH3pr-BFP-hphR natR::GEM,GAL1pr-ROQ1*	this study
SSY1857	*HIS3::TDH3pr-BFP-hphR natR::GEM,GAL1pr-ROQ1 ubr1Δ::HIS3*	this study
SSY1858	*HIS3::TDH3pr-BFP-hphR natR::GEM,GAL1pr-ROQ1 ynm3Δ::HIS3*	this study

Alias	Genotype	Source
SSY2376	ubr1Δ::natR roq1Δ::HIS3 ura3Δ::TDH3pr-Ub-roq1Δ21-HA(74)-ura3::TDH3pr-Ub-R-mCherry-sfGFP-kanR	this study
SSY1621	HIS3::TDH3pr-BFP-hphR LEU2::ADH1pr-Yop1Pho8*-sfGFP	this study
SSY1393	HIS3::TDH3pr-BFP-hphR LEU2::ADH1pr-Yop1Pho8*-GFP	this study
SSY1394	HIS3::TDH3pr-BFP-hphR ubr1Δ::natR LEU2::ADH1pr-Yop1Pho8*-GFP	this study
SSY1395	HIS3::TDH3pr-BFP-hphR ynm3Δ::HIS3 LEU2::ADH1pr-Yop1Pho8*-GFP	this study
SSY1396	HIS3::TDH3pr-BFP-hphR roq1Δ::kanR LEU2::ADH1pr-Yop1Pho8*-GFP	this study
SSY1388	HIS3::TDH3pr-BFP-hphR LEU2::ADH1pr-Rtn1CPY*-GFP	this study
SSY1389	HIS3::TDH3pr-BFP-hphR ubr1Δ::natR LEU2::ADH1pr-Rtn1CPY*-GFP	this study
SSY1390	HIS3::TDH3pr-BFP-hphR ynm3Δ::HIS3 LEU2::ADH1pr-Rtn1CPY*-GFP	this study
SSY1391	HIS3::TDH3pr-BFP-hphR roq1Δ::kanR LEU2::ADH1pr-Rtn1CPY*-GFP	this study
SSY800	HIS3::TDH3pr-BFP-hphR hrd1Δ::HIS3 doa10Δ::TRP1	this study
SSY816	HIS3::TDH3pr-BFP-hphR hrd1Δ::HIS3 doa10Δ::TRP1 ubr1Δ::natR	this study
SSY860	HIS3::TDH3pr-BFP-hphR hrd1Δ::HIS3 doa10Δ::TRP1 ynm3Δ::natR	this study
SSY861	HIS3::TDH3pr-BFP-hphR hrd1Δ::HIS3 doa10Δ::TRP1 roq1Δ::kanR	this study
SSY1577	HIS3::TDH3pr-BFP-hphR ura3::TEF1pr-Luciferase-mCherry-natR	this study
SSY1521	HIS3::TDH3pr-BFP-hphR ura3::TEF1pr-Luciferase(DM)-mCherry-natR	this study
SSY1522	HIS3::TDH3pr-BFP-hphR ubr1Δ::kanR ura3::TEF1pr-Luciferase(DM)-mCherry-natR	this study
SSY1523	HIS3::TDH3pr-BFP-hphR ynm3Δ::HIS3 ura3::TEF1pr-Luciferase(DM)-mCherry-natR	this study
SSY1524	HIS3::TDH3pr-BFP-hphR roq1Δ::kanR ura3::TEF1pr-Luciferase(DM)-mCherry-natR	this study
SSY2031	HIS3::TDH3pr-BFP-hphR ura3::TEF1pr -Luciferase-mCherry-natR LEU2::GEM	this study
SSY2033	HIS3::TDH3pr-BFP-hphR ura3::TEF1pr -Luciferase-mCherry-natR LEU2::GEM kanR::GAL1pr-ROQ1	this study
SSY2032	HIS3::TDH3pr-BFP-hphR ura3::TEF1pr-Luciferase(DM)-mCherry-natR LEU::GEM	this study
SSY2034	HIS3::TDH3pr-BFP-hphR ura3::TEF1pr-Luciferase(DM)-mCherry-natR LEU::GEM kanR::GAL1pr-ROQ1	this study
SSY1572	HIS3::TDH3pr-BFP-hphR ura3::TEF1pr-stGnd1-mCherry-natR	this study
SSY1573	HIS3::TDH3pr-BFP-hphR ubr1Δ::kanR ura3::TEF1pr-stGnd1-mCherry-natR	this study
SSY1574	HIS3::TDH3pr-BFP-hphR ynm3Δ::HIS3 ura3::TEF1pr-stGnd1-mCherry-natR	this study
SSY1575	HIS3::TDH3pr-BFP-hphR roq1Δ::kanR ura3::TEF1pr-stGnd1-mCherry-natR	this study
SSY1588	BY4741 HIS3::TDH3pr-BFP-hphR ura3Δ::kanR	this study
SSY1590	BY4741 HIS3::TDH3pr-BFP-hphR roq1Δ::kanR	this study
SSY1745	YJLM11-1 HIS3::TDH3pr-BFP-hphR URA3::TEF1pr-Rtn1-mCherry-sfGFP-natR	this study
SSY1747	YJLM11-1 HIS3::TDH3pr-BFP-hphR roq1Δ::kanR URA3::TEF1pr-Rtn1-mCherry-sfGFP-natR	this study
SSY1748	YJLM11-1 HIS3::TDH3pr-BFP-hphR URA3::TEF1pr-Rtn1Pho8*-mCherry-sfGFP-natR	this study
SSY1750	YJLM11-1 HIS3::TDH3pr-BFP-hphR roq1Δ::kanR URA3::TEF1pr-Rtn1Pho8*-mCherry-sfGFP-natR	this study
SSY1754	YMAM-330 MATa HIS3::TDH3pr-BFP-hphR ura3Δ::kanR Cam1-mCherry-sfGFP	this study
SSY1756	YMAM-330 MATa HIS3::TDH3pr-BFP-hphR roq1Δ::kanR Cam1-mCherry-sfGFP	this study
SSY1751	YMAM-330 MATa HIS3::TDH3pr-BFP-hphR ura3Δ::kanR Tef4-mCherry-sfGFP	this study
SSY1753	YMAM-330 MATa HIS3::TDH3pr-BFP-hphR roq1Δ::kanR Tef4-mCherry-sfGFP	this study
SSY2380	YMAM-330 MATa HIS3::TDH3pr-BFP-hphR ura3Δ::kanR Sfa1-mCherry-sfGFP	this study
SSY2381	YMAM-330 MATa HIS3::TDH3pr-BFP-hphR roq1Δ::kanR Sfa1-mCherry-sfGFP	this study
SSY2378	YMAM-330 MATa HIS3::TDH3pr-BFP-hphR ura3Δ::kanR Glo1-mCherry-sfGFP	this study
SSY2379	YMAM-330 MATa HIS3::TDH3pr-BFP-hphR roq1Δ::kanR Glo1-mCherry-sfGFP	this study
SSY1711	Cam1-HA::HIS3	this study
SSY1714	Cam1-HA::HIS3 ubr1Δ::natR	this study
SSY1715	Cam1-HA::HIS3 ynm3Δ::natR	this study
SSY1716	Cam1-HA::HIS3 roq1Δ::natR	this study
SSY1712	Tef4-HA::HIS3	this study

Alias	Genotype	Source
SSY1718	*Tef4-HA::HIS3 ubr1Δ::natR*	this study
SSY1719	*Tef4-HA::HIS3 ynm3Δ::natR*	this study
SSY1720	*Tef4-HA::HIS3 roq1Δ::natR*	this study

Table 3. Oligos used in the study

Only the oligos used to create knockout or knock-in strains and the oligos used in qPCR experiments are listed here. Sequences of oligos used for cloning are available upon request.

Name	Sequence
Knockout oligos	
ATG7-F1	ATGTCGTCAGAAAGGGTCTTAAGTTATGCACCAGCTTTTACGGATCCCCGGGTTAATTAA
ATG7-R1	TGGCACCACAATATGTACCAATGCTATTATATGCAAAATAGAATTCGAGCTCGTTTAAAC
DOA10-F1	TACCACTAATTGAATCAAAGAGACTAGAAGTGTGAAAGTCCGGATCCCCGGGTTAATTAA
DOA10-R1	TATGCTAGCATTCATTTTAAATGTAAGGAAGAAAACGCCTGAATTCGAGCTCGTTTAAAC
HAC1-F1	ACAACCTCCTCCTCCCCCACCTACGACAACAACCGCCACTCGGATCCCCGGGTTAATTAA
HAC1-R1	ATAACGAGAAAAAAAAATTATACCCTCTTGCGATTGTCTGAATTCGAGCTCGTTTAAAC
HIS3-F1	TATACTAAAAAATGAGCAGGCAAGATAAACGAAGGCAAAGCGGATCCCCGGGTTAATTAA
HIS3-R1	TATATATATCGTATGCTGCAGCTTTAAATAATCGGTGTCAGAATTCGAGCTCGTTTAAAC
HRD1-F1	TGCAATTTGTAAGAGAAGGGGAGAAAGACAAAATAATAATCGGATCCCCGGGTTAATTAA
HRD1-R1	TTTCTTTAAAAAAAACTATGTATAATATAAAACATGCAATGAATTCGAGCTCGTTTAAAC
IRE1-F1	ACAGCATATCTGAGGAATTAATATTTTAGCACTTTGAAAACGGATCCCCGGGTTAATTAA
IRE1-R1	GCAATAATCAACCAAGAAGAAGCAGAGGGGCATGAACATGGAATTCGAGCTCGTTTAAAC
PDR5-F1	AAGTTTTCGTATCCGCTCGTTCGAAAGACTTTAGACAAAACGGATCCCCGGGTTAATTAA
PDR5-R1	TCTTGGTAAGTTTCTTTTCTTAACCAAATTCAAAATTCTAGAATTCGAGCTCGTTTAAAC
PEP4-F1	ATTTAATCCAAATAAAATTCAAACAAAAACCAAAACTAACCGGATCCCCGGGTTAATTAA
PEP4-R1	GGCAGAAAAGGATAGGGCGGAGAAGTAAGAAAAGTTTAGCGAATTCGAGCTCGTTTAAAC
PHO13-F1	CTTATAGCTTGCCCTGACAAAGAATATACAACTCGGGAAACGGATCCCCGGGTTAATTAA
PHO13-R1	TTCAAAAAGTAATTCTACCCCTAGATTTTGCATTGCTCCTGAATTCGAGCTCGTTTAAAC
PRB1-F1	CAATAAAAAAACAAACTAAACCTAATTCTAACAAGCAAAGCGGATCCCCGGGTTAATTAA
PRB1-R1	AAGAAAAAAAAAGCAGCTGAAATTTTTCTAAATGAAGAAGAATTCGAGCTCGTTTAAAC
RAD6-S1	AAGATTATTTTTAGGCAGACAGAGACTAAAAGATAAAGCGTCCGTACGCTGCAGGTCGAC
RAD6-S2	TATCGGCTCGGCATTCATCATTAAGATTCTTTTGATTTTTCATCGATGAATTCGAGCTCG
ROQ1-F1	AAAAGTCAGCAAAACAAGAGATAAGATAACAAGAAGAAGCGGATCCCCGGGTTAATTAA
ROQ1-R1	CCCGAATGGTATTGTTAGATATGCTTTATAATGCTGGAGTGAATTCGAGCTCGTTTAAAC
ROQ1-S1	AAAAAAGTCAGCAAAACAAGAGATAAGATAACAAGAAGAAGCGTACGCTGCAGGTCGAC
ROQ1-S2	ACCCGAATGGTATTGTTAGATATGCTTTATAATGCTGGAGTATCGATGAATTCGAGCTCG
SAN1-F1	GTTTTCTCTCATAGTCTTGTAACCTCAGCTTTTGTTCATTCGGATCCCCGGGTTAATTAA
SAN1-R1	GACATATTTTCATATTAACATACTTCAGAAGCGGTATTGTGAATTCGAGCTCGTTTAAAC
UBR1-F1	AATCTTTACAGGTCACACAAATTACATAGAACATTCCAATCGGATCCCCGGGTTAATTAA
UBR1-R1	ACAAATATGTCAACTATAAAACATAGTAGAGGGCTTGAATGAATTCGAGCTCGTTTAAAC
UBR1-S1	CTAATCTTTACAGGTCACACAAATTACATAGAACATTCCAATCGTACGCTGCAGGTCGAC
UBR1-S2	TACAAATATGTCAACTATAAAACATAGTAGAGGGCTTGAATATCGATGAATTCGAGCTCG
UBR2-F1	AGATTCGTTAACTAAATTAATAGCTACTTAACAAGCACGCCGGATCCCCGGGTTAATTAA
UBR2-R1	TTTCGTAGCAATTTTGAATGACTAGACATTTGTTGGATAAGAATTCGAGCTCGTTTAAAC
pURA3-F1	ATTTATGGTGAAGGATAAGTTTTGACCATCAAAGAAGGTTCGGATCCCCGGGTTAATTAA

Name	Sequence
pURA3-R1	GAAGCTTTTTCTTTCCAATTTTTTTTTTTTTCGTCATTATAGAATTCGAGCTCGTTTAAAC
YNM3-F1	TACACACGTAGAGTACAGTAAAGGTTTTTTAGATCTACTACGGATCCCCGGGTTAATTAA
YNM3-R1	CATACATACATACATATATAAATGTTTTATCAAATCTGGCGAATTCGAGCTCGTTTAAAC
YNM3-S1	AATACACACGTAGAGTACAGTAAAGGTTTTTTAGATCTACTACGTACGCTGCAGGTCGAC
YNM3-S2	ACATACATACATACATATATAAATGTTTTATCAAATCTGGCATCGATGAATTCGAGCTCG

Knock-in oligos	
CAM1-F2	TGGCGAACCAAAGGAAATTGTTGACGGTAAGGTCTTAAAACGGATCCCCGGGTTAATTAA
knock-in_URA3_fw	ATTTATGGTGAAGGATAAGTTTTGACCATCAAAGAAGGTTAGCTTGTCTGTAAGCGGATG
knock-in_URA3_rev	GAAGCTTTTTCTTTCCAATTTTTTTTTTTTTCGTCATTATACATGTTCTTTCCTGCGTTATCC
PHO8 +708	TGGAAGAGATTTAATCGATGAG
PHO8-R1	ATTAAATAATATGTGAAAAAAGAGGGAGAGTTAGATAGGAGAATTCGAGCTCGTTTAAAC
SEC63-F2	CGATACGGATACAGAAGCTGAAGATGATGAATCACCAGAACGGATCCCCGGGTTAATTAA
TEF4-F2	TGGCGAAGATAAGGAAATTGTTGACGGTAAGGTTTTGAAACGGATCCCCGGGTTAATTAA
URApart2_fw	TTGTGAGTTTAGTATACATGC
URApart1_rev	ATTCGGTAATCTCCGAACAG
YNM3-F2	GATTGAAAAGGAATTTACCGGCAACAGCCAAAGTGAAAAACGGATCCCCGGGTTAATTAA

qPCR oligos	
PTR2_fw	CGTTGGTAACAGAGACAGTGC
PTR2_rev	CTGGTCGGCAATCAACACG
ROQ1_fw	TCAATAACCAGCCTACACAGC
ROQ1_rev	GCTTGTGTTTTCCTGTATGCC
TAF10_fw	GGATCAGGTCTTCCGTAGCG
TAF10_rev	AGGCTGTTGCTGTCCTTGC

Table 4. Antibodies

Antibody	Dilution for western blot	Source/Supplier	Catalogue no.
Primary antibodies			
anti-FLAG (M2) mouse	1:5,000	Sigma	F1804
anti-GFP (7.1/13.1) mouse	1:5,000	Roche	11814460001
anti-HA (3F10) rat	1:5,000	Roche	11867423001
anti-HA (6E2) mouse	1:5,000	NEB	2367S
anti-mCherry (1C51) mouse	1:5,000	Abcam	ab125096
anti-mCherry rabbit	1:5,000	Biovision	5993
anti-PGK1 mouse	1:50,000	Abcam	ab113687
anti-PHO8 (1D3A10) mouse	1:5,000	Abcam	ab113688
anti-SEC61 rabbit	1:5,000	Peter Walter	
Secondary antibodies			
anti-mouse-HRP goat	1:10,000	Pierce	31432
anti-rabbit-HRP goat	1:10,000	Pierce	31462
anti-rat-HRP donkey	1:10,000	Jackson	712035150

Table 5. Antibody coupled beads for immunoprecipitation

Antibody	Amount used for IP	Source/Supplier	Catalogue no.
anti-FLAG (M2) mouse agarose beads	30 µL / sample	Sigma	A2220
anti-HA (HA-7) mouse agarose beads	30 µL / sample	Sigma	A2095

Table 6. Enzymes

Enzyme	Supplier
FastAP alkaline phosphatase	Thermo Fisher Scientific
Gibson Assembly Master Mix	New England Biolabs
HiFi DNA Assembly Master Mix	New England Biolabs
Optitaq DNA polymerase	Roboklon
Phusion® High-Fidelity DNA polymerase	New England Biolabs
Enzyme	**Supplier**
Q5 High-Fidelity DNA polymerase	New England Biolabs
Restriction enzymes	New England Biolabs, Thermo Fisher Scientific
RevertAid reverse transcriptase	Thermo Fisher Scientific
SensiFAST SYBR No-ROX mix	Bioline
T4 DNA ligase	Thermo Fisher Scientific
Taq polymerase	Sigma-Aldrich
hTaq polymerase	Lab collection

Table 7. Standards and kits

Standards and kits	Supplier
BCA kit	Thermo Fisher Scientific
GeneRuler 1kb Plus DNA Ladder	Thermo Fisher Scientific
NucleoSpin Plasmid Mini-Prep Kit	Macherey-Nagel
NucleoSpin Gel and PCR Clean.up	Macherey-Nagel
PageRuler Plus Prestained Protein Ladder	Thermo Fisher Scientific

Table 8. Growth media

Media	Composition
Lysogeny broth (LB) ampicillin medium	1% (w/v) tryptone
	0.5% (w/v) yeast extract
	1% (w/v) NaCl
	100 µg/mL ampicillin
Synthetic complete (SC) medium	0.69% (w/v) yeast nitrogen base (with ammonium sulphate)
	2% (w/v) glucose
	0.2% (w/v) desired amino acid mixture*
Synthetic complete raffinose (SC Raf) medium	0.69% (w/v) yeast nitrogen base (with ammonium sulphate)
	2% (w/v) raffinose
	0.2% (w/v) desired amino acid mixture*
Synthetic complete raffinose/galactose (SC Raf/Gal) medium	0.69% (w/v) yeast nitrogen base (with ammonium sulphate)
	2% (w/v) raffinose
	2% (w/v) galactose
	0.2% (w/v) desired amino acid mixture*
Yeast peptone dextrose (YPD) medium	1% (w/v) yeast extract
	2% (w/v) peptone
	2% (w/v) glucose

Table 9. Plates

Plates	Composition
LB ampicillin plates	1% (w/v) tryptone
	0.5% (w/v) yeast extract
	1% (w/v) NaCl
	2% (w/v) agar
	100 µg/mL ampicillin
SC plates	0.69% (w/v) yeast nitrogen base (with ammonium sulphate)
	0.2% (w/v) desired amino acid mixture*
	2% (w/v) glucose
	2% (w/v) agar

Plates	Composition
SC (-HIS/ARG/LYS) plates for SGA	0.17% (w/v) yeast nitrogen base (without amino acids and ammonium sulphate)
	0.1% (w/v) monosodium glutamate
	0.2% (w/v) desired amino acid mixture*
	2% (w/v) glucose
	2% (w/v) agar
	50 µg/mL canavanine
	50 µg/mL thialysine
SC (-HIS/ARG/LYS/URA) Raf/Gal plates for SGA	0.17% (w/v) yeast nitrogen base (without amino acids or ammonium sulphate)
	0.1% (w/v) monosodium glutamate
	0.2% (w/v) desired amino acid mixture*
	2% (w/v) raffinose
	2% (w/v) galactose
	2% (w/v) agar
	50 µg/mL canavanine
	50 µg/mL thialysine
SC (-HIS/ARG/LYS) 5-FOA plates for SGA	0.17% (w/v) yeast nitrogen base (without amino acids or ammonium sulphate)
	0.1% (w/v) monosodium glutamate
	0.2% (w/v) desired amino acid mixture*
	1 mg/mL 5-FOA
	2% (w/v) glucose
	2% (w/v) agar
	50 µg/mL canavanine
	50 µg/mL thialysine
Sporulation plates	0.1% (w/v) yeast extract
	1% (w/v) potassium acetate
	0.01% (w/v) amino acid supplement†
	0.05% (w/v) glucose
	2% (w/v) agar
YPD plates	1% (w/v) yeast extract
	2% (w/v) peptone
	2% (w/v) glucose
	2% (w/v) agar

Plates	Composition
YPD G418 plates	1% (w/v) yeast extract
	2% (w/v) peptone
	2% (w/v) glucose
	2% (w/v) agar
	200 µg/mL geneticin (G418)
YPD hph plates	1% (w/v) yeast extract
	2% (w/v) peptone
	2% (w/v) glucose
	2% (w/v) agar
	300 µg/mL hygromycin B
YPD nat plates	1% (w/v) yeast extract
	2% (w/v) peptone
	2% (w/v) glucose
	2% (w/v) agar
	100 µg/mL nourseothricin (ClonNat)

*synthetic complete amino acid mixture is made up as follows:

Component	Amount	Component	Amount
adenine	0.5 g	isoleucine	2 g
alanine	2 g	leucine	4 g
para-aminobenzoic acid	0.2 g	lysine	2 g
arginine	2 g	methionine	2 g
asparagine	2 g	phenylalanine	2 g
aspartic acid	2 g	proline	2 g
cysteine	2 g	serine	2 g
glutamic acid	2 g	threonine	2 g
glutamine	2 g	tyrosine	2 g
glycine	2 g	tryptophan	2 g
histidine	2 g	uracil	2 g
inositol	2 g	valine	2 g

Drop out variants of amino acid mixtures follow the same recipe without the desired amino acid(s).

† amino acid supplement is made up as follows:

Component	Amount
histidine	2 g
leucine	4 g
lysine	2 g
uracil	2 g

Table 10. Buffers and solutions

Buffers, solutions	Composition
1NM-PP1	3 mM in DMSO
Acrylamide mix (30%)	29.2% (w/v) acrylamide
	0.8% (w/v) N,N'-methylenbisacrylamide (ratio 37.5:1)
Acrylamide mix (49.5%)	46.5% (w/v) acrylamide
	3.0% (w/v) bisacrylamide (ratio 15.5:1)
Amino acid mix (10x)	20 g/L amino acid mixture in water
Ammonium persulfate (10x)	10% (w/v) in water
Ampicillin	100 mg/mL in water
Anode buffer (5x)	1 M Tris-HCl pH 8.9
Blocking buffer (1x) for western blot	10 mM Tris-HCl pH 7.4
	150 mM NaCl
	0.1% (v/v) Tween-20
	5% (w/v) nonfat dry milk
Blotting buffer (1x)	25 mM Tris
	192 mM glycine
	20% (v/v) methanol
Canavanine	50 mg/mL in water
Cathode buffer (5x)	500 mM Tris
	500 mM Tricine
	0.5% (v/v) SDS
Colony PCR buffer (10x)	200 mM Tris pH 8.8
	100 mM (NH4)2SO4
	100 mM KCl
	25 mM MgCl2

Buffers, solutions	Composition
Complete protease inhibitors mix (25x)	1 tablet in 2mL 0.1 M Na3PO4 pH 7.0
p-Coumaric acid	90 mM in DMSO
Cycloheximide	50 mg/mL in DMSO
DNA loading dye (6x)	50% (v/v) glycerol 10% (v/v) 10x TBE buffer 0.05% (w/v) Orange G
dNTPs	10 mM of each nucleotide in water
Dithiothreitol (DTT)	1M in water
ECL solution (1x)	100 mM Tris pH 8.5 1.25 mM Luminol 0.198 mM p-Coumaric acid 0.9% (v/v) H2O2 add just before use
β-estradiol	1 mM in ethanol
Galactose (10x)	20% (w/v) in water
Geneticin (G418)	200 mg/mL in water
Glucose (10x)	20% (w/v) in water
Hygromycin B	100 mg/mL in water
Lithium acetate	1 M in water
Luminol	250 mM in DMSO
Lysis buffer (1x) for cell lysis	50 mM Tris-HCl pH7.5 0.5 mM EDTA add 1 mM PMSF just before use add 1x complete protease inhibitors just before use

Buffers, solutions	Composition
Lysis buffer (1x) for immunoprecipitation	25 mM HEPES pH 7.5 100 mM NaCl 0.5 mM EDTA 10% glycerol 0.1% NP-40 add 1 mM PMSF just before use add 1x complete protease inhibitors just before use
Lysis buffer (1x) for subcellular fractionation	50 mM HEPES-HCl pH 7.5 1 mM EDTA 200 mM sorbitol add 1 mM PMSF just before use add 1x complete protease inhibitors just before use
MG132	40mM in DMSO
Nourseothricin (ClonNat)	100 mg/mL in water
PEG 3350	50% (w/v) in water
Phenylmethylsulfonyl fluoride (PMSF)	1 M in DMSO
Ponceau S	0.1% (w/v) Ponceau S 5% (v/v) acetic acid
Raffinose (10x)	20% (w/v) in water
Rapamycin	0.2 mg/mL in DMSO
Reducing buffer (1x) for spheroplasting	100 mM Tris-HCl pH 9.4 add 10 mM NaN3 just before use
Reducing buffer with DTT (1x) for spheroplasting	100 mM Tris-HCl pH 9.4 add 10 mM NaN3 just before use add 10 mM DTT just before use

Buffers, solutions	Composition
Running buffer (1x)	0.1% (w/v) SDS 25 mM Tris 192 mM glycine
Salmon sperm DNA	10 mg/mL in water
Sample buffer (4x)	278 mM Tris-HCl pH 6.8 44.4% (v/v) glycerol 4.4% (w/v) LDS 0.02% bromophenol blue add 10% (v/v) β-mercaptoethanol just before use
Separating gel buffer (1x)	2 M Tris-HCl pH 8.8
Solution B (3x)	3 M Tris-HCl pH 8.5 0.3% SDS
Spheroblast buffer (1x)	50 mM Tris-HCl pH 7.5 1 M sorbitol add 1 mM PMSF just before use add 1x complete protease inhibitors just before use
Stacking gel buffer (1x)	0.5 Tris-HCl pH 6.8
TAE buffer (50x)	2 M Tris 1 M acetic acid 50 mM EDTA
TBE buffer (10x)	1 M Tris 1 M boric acid 0.02 M EDTA
TBS-T buffer (1x)	10 mM Tris-HCl pH 7.4 150 mM NaCl 0.1% (v/v) Tween-20
TES buffer (1x)	10 mM Tris-HCl pH 7.5 10 mM EDTA 0.5% SDS

Buffers, solutions	Composition
Thialysine	50 mg/mL
Transformation mix	33.33 % (w/v) PEG 3350
	100 mM Lithium acetate
	0.27 mg/mL freshly boiled salmon sperm DNA
Tunicamycin	1 mg/mL in DMSO
Zymolyase T20	50 mg/mL zymolyase T20 (1 U/µL)
	50 mM Tris-HCl pH 7.5

4.2 Molecular biology methods

All methods were performed according to the standard lab protocols unless noted otherwise.

4.2.1 Plasmids

Plasmids used in the study are listed in **Table 1**. The Pho8* constructs contain the luminal domain (60-550) of the vacuolar phosphatase Pho8 with two point mutations. The F352S mutation is responsible for its degradation phenotype while the N247D mutation is irrelevant. CPY* constructs contain the full-length vacuolar carboxy peptidase Prc1 with the destabilizing G255R mutation. The Hmg2-GFP plasmid contains residues 1-671 of Hmg2. CFTR plasmids contain the full-length human cystic fibrosis transmembrane conductance regulator sequence. The Luciferase(WT)-mCherry and the Luciferase(DM)-mCherry plasmids contain the wild-type or the double mutant (R188Q, R261Q) versions of the firefly luciferase respectively. The stGnd1-mCherry construct contains residues 1-150 of the phosphogluconate dehydrogenase Gnd1.

4.2.2 Molecular cloning

Plasmids were isolated from chemically competent *Escherichia coli* DH5α strain using the mini-prep kit from Macherey-Nagel and following the manufacturer's manual. Oligos used for cloning and yeast manipulations (**Table 3**), were synthesized by Sigma-Aldrich or Integrated DNA Technologies (IDT). Home-made hTaq or Sigma Taq polymerase was used for polymerase chain reactions (PCR) from bacteria or yeast colonies. For standard PCR reactions OptiTaq (Roboklon), Q5 (NEB) or Phusion

(NEB) DNA polymerase was employed. Amplified DNA products were purified from 0.7% agarose gels using the NucleoSpin Gel and PCR Clean-up kit (Macherey-Nagel) following the manufacturer's manual. For molecular cloning, amplified inserts with homologues ends to linearized recipient vectors were mixed in a 1:2 molar ratio and ligated with the NEBuilder HiFi DNA assembly mix. Point mutations were introduced according to the manufacturer's manual of Quikchange site-directed mutagenesis kit (Stratagene). Deletions were introduced by inverse PCR of vectors with primers removing the desired sequences and enabling re-ligation of homologues ends. The generated constructs were transformed into competent bacteria according to the standard lab protocol. The candidate clones were screened by bacterial colony PCR and confirmed by sequencing using GATC or SeqLab.

4.3 Yeast methods

4.3.1 Yeast strains

Yeast strains used in the study are listed in **Table 2**. Unless noted otherwise the strains were derived from the *Saccharomyces cerevisiae* W303 mating type a (SSY122). Chromosomal modifications including gene tagging, deletions and integrations were achieved by homologous recombination. The desired chromosomal modifications, with a selective marker, were introduced into the chromosome using PCR products (Janke et al., 2004) or linearized integrative plasmids via flanking homologues sequences (Taxis and Knop, 2006). Gene tagging or deletion was confirmed by yeast colony PCR using primers that bind in the selection cassette and up- or downstream of the desired locus in the chromosome. Single copy chromosomal integrations were identified using flow cytometry or western blot. The F352S mutation was introduced into the *PHO8* gene using a PCR product including the Pho8(136-567) sequence with the F352S mutation, the kanamycin resistance cassette and flanking homologues regions to target it into the *PHO8* locus (Schuck et al., 2014). To generate strains SSY2323 and SSY2324 the sequence encoding Ub-Roq1Δ21-HA(74) or Roq1(R22A)Δ21-HA(74) together with the *URA3* gene was amplified from pSS764 and pSS927 using primers knock-in_URA_fw and knock-in_URA_rev and integrated into the *ura3* locus of SSY792. To generate the strains containing chromosomally integrated Ub-X-mCherry-sfGFP the constructs from plasmids pAK146-160, pMaM46-48 or pMaM66-67 were amplified with primers URApart2_fw and URApart1_rev and integrated into the *URA3* locus. The analogue sensitive *tpk1/2/3-as* strain contains the following point mutations:

TPK1(M164G), TPK2(M147G) and TPK3(M165G) (Hao and O'Shea, 2012). The temperature sensitive *cdc48-3* allele contains two point mutations (P257L and R387K) in the Cdc48 protein (Verma et al., 2011).

4.3.2 Growth conditions

Yeast cells were cultured at 30°C in SC, SC -URA or SC -LEU media where uracil or leucine selection was required to maintain plasmid selection. In general experiments were performed in mid-log growth phase between OD_{600} 0.5-1 (in short OD from now on) unless noted otherwise. Cells were inoculated in liquid media for 5-10 hours ("pre-culture"), followed by diluting back to reach mid-log phase the following morning ("overnight culture"). During cycloheximide (CHX) chase, cells in mid-log phase were treated with 50 µg/mL cycloheximide (Sigma). In the CHX chase experiments the reporters harboured the fast folding superfolder GFP (sfGFP), (Pédelacq et al., 2006) instead of regular GFP. Since sfGFP folds in ~5 minutes the last reporter molecules, with the sfGFP fluorophore generated prior to addition of cycloheximide will be detected shortly after inhibiting protein translation. This enabled us to reduce the side effect coming from the slower maturation kinetics of GFP and thus a slight increase in GFP fluorescence after CHX treatment. During ER-stress experiments, cells in mid-log phase were diluted back to OD 0.05 and treated with tunicamycin (1 µg/mL for western blot experiments and 2 µg/mL for flow cytometry assays, Merck) or 8mM dithiothreitol (DTT) (Applichem) (Cleland, 1964; Takatsuki et al., 1971). To inhibit serine proteases, PMSF (Fahrney and Gold, 1963) was used at 1 mM final concentration, while inhibiting the proteasome was achieved by MG132 (Merck) at 80 µM (Rock et al., 1994). For efficient inhibition of the proteasome a strain lacking the plasma membrane ABC transporter *PDR5* was used (Leppert et al., 1990). For starvation experiments, cells in mid-log phase were diluted back to OD 0.05 and rapamycin (Sehgal et al., 1975) was used at a final concentration of 0.2 µg/mL. For growth into post-diauxic phase, cells in mid-log phase were normalized to OD 0.5 and were grown for 24 hours. To inhibit the PKA homologue Tpk1/2/3, the analogue sensitive *tpk1/2/3-as* cells in mid-log phase were diluted back to OD 0.05 and treated with 1NMPP-1 at a final concentration of 3 µM (Merck). To activate the Gal4-Estrogen-Receptor-Msn2 (GEM) chimeric transcription factor, β-estradiol (Sigma) was used in the final concentration of 400 nM for 6 hours for flow cytometry experiments and 8 hours for mass spectrometry analysis. To induce expression with galactose, cells were inoculated from plates into SC Raf

medium for 5-10 hours followed by diluting back to reach OD 0.2 the following morning. Galactose was supplemented to a final concentration of 2% and cells were grown for an additional 2 hours. Two hours of promoter induction by galactose resulted in a comparable expression level to the constitutive *ADH1* promoter. Promoter shut-off was achieved by diluting the cells back to SC medium in a 1:9 ratio. As in the CHX chase experiments (see above), *GAL1*-driven reporters harboured sfGFP instead of regular GFP.

4.3.3 Flow cytometry

The flow cytometry experiments were performed in 96-well deep-well plates. Saturated pre-cultures were diluted back to OD 0.02 in 1 mL medium and were placed in a programmable incubator (Memmert, "Jesus"). The incubator kept the temperature at 14°C until midnight, followed by increasing the temperature to 30°C to reach the desired OD the following morning. Cells in mid-log phase were normalized to OD 0.05 in 1 mL medium containing the appropriate drug or left untreated (see "yeast culture" for details on treatments) and were grown at 30°C for the indicated time. At each time point 100 µL of sample was measured for fluorescence and cell number with the FACS Canto (BD Biosciences) flow cytometer equipped with a high-throughput sampler. In order to determine the reporter levels, the mean GFP fluorescence was corrected for autofluorescence by subtracting the fluorescence values measured in identically treated control cells without any GFP-tagged proteins. The corrected GFP values were normalized to cell volume by dividing it with the mean fluorescence of a constitutively expressed cytosolic BFP fluorophore. To assess the effect of different stressors, the GFP/BFP ratios in treated cells were divided by the corresponding ratios in non-treated cells. Finally, the reporter levels were plotted in percent of the levels at time point 0. In the cycloheximide chase experiments total GFP fluorescence was determined by multiplying mean GFP fluorescence by cell number and the values were plotted in percent of the levels at time point 0.

4.3.4 Transformation of yeast

A saturated overnight culture in YPD media was diluted back to OD 0.4 in 5 mL YPD and was grown for 4 hours at 30°C to reach approximately OD 1. Cells were pelleted at 1,000 g for 5 minutes and the pellet was washed in 5 mL water. Cells were pelleted again and transferred to a microcentrifuge tube in 1 mL water. After centrifugation at 10,000 g for 2 minutes the supernatant was completely removed. Transforming DNA

(1/10th of a purified PCR product, ~250 ng of linearized integrative plasmid or ~25-100 ng of episomal plasmids) was added directly to the cell pellet followed by resuspending the pellet in 360 µL freshly prepared transformation mix. The reaction mix per sample contained the following components:

Constituent	Volume
50% (w/v) PEG 3350	240 µL
1 M lithium acetate	36 µL
10 mg/mL salmon sperm DNA	10 µL
ddH2O	74 µL

Transformation was performed at 42°C for 40 minutes. Afterwards cells were pelleted at 10,000 g for 2 minutes and resuspended in 1 mL YPD. Transformants with auxotrophic selection markers were plated on selective plates directly after transformation while transformants with antibiotic selection markers were grown for 4-6 hours at 30°C before plating them on selection plates. Plates were incubated at 30°C until visible colonies were formed.

4.3.5 Yeast cell lysis

Cells were pelleted by centrifugation at 1,000g for 5 minutes at 4°C followed by resuspending in 1 mL cold water and transferring to a microcentrifuge tube to pellet again. After careful removal of the supernatant, cell pellets were resuspended in 200 µL cold lysis buffer supplemented with PMSF and complete protease inhibitors (Roche) and transferred to 2 mL screw-cap tubes with 0.7 g of 1 mm glass beads. Cells were disrupted using FastPrep 24 (MP Biomedicals) for 40 seconds at 6.0 m/s. Proteins were solubilized by addition of 1.5% SDS and incubation at 65°C for 5 minutes. Lysates were clarified at 16,000 g for 2 minutes at 4°C.

4.3.6 Generation of spheroplasts for subcellular fractionation

In order to preserve the reticulon-based reporters in the ER membranes we employed a gentler cell lysis method, which included generation of spheroplasts (yeast cells without cell wall). Cells in mid-log phase were pelleted by centrifugation at 1,000g for 5 minutes at room temperature (RT) followed by resuspending in 4 mL reducing buffer containing freshly added 10 mM NaN_3 to kill the cells. After pelleting again at RT, cells were resuspended in 4 mL reducing buffer containing freshly added 10 mM NaN_3 and 10 mM DTT to break disulfide bonds in the cell wall to ensure efficient zymolyase

treatment. Cells were pelleted and resuspended in 1 mL spheroplast buffer containing zymolyase T20 at a final concentration of 0.2 U/OD. In order to monitor the conversion to spheroplasts, 25 µL of cells were diluted in 975 µL water and the initial OD was determined. Cells were incubated at 30°C for 10 minutes. If spheroplasting was successful, osmotic lysis occurs when spheroplasts are diluted in water and the OD should drop below 10% of the initial value. Spheroplasts were collected by centrifugation at 1,000 g for 5 minutes at 4°C. Supernatant was carefully removed and the pellet was gently washed three times with 1 mL cold spheroplast buffer to ensure complete removal of zymolyase.

4.3.7 Yeast spotting assay

Cells in mid-log phase were diluted back to OD 0.2 in 1 mL YPD and a dilution series, with five-fold dilution steps, were prepared in a flat bottom 96-well plate. Using a manual pinning tool, the cells were spotted on YPD agar plates. Plates were incubated at 30°C until visible colonies were formed.

4.3.8 Liquid growth assay

Cells in mid-log phase were diluted back to OD 0.05 in 500 µL SC containing 400 nM estradiol or left untreated. Cells were seeded in a 48-well plate. Absorbance was measured at 600 nm for ~24 hours in 5-minute intervals with the Tecan Infinite M1000 Pro machine. A shaking routine consisting of 120 s orbital shaking, 30 s rest and 90 s linear shaking was used to keep cells in suspension between OD measurements. Area under the curve (total growth) was determined using the R package "Growthcurver" (Sprouffske and Wagner, 2016).

4.3.9 Light microscopy

Cells in mid-log phase were imaged at RT with a spinning disk confocal microscope (Nikon TE2000 inverted microscope). The acquired images were processed by Adobe Photoshop.

4.3.10 RNA preparation

RNA was isolated from cells by phenol/chloroform extraction. Briefly, 5 ODs of cells were harvested from mid-log phase by centrifugation at 1,000 g for 5 minutes at 4°C. After washing the pellets once with cold water, the pellets were resuspended in 400 µL TES buffer. Afterwards, 400 µL of water-saturated phenol was added and vortexed vigorously for 10 seconds. The mixture was incubated at 65°C for 60 minutes and

vortexed every 10 minutes for 10 seconds. Phase separation was induced by centrifugation at 16,000 g for 5 minutes at 4°C. The aqueous top phase was collected to a fresh microcentrifuge tube. RNA was extracted twice more with 400 µL phenol and once with 400 µL chloroform. RNA was precipitated by addition of 40 µL 3M NaOAc pH 5.3 and 1 mL of cold 100% ethanol. RNA was pelleted by centrifugation at 16,000 g for 5 minutes at 4°C and washed once with 1 mL cold 70% ethanol. After the complete removal of ethanol, the pellet was resuspended in 30 µL water and RNA concentration was determined with NanoDrop.

4.3.11 Tandem fluorescence timer (tFT) screen

The tFT library was constructed in the yMaM330 strain where 4081 pre-selected ORFs were tagged with a tFT tagging module on the C-terminus (Khmelinskii et al., 2014). The module contains the following elements in this order: mCherry, I-SceI cut site, *CYC1* terminator, *URA3* selection marker, second I-SceI cut site, mCherryΔN-sfGFP (C-terminal fragment of mCherry followed by sfGFP). Induced expression of the I-SceI endonuclease allows the removal of both the *CYC1* terminator and the *URA3* gene and induces homologues recombination to generate the full tFT tag. This seamless tagging approach reduces the negative impact of introducing excessive amount of foreign genetic material into the chromosome. Moreover, it maintains the expression of gene fusions under the control of endogenous up- and downstream regulatory elements.

The following query strains were mated against the entire tFT library: SSY1588 (*ura3Δ*) and SSY1590 (*roq1Δ*). Additionally, the top 56 hits from a tFT screen aimed to find endogenous *UBR1* substrates (performed by Anton Khmelinskii) were manually arrayed on an extra plate and mated with SSY1475 (*ynm3Δ*). Each array plate also contained a negative and a positive control, SSY552 (Rtn1-tFT + p316) and SSY553 (Rtn1Pho8*-tFT + p316) respectively. The p316 plasmid was required for selection on SC -URA plates. Mass mating and sequential steps in the synthetic genetic array (SGA) analysis (Tong and Boone, 2005) were performed using the Singer ROTOR HDA (Singer Instruments) colony-arraying robot. The SGA procedure is summarized below and the individual steps are listed in **Table 12**:

1. **Mating of the query strains with the tFT library**

    Saturated cultures of the query strains were arrayed into a 384 colony/plate format on YPD plates to match the density of the tFT library. The *MATa* query

strains were pinned on a new YPD plate and the strains from the *MATα* tFT library were directly pinned on top to allow mating to occur. Plates were incubated at 30°C overnight.

2. **Diploid selection**

   MATa/α diploids were selected on YPD G418/nat plates. This selection eliminated unmated haploid cells.

3. **Sporulation**

   Diploid cells were pinned onto sporulation plates and were incubated for 7 days at 20°C to let cells undergo meiosis and produce spores.

4. **Mating type selection**

   After sporulation haploid spores with *MATa* were selected by pinning them on SC (-HIS/ARG/LYS) plates. The selection was achieved by using a *MATa* specific *STE2* promoter that drives the expression of the *Schizosaccharomyces pombe HIS5* gene. Additionally, the mating type selection cassettes were integrated into the *CAN1* and *LYP1* loci that encode plasma membrane arginine and lysine permeases respectively. Addition of toxic arginine and lysine analogues to the media (canavanine and thialysine respectively) results in selection for cells containing the mating type selection cassettes (*can1Δ::STE2pr-SpHIS5 lyp1Δ::STE3pr-LEU2*).

5. **Allele selection**

   After selection for *MATa* spores we selected for all the desired alleles in a step-wise manner. In brief, first we selected for the tFT tag, followed by selection for the knockout, BFP and finally the endonuclease.

6. **Excision of the *URA3* marker and generating the full tFT tag**

   In order to generate the full tFT tag the I-SceI endonuclease had to be expressed. The endonuclease was placed under the inducible *GAL1* promoter thus pinning the cells on SC RAF/GAL plates initiated endonuclease expression, excision of the *URA3* selection marker gene and generation of the full tFT tag via homologues recombination. This step was repeated twice.

7. **Full tFT tag selection**

   The cleavage by endonuclease removed the *URA3* selection cassette. To successfully select for cells that lost the *URA3* marker we pinned the cells on plates containing 5-fluoroorotic acid (5-FOA).

Table 12. Plates used during SGA

SGA steps	Plates
Mating	YPD
Diploid selection	YPD + G418/nat
Sporulation	Sporulation plates
Mating type selection	SC (-HIS/ARG/LYS) + can/thia
tFT selection	SC (-HIS/ARG/LYS/URA) + can/thia
KO selection	SC (-HIS/ARG/LYS/URA) + can/thia/G418
BFP selection	SC (-HIS/ARG/LYS/URA) + can/thia/G418/hph
Endonuclease selection	SC (-HIS/ARG/LYS/URA) + can/thia/G418/hph/nat
Excision of the URA3 marker	SC (-HIS/ARG/LYS) RAF/GAL + can/thia/G418/hph/nat
Full tFT tag selection	SC (-HIS/ARG/LYS) + can/thia/5-FOA
Final selection	SC (-HIS/ARG/LYS) + can/thia/G418/hph/nat
Screening	SC

The screening was performed on SC plates after ~20-24 hours of growth. On each screening plate (total of 77 plates in 1536 colony/plate format) the identical tFT-tagged strains from the *ura3Δ* (control) and *roq1Δ* SGA were pinned next to each other together with control strains expressing no fluorophores (autofluorescence control, SSY765) and reference strains. The reference strains included tFT protein fusions with a broad range of protein half-life. The same reference strains were used on each screening plate in order to remove any plate-to-plate variation. Fluorescence intensities from colonies were measured by the Tecan Infinite M1000 Pro microplate reader. Following the screen, each screening plate was imaged by Gel Doc XR+ (BioRad).

4.3.12 Quantification and validation of the tFT screen

An R script, written in the Knop lab, was used to quantify the data from the tFT screen. In brief, yeast colonies were segmented from the plate images to determine locations with empty slots and abnormal colony shapes. In order to remove spatial effects of screening plates, sfGFP and mCherry fluorescence was corrected locally according to the reference colonies. In order to correct for autofluorescence, mCherry and sfGFP intensities were corrected by subtracting fluorescence values from strains expressing no fluorophores. Finally, to remove any plate-to-plate variations mCherry and sfGFP values were rescaled according to the intensities from the reference colonies in all 77 plates.

Candidate substrates were selected where the mCherry/sfGFP ratio difference between *roq1Δ* and *ura3Δ* strains is higher than log2 0.2 (p< 0.1). This filtering resulted in a total of 332 candidate substrates. In order to validate the hits 152 candidates were re-screened in liquid culture with flow cytometry. In brief, saturated pre-cultures in 96-well plates were diluted back to OD 0.05 in 1 mL SC and measured 5 (log phase) and 24 hours (diauxic phase) later with FACS Canto flow cytometer equipped with a high-throughput sampler.

4.3.13 Mass spectrometry (analysis was performed by Daniel Itzhak and Georg Borner)

The following strains were used for mass spectrometry analysis: SSY1488 (WT), 1559 (WT + Roq1 OE), 2143 (*ubr1Δ*) and 1561 (*ubr1Δ* + Roq1 OE). Cells were grown to mid-log phase and diluted back to OD 0.05 followed by treatment with 400 nM estradiol for 8 hours. Three ODs of cells were harvested and lysed as described above ("yeast cell lysis") except that PMSF was not used. Lysates were processed and analysed on a Q Exactive HF Hybrid Quadrupole-Orbitrap mass spectrometer (Itzhak et al., 2016). Full proteomes of the four strains were analysed from four biological replicates. For each identified protein the difference between WT and WT + Roq1 OE was determined and averaged over the four replicates. Candidate SHRED substrates were selected whose levels in WT + Roq1 OE cells were at least 0.75 fold lower compared to WT cells and whose protein levels in *ubr1Δ* and *ubr1Δ* + Roq1 OE cells were similar (between 0.9 and 1.1 fold). These selected thresholds were based on the observed change in GFP and Pho8 levels that served as positive control. All differences were subjected to a paired, one-tailed t-test and filtered by false discovery rate (FDR)-controlled analysis.

4.4 Biochemistry methods

4.4.1 Subcellular fractionation

Spheroplasts were resuspended in 900 µL lysis buffer and 500 µL were transferred into a 2 mL Dounce homogenizer with a tight-fitting pestle B (clearance 0.01 – 0.06 mm). Cells were disrupted with 20 strokes and the lysate was transferred to a fresh microcentrifuge tube. Lysates were cleared at 500 g for 5 minutes at 4°C and 400 µL lysate was removed without disturbing the pellet. 200 µL was set aside as total (T) and the remaining 200 µL was centrifuged at 16,000 g for 15 minutes at 4°C.

Supernatant (S) was collected and set aside. The pellet (P) was resuspended in 200 µL cold lysis buffer. Proteins in total (T), supernatant (S) and pellet (P) fraction were solubilized by addition of 1.5% SDS and incubation at 65°C for 5 minutes. Equal volumes were resolved on a SDS PAGE gel.

4.4.2 Protein determination

Total protein concentration was determined using the bicinchoninic acid assay (BCA) following the manufacturer's manual. In brief, a reference serial dilution (0 – 1 µg) of bovine serum albumin (BSA) solution was loaded in a 96-well plate in 150 µL water. In the sample wells 0.5 – 1 µL of yeast lysate was mixed in a total volume of 150 µL water. BCA reagents A and B were mixed in a 1:49 ratio and 150 µL pf mixture was added to every well generating a total of 300 µL reaction volume. The plate was incubated at 37°C for 15-45 minutes and absorbance was measured at 562 nm with a plate reader. Protein concentrations of the samples were calculated based on the reference series.

4.4.3 Western blot

Equal amounts of protein lysate were resolved on 10% SDS-PAGE or 16% Tris-Tricine SDS-PAGE gels. The composition of the gels is listed in **Table 13**. Proteins were resolved using constant 200 V for the SDS-PAGE gels while proteins on Tris-Tricine gels were resolved initially at 30 V for 30 minutes followed by 60 minutes at 200 V and finally 30 minutes at 300 V. The proteins were transferred to a nitrocellulose membrane using wet electroblotting systems (BioRad) for 1 hour at 100 V. Membranes were incubated in blocking buffer for 30 minutes and probed overnight with primary antibody. The following morning the membranes were rinsed three times with TBST for 5 minutes and incubated with horseradish peroxidase (HRP) coupled secondary antibodies for 1 hour. After rinsing the membranes with TBST three times the membranes were incubated with homemade ECL solution and chemiluminescence was detected using the ImageQuant LAS 4000 imaging system. The acquired images were quantified by Fiji and processed by Adobe Photoshop. Antibodies used in the study are listed in **Table 4**.

Table 13. Composition of the SDS-PAGE gels

Separating gel			
10% SDS-PAGE		**16% Tris-tricine SDS-PAGE**	
H$_2$O	2.7 mL	H$_2$O	1.34 mL
separating gel buffer	1.2 mL	3x solution B	2 mL
30% acrylamide mix	2.0 mL	49.5% acrylamide mix	1.94 mL
15% SDS	40 µL	87% glycerol	0.72 mL
10% APS	60 µL	10% APS	30 µL
TEMED	6 µL	TEMED	3 µL
4% stacking gel			
H$_2$O	1.2 mL	H$_2$O	1.17 mL
stacking gel buffer	0.5 mL	3x solution B	0.67 mL
30% acrylamide mix	0.27 mL	49.5% acrylamide mix	0.16 mL
15% SDS	13 µL		
10% APS	20 µL	10% APS	20 µL
TEMED	2 µL	TEMED	2 µL

4.4.4. Immunoprecipitation

Ten ODs of cells in mid-log phase were harvested and lysed as described above in lysis buffer for IP supplemented with complete protease inhibitors and 1mM PMSF. Lysates were cleared at 12,000g for 10 minutes at 4°C. Roq1Δ21-HA(74) or FLAG-Ubr1 variants were immunoprecipitated with anti-HA or anti-FLAG coupled agarose beads for 30 minutes at 4°C. Beads were washed three times with cold lysis buffer and boud proteins were eluted using 1X SDS-PAGE sample buffer at 95°C for 5 minutes. Six percent of total lysate (~60 µg of protein) served as "input". Samples were separated on 4-15% gradient gels (BioRad) and co-immunoprecipitated proteins were detected by anti-FLAG, anti-HA or anti-mCherrry antibody.

4.4.5. Quantitative real-time PCR (performed by Rolf Schmidt)

cDNA was synthesized from the isolated mRNA using the Protoscript II synthesis kit following the manufacturer's manual. In brief, RNA samples were normalized to 167 ng/µL and 3 µL of sample was mixed with 3 µL of mix A (**Table 14**) followed by incubation at 65°C for 5 minutes. cDNA synthesis was initiated by addition of 4 µL mix B (**Table 14**) and incubation at 42°C for 1 hour. The enzyme was inactivated at 70°C for 5 minutes. qPCR was performed in a 384-well plate format with LightCycler II 480 using the SensiFAST SYBR No-ROX kit. For each primer pair a

control well with water instead of cDNA was used. Approximately 5 ng of cDNA was used per reaction. *TAF10* mRNA served as internal control to determine the relative amounts of *ROQ1* or *PTR2* mRNA. Primers for the qPCR reactions are listed in **Table 3**.

Table 14. Composition of cDNA synthesis mix and qPCR reaction

Mix A	
Nuclease free water	2.5 µL
Oligo(dT)18 primer	0.5 µL
Mix B	
5x reaction buffer	2 µL
RiboLock RNase inhibitor	0.5 µL
10 mM dNTP mix	1 µL
RevertAid M-MuLV reverse transcriptase	0.5 µL
qPCR reaction	
2x SensiFAST SYBR Green	5 µL
2.5 µM fw primer	1 µL
2.5 µM rev primer	1 µL
cDNA (~5 ng)	3 µL

CONTRIBUTION BY CO-WORKERS

Characterization and mechanistic analysis of the SHRED pathway would not have been possible without contribution from co-workers in the Schuck Lab and collaborators from the Max Planck Institute of Biochemistry in Martinsried, Germany. Hereby, I single out their contributions to the Results section: Sebastian Schuck, together with Enrique Garcia-Rivera, Vivian Chen and Dale Muzzey performed the random mutagenesis screen. Katharina Schaeff and Kevin Leiss contributed in the characterization of both the misfolded reporter protein and the SHRED pathway. Juan Diaz-Miyar helped out in the tandem fluorescent timer screen and in the characterization of SHRED substrates. Rolf Schmidt and Peter Bircham contributed with qPCR and growth assay experiments, respectively. Finally, the mass spectrometry analysis was performed by Daniel Itzhak and Georg Borner.

REFERENCES

Akiyoshi, B., Nelson, C.R., Duggan, N., Ceto, S., Ranish, J.A., Biggins, S., 2013. The Mub1/Ubr2 ubiquitin ligase complex regulates the conserved Dsn1 kinetochore protein. PLoS Genet. 9, e1003216.

Bachmair, A., Finley, D., Varshavsky, A., 1986. In vivo half-life of a protein is a function of its amino-terminal residue. Science (80-.). 234, 179–186.

Bagola, K., Sommer, T., 2008. Protein quality control: On IPODs and other JUNQ. Curr. Biol. 18, 1019–1021.

Baker, R.T., Varshavsky, A., 1995. Yeast N-terminal amidase. J. Biol. Chem. 270, 12065–12074.

Baker, R.T., Varshavsky, A., 1991. Inhibition of the N-end rule pathway in living cells. Proc. Natl. Acad. Sci. U. S. A. 88, 1090–1094.

Balchin, D., Hayer-Hartl, M., Hartl, F.U., 2016. In vivo aspects of protein folding and quality control. Science (80-.). 353, aac4354. doi:10.1126/science.aac4354

Baler, R., Dahl, G., Voellmy, R., 1993. Activation of human heat shock genes is accompanied by oligomerization, modification, and rapid translocation of heat shock transcription factor HSF1. Mol. Cell. Biol. 13, 2486–2496.

Balzi, E., Choder, M., Chen, W., Varshavsky, A., Goffeau, A., 1990. Cloning and functional analysis of the arginyl-tRNA-protein transferase gene ATE1 of Saccharomyces cerevisiae. J. Biol. Chem. 265, 7464–7471.

Bartel, B., Wünning, I., Varshavsky, A., 1990. The recognition component of the N-end rule pathway. EMBO J. 9, 3179–3189.

Battaglia, M., Olvera-Carrillo, Y., Garciarrubio, A., Campos, F., Covarrubias, A.A., 2008. The enigmatic LEA proteins and other hydrophilins. Plant Physiol. 148, 6–24.

Bays, N.W., Gardner, R.G., Seelig, L.P., Joazeiro, C.A., Hampton, R.Y., 2001. Hrd1p/Der3p is a membrane-anchored ubiquitin ligase required for ER-associated degradation. Nat. Cell Biol. 3, 24–29.

Becker, J., Walter, W., Yan, W., Craig, E.A., 1996. Functional interaction of cytosolic hsp70 and a DnaJ-related protein, Ydj1p, in protein translocation in vivo. Mol. Cell. Biol. 16, 4378–4386.

Belanger, K.D., Walter, D., Henderson, T.A., Yelton, A.L., O'Brien, T.G., Belanger, K.G., Geier, S.J., Fahrenkrog, B., 2009. Nuclear localisation is crucial for the proapoptotic activity of the HtrA-like serine protease Nma111p. J. Cell Sci. 122, 3931–3941.

Bengtson, M.H., Joazeiro, C.A.P., 2010. Role of a ribosome-associated E3 ubiquitin ligase in protein quality control. Nature 467, 470–473.

Berner, N., Reutter, K., Wolf, D.H., 2018. Protein Quality Control of the Endoplasmic Reticulum and Ubiquitin – Proteasome- Triggered Degradation of Aberrant Proteins : Yeast Pioneers the Path. Annu. Rev. Biochem. 1–32.

Bishop, A.C., Ubersax, J.A., Petsch, D.T., Matheos, D.P., Gray, N.S., Blethrow, J., Shimizu, E., Tsien, J.Z., Schultz, P.G., Rose, M.D., Wood, J.L., Morgan, D.O., Shokat, K.M., 2000. A chemical switch for inhibitor-sensitive alleles of any protein kinase. Nature 407, 395–401.

Bordallo, J., Plemper, R.K., Finger, A., Wolf, D.H., 1998. Der3p/Hrd1p is required for endoplasmic reticulum-associated degradation of misfolded lumenal and integral membrane proteins. Mol. Biol. Cell 9, 209–222.

Braakman, I., Hebert, D.N., 2013. Protein folding in the endoplasmic reticulum. Cold Spring Harb. Perspect. Biol. 5, a013201. doi:10.1101/cshperspect.a013201

Brady, J.P., Claridge, J.K., Smith, P.G., Schnell, J.R., 2015. A conserved amphipathic helix is required for membrane tubule formation by Yop1p. Proc. Natl. Acad. Sci. U. S. A. 112, E639–E648.

Brandman, O., Hegde, R.S., 2016. Ribosome-associated protein quality control. Nat. Struct. Mol. Biol. 23, 7–15.

REFERENCES

Brandman, O., Stewart-Ornstein, J., Wong, D., Larson, A., Williams, C.C., Li, G.-W., Zhou, S., King, D., Shen, P.S., Weibezahn, J., Dunn, J.G., Rouskin, S., Inada, T., Frost, A., Weissman, J.S., 2012. A ribosome-bound quality control complex triggers degradation of nascent peptides and signals translation stress. Cell 151, 1042–1054.

Brauer, M.J., Saldanha, A.J., Dolinski, K., Botstein, D., 2005. Homeostatic adjustment and metabolic remodeling in glucose-limited yeast cultures. Mol. Biol. Cell 16, 2503–2517.

Braun, M.A., Costa, P.J., Crisucci, E.M., Arndt, K.M., 2007. Identification of Rkr1, a nuclear RING domain protein with functional connections to chromatin modification in Saccharomyces cerevisiae. Mol. Cell. Biol. 27, 2800–2811.

Breitschopf, K., Bengal, E., Ziv, T., Admon, A., Ciechanover, A., 1998. A novel site for ubiquitination: The N-terminal residue, and not internal lysines of MyoD, is essential for conjugation and degradation of the protein. EMBO J. 17, 5964–5973.

Buchberger, A., Bukau, B., Sommer, T., 2010. Protein quality control in the cytosol and the endoplasmic reticulum: brothers in arms. Mol. Cell 40, 238–252.

Buck, T.M., Jordan, R., Lyons-Weiler, J., Adelman, J.L., Needham, P.G., Kleyman, T.R., Brodsky, J.L., 2015. Expression of three topologically distinct membrane proteins elicits unique stress response pathways in the yeast Saccharomyces cerevisiae. Physiol. Genomics 47, 198–214.

Cadwell, K., Coscoy, L., 2005. Ubiquitination on nonlysine residues by a viral E3 ubiquitin ligase. Science (80-.). 309, 127–130.

Carvalho, P., Goder, V., Rapoport, T.A., 2006. Distinct ubiquitin-ligase complexes define convergent pathways for the degradation of ER proteins. Cell 126, 361–373.

Causton, H.C., Ren, B., Koh, S.S., Harbison, C.T., Kanin, E., Jennings, E.G., Lee, T.I., True, H.L., Lander, E.S., Young, R.A., 2001. Remodeling of yeast genome expression in response to environmental changes. Mol. Biol. Cell 12, 323–337.

Chen, B., Retzlaff, M., Roos, T., Frydman, J., 2011. Cellular strategies of protein quality control. Cold Spring Harb. Perspect. Biol. 3:a004374.

Choi, W.S., Jeong, B.-C., Joo, Y.J., Lee, M.-R., Kim, J., Eck, M.J., Song, H.K., 2010. Structural basis for the recognition of N-end rule substrates by the UBR box of ubiquitin ligases. Nat. Struct. Mol. Biol. 17, 1175–1181.

Christiano, R., Nagaraj, N., Fröhlich, F., Walther, T.C., 2014. Global proteome turnover analyses of the yeasts S. cerevisiae and S. pombe. Cell Rep. 9, 1959–1966.

Clausen, T., Kaiser, M., Huber, R., Ehrmann, M., 2011. HTRA proteases: Regulated proteolysis in protein quality control. Nat. Rev. Mol. Cell Biol. 12, 152–162.

Clausen, T., Southan, C., Ehrmann, M., 2002. The HtrA family of proteases: implications for protein composition and cell fate. Mol. Cell 10, 443–455.

Cleland, W.W., 1964. Dithiothreitol, a new protective reagent for SH groups. Biochemistry 3, 480–482.

Connell, P., Ballinger, C.A., Jiang, J., Wu, Y., Thompson, L.J., Höhfeld, J., Patterson, C., 2001. The co-chaperone CHIP regulates protein triage decisions mediated by heat-shock proteins. Nat. Cell Biol. 3, 93–96.

Cox, J.S., Shamu, C.E., Walter, P., 1993. Transcriptional Induction of Genes Encoding Endoplasmic-Reticulum Resident Proteins Requires a Transmembrane Protein-Kinase. Cell 73, 1197–1206. doi:10.1016/0092-8674(93)90648-a

Credle, J.J., Finer-Moore, J.S., Papa, F.R., Stroud, R.M., Walter, P., 2005. On the mechanism of sensing unfolded protein in the endoplasmic reticulum. Proc. Natl. Acad. Sci. U. S. A. 102, 18773–18784.

Crosas, B., Hanna, J., Kirkpatrick, D.S., Zhang, D.P., Tone, Y., Hathaway, N.A.A., Buecker, C., Leggett, D.S., Schmidt, M., King, R.W., Gygi, S.P., Finley, D., 2006. Ubiquitin chains are remodeled at the proteasome by opposing ubiquitin ligase and deubiquitinating activities. Cell 127, 1401–1413.

Crowder, J.J., Geigges, M., Gibson, R.T., Fults, E.S., Buchanan, B.W., Sachs, N., Schink, A., Kreft, S.G., Rubenstein, E.M., 2015. Rkr1/Ltn1 ubiquitin ligase-mediated degradation of translationally stalled endoplasmic reticulum proteins. J. Biol. Chem. 290, 18454–18466.

Dang, N.X., Hincha, D.K., 2011. Identification of two hydrophilins that contribute to the desiccation and freezing tolerance of yeast (Saccharomyces cerevisiae) cells. Cryobiology 62, 188–193.

Dasgupta, A., Ramsey, H.L., Smith, J.S., Auble, D.T., 2004. Sir antagonist 1 (San1) is a ubiquitin ligase. J. Biol. Chem. 279, 26830–26838.

De Craene, J.-O., Coleman, J., de Martin, P.E., Pypaert, M., Anderson, S., Yates III, J.R., Ferro-Novick, S., Novick, P., 2006. Rtn1p is involved in structuring the cortical endoplasmic reticulum. Mol. Biol. Cell 17, 3009–3020.

Deng, M., Hochstrasser, M., 2006. Spatially regulated ubiquitin ligation by an ER/nuclear membrane ligase. Nature 443, 827–831.

Denic, V., Quan, E.M., Weissman, J.S., 2006. A luminal surveillance complex that selects misfolded glycoproteins for ER-associated degradation. Cell 126, 349–359.

DeRisi, J.L., Iyer, V.R., Brown, P.O., 1997. Exploring the metabolic and genetic control of gene expression on a genomic scale. Science (80-.). 278, 680–686.

Dohmen, R.J., Madura, K., Bartel, B., Varshavsky, A., 1991. The N-end rule is mediated by the UBC2(RAD6) ubiquitin-conjugating enzyme. Proc. Natl. Acad. Sci. U. S. A. 88, 7351–7355.

Du, F., Navarro-Garcia, F., Xia, Z., Tasaki, T., Varshavsky, A., 2002. Pairs of dipeptides synergistically activate the binding of substrate by ubiquitin ligase through dissociation of its autoinhibitory domain. Proc. Natl. Acad. Sci. U. S. A. 99, 14110–14115.

Eisele, F., Wolf, D.H., 2008. Degradation of misfolded protein in the cytoplasm is mediated by the ubiquitin ligase Ubr1. FEBS Lett. 582, 4143–4146.

Ellis, R.J., van der Vies, S.M., 1991. Molecular chaperones. Annu. Rev. Biochem. 60, 321–347.

Escusa-Toret, S., Vonk, W.I.M., Frydman, J., 2013. Spatial sequestration of misfolded proteins by a dynamic chaperone pathway enhances cellular fitness during stress. Nat. Cell Biol. 15, 1231–43.

Fahrenkrog, B., 2011. Nma111p, the pro-apoptotic HtrA-like nuclear serine protease in Saccharomyces cerevisiae: A short survey. Biochem. Soc. Trans. 39, 1499–1501.

Fahrenkrog, B., Sauder, U., Aebi, U., 2004. The S. cerevisiae HtrA-like protein Nma111p is a nuclear serine protease that mediates yeast apoptosis. J. Cell Sci. 117, 115–126.

Fahrney, D.E., Gold, A.M., 1963. Sulfonyl fluorides as inhibitors of esterases. I. Rates of reaction with acetylcholinesterase, α-Chymotrypsin, and trypsin. J. Am. Chem. Soc. 85, 997–1000.

Fang, N.N., Chan, G.T., Zhu, M., Comyn, S.A., Persaud, A., Deshaies, R.J., Rotin, D., Gsponer, J., Mayor, T., 2014. Rsp5/Nedd4 is the main ubiquitin ligase that targets cytosolic misfolded proteins following heat stress. Nat. Cell Biol. 16, 1227–1237.

Fang, N.N., Ng, A.H.M., Measday, V., Mayor, T., 2011. Hul5 HECT ubiquitin ligase plays a major role in the ubiquitylation and turnover of cytosolic misfolded proteins. Nat. Cell Biol. 13, 1344–1352.

Finger, A., Knop, M., Wolf, D.H., 1993. Analysis of two mutated vacuolar proteins reveals a degradation pathway in the endoplasmic reticulum or a related compartment of yeast. Eur. J. Biochem. 218, 565–574.

Finley, D., Chen, X., Walters, K.J., 2016. Gates, channels, and switches: Elements of the proteasome machine. Trends Biochem. Sci. 41, 77–93. doi:10.1016/j.tibs.2015.10.009

Finley, D., Ulrich, H.D., Sommer, T., Kaiser, P., 2012. The ubiquitin-proteasome system of Saccharomyces cerevisiae. Genetics 192, 319–360.

Foresti, O., Rodriguez-Vaello, V., Funaya, C., Carvalho, P., 2014. Quality control of inner nuclear membrane proteins by the Asi complex. Science (80-.). 346, 751–755.

Fredrickson, E.K., Gallagher, P.S., Candadai, S.V.C., Gardner, R.G., 2013. Substrate recognition in nuclear protein quality control degradation is governed by exposed hydrophobicity that correlates with aggregation and insolubility. J. Biol. Chem. 288, 6130–6139.

Fredrickson, E.K., Rosenbaum, J.C., Locke, M.N., Milac, T.I., Gardner, R.G., 2011. Exposed hydrophobicity is a key determinant of nuclear quality control degradation. Mol. Biol. Cell 22, 2384–2395.

REFERENCES

Garay-Arroyo, A., Colmenero-Flores, J.M., Garciarrubio, A., Covarrubias, A.A., 2000. Highly hydrophilic proteins in prokaryotes and eukaryotes are common during conditions of water deficit. J. Biol. Chem. 275, 5668–5674.

Gardner, R.G., Nelson, Z.W., Gottschling, D.E., 2005. Degradation-mediated protein quality control in the nucleus. Cell 120, 803–815.

Gasch, A.P., 2003. The environmental stress response: A common yeast response to diverse environmental stresses, in: Hohmann, S., Mager, W. (Eds.), Yeast Stress Responses. Topics in Current Genetics, Vol 1. Springer, Berlin, Heidelberg, pp. 11–70.

Gasch, A.P., Spellman, P.T., Kao, C.M., Carmel-Harel, O., Eisen, M.B., Storz, G., Botstein, D., Brown, P.O., 2000. Genomic expression programs in the response of yeast cells to environmental changes. Mol. Biol. Cell 11, 4241–4257.

Gerlach, J.Q., Sharma, S., Leister, K.J., Joshi, L., 2012. A tight-knit group: Protein glycosylation, endoplasmic reticulum stress and the unfolded protein response, in: Agostinis, P., Samali, A. (Eds.), Endoplasmic Reticulum Stress in Health and Disease. Springer, Dordrecht, Heidelberg, New York, London, pp. 23–40.

Ghaemmaghami, S., Huh, W.-K., Bower, K., Howson, R.W., Belle, A., Dephoure, N., O'Shea, E.K., Weissman, J.S., 2003. Global analysis of protein expression in yeast. Nature 425, 737–741.

Glover, J.R., Lindquist, S., 1998. Hsp104, Hsp70, and Hsp40: A novel chaperone system that rescues previously aggregated proteins. Cell 94, 73–82. doi:10.1016/S0092-8674(00)81223-4

Goffeau, A., Barrell, B.G., Bussey, H., Davis, R.W., Dujon, B., Feldmann, H., Galibert, F., Hoheisel, J.D., Jacq, C., Johnston, M., Louis, E.J., Mewes, H.W., Murakami, Y., Philippsen, P., Tettelin, H., Oliver, S.G., 1996. Life with 6000 genes. Science (80-.). 274, 546–567.

Görner, W., Durchschlag, E., Martinez-Pastor, M.T., Estruch, F., Ammerer, G., Hamilton, B., Ruis, H., Schüller, C., 1998. Nuclear localization of the C2H2 zinc finger protein Msn2p is regulated by stress and protein kinase A activity. Genes Dev. 12, 586–597.

Guan, Q., Haroon, S., Bravo, D.G., Will, J.L., Gasch, A.P., 2012. Cellular memory of acquired stress resistance in Saccharomyces cerevisiae. Genetics 192, 495–505.

Gupta, R., Kasturi, P., Bracher, A., Loew, C., Zheng, M., Villella, A., Garza, D., Hartl, F.U., Raychaudhuri, S., 2011. Firefly luciferase mutants as sensors of proteome stress. Nat. Methods 8, 879–884.

Gupta, R., Kus, B., Fladd, C., Wasmuth, J., Tonikian, R., Sidhu, S., Krogan, N.J., Parkinson, J., Rotin, D., 2007. Ubiquitination screen using protein microarrays for comprehensive identification of Rsp5 substrates in yeast. Mol. Syst. Biol. 3, 1–12. doi:10.1038/msb4100159

Habeck, G., Ebner, F.A., Shimada-Kreft, H., Kreft, S.G., 2015. The yeast ERAD-C ubiquitin ligase Doa10 recognizes an intramembrane degron. J. Cell Biol. 209, 261–73.

Halbleib, K., Pesek, K., Covino, R., Hofbauer, H.F., Wunnicke, D., Hänelt, I., Hummer, G., Ernst, R., 2017. Activation of the unfolded protein response by lipid bilayer stress. Mol. Cell 67, 673–684.

Hampton, R.Y., Gardner, R.G., Rine, J., 1996. Role of 26S proteasome and HRD genes in the degradation of 3-hydroxy-3-methylglutaryl-CoA reductase, an integral endoplasmic reticulum membrane protein. Mol. Biol. Cell 7, 2029–2044. doi:c.7.12.2029

Hampton, R.Y., Rine, J., 1994. Regulated degradation of HMG-CoA reductase, an integral membrane protein of the endoplasmic reticulum, in yeast. J. Cell Biol. 125, 299–312.

Hao, N., O'Shea, E.K., 2012. Signal-dependent dynamics of transcription factor translocation controls gene expression. Nat. Struct. Mol. Biol. 19, 31–39.

Hartl, F.U., 2017. Protein misfolding diseases. Annu. Rev. Biochem. 86, 21–26.

Hartl, F.U., Hayer-Hartl, M., 2009. Converging concepts of protein folding in vitro and in vivo. Nat. Struct. Mol. Biol. 16, 574–581.

Heck, J.W., Cheung, S.K., Hampton, R.Y., 2010. Cytoplasmic protein quality control degradation mediated by parallel actions of the E3 ubiquitin ligases Ubr1 and San1. Proc. Natl. Acad. Sci. U. S. A. 107, 1106–1111.

Hegde, R., Srinivasula, S.M., Zhang, Z., Wassell, R., Mukattash, R., Cilenti, L., Dubois, G., Lazebnik,

Y., Zervos, A.S., Fernandes-Alnemri, T., Alnemri, E.S., 2002. Identification of Omi/HtrA2 as a mitochondrial apoptotic serine protease that disrupts inhibitor of apoptosis protein-caspase interaction. J. Biol. Chem. 277, 432–438. doi:10.1074/jbc.M109721200

Heinemeyer, W., Cruhler, A., Mohrle, V., Mahe, Y., Wolf, D.H., 1993. PRE2, highly homologous to the human major histocompatibility complex- linked Ring10 gene, codes for a yeast proteasome subunit necessary for chymotryptic activity and degradation of ubiquitinated proteins. J. Biol. Chem. 268, 5115–5120.

Herrero, E., Thorpe, P.H., 2016. Synergistic control of kinetochore protein levels by Psh1 and Ubr2. PLoS Genet. 12, 1–23.

Hershko, A., Ciechanover, A., 1998. The ubiquitin system. Annu. Rev. Biochem. 67, 425–479.

Higuchi-Sanabria, R., Frankino, P.A., Paull III, J.W., Tronnes, S.U., Dillin, A., 2018. A futile battle? Protein quality control and the stress of aging. Dev. Cell 44, 139–163. doi:10.1016/j.devcel.2017.12.020

Hiller, M.M., Finger, A., Schweiger, M., Wolf, D.H., 1996. ER degradation of a misfolded luminal protein by the cytosolic ubiquitin-proteasome pathway. Science (80-.). 273, 1725–1728.

Hochstrasser, M., 1996. Ubiquitin-dependent protein degradation. Annu. Rev. Genet. 30, 405–439.

Horn, S.C., Hanna, J., Hirsch, C., Volkwein, C., Schütz, A., Heinemann, U., Sommer, T., Jarosch, E., 2009. Usa1 Functions as a Scaffold of the HRD-Ubiquitin Ligase. Mol. Cell 36, 782–793. doi:10.1016/j.molcel.2009.10.015

Horton, L.E., James, P., Craig, E.A., Hensold, J.O., 2001. The yeast hsp70 homologue Ssa is required for translation and interacts with Sis1 and Pab1 on translating ribosomes. J. Biol. Chem. 276, 14426–14433.

Huibregtse, J.M., Scheffner, M., Beaudenon, S., Howley, P.M., 1995. A family of proteins structurally and functionally related to the E6-AP ubiquitin-protein ligase. Proc. Natl. Acad. Sci. U. S. A. 92, 2563–2567.

Huttunen, H.J., Guénette, S.Y., Peach, C., Greco, C., Xia, W., Doo, Y.K., Barren, C., Tanzi, R.E., Kovacs, D.M., 2007. HtrA2 regulates β-amyloid precursor protein (APP) metabolism through endoplasmic reticulum-associated degradation. J. Biol. Chem. 282, 28285–28295.

Itzhak, D.N., Tyanova, S., Cox, J., Borner, G.H.H., 2016. Global, quantitative and dynamic mapping of protein subcellular localization. Elife 5, 1–36.

Janke, C., Magiera, M.M., Rathfelder, N., Taxis, C., Reber, S., Maekawa, H., Moreno-Borchart, A., Doenges, G., Schwob, E., Schiebel, E., Knop, M., 2004. A versatile toolbox for PCR-based tagging of yeast genes: New fluorescent proteins, more markers and promoter substitution cassettes. Yeast 21, 947–962. doi:10.1002/yea.1142

Kaganovich, D., Kopito, R., Frydman, J., 2008. Misfolded proteins partition between two distinct quality control compartments. Nature 454, 1088–1095. doi:10.1038/nature07195

Kambouris, N.G., Burke, D.J., Creutz, C.E., 1993. Cloning and genetic characterization of a calcium- and phospholipid-binding protein from Saccharomyces cerevisiae that is homologous to translation elongation factor-1γ. Yeast 9, 151–163.

Kampinga, H.H., Craig, E.A., 2010. The HSP70 chaperone machinery: J proteins as drivers of functional specificity. Nat. Rev. Mol. Cell Biol. 11, 579–592. doi:10.1038/nrm2941

Kanehara, K., Xie, W., Ng, D.T.W., 2010. Modularity of the Hrd1 ERAD complex underlies its diverse client range. J. Cell Biol. 188, 707–716.

Khmelinskii, A., Blaszczak, E., Pantazopoulou, M., Fischer, B., Omnus, D.J., Le Dez, G., Brossard, A., Gunnarsson, A., Barry, J.D., Meurer, M., Kirrmaier, D., Boone, C., Huber, W., Rabut, G., Ljungdahl, P.O., Knop, M., 2014. Protein quality control at the inner nuclear membrane. Nature 516, 410–413.

Khmelinskii, A., Keller, P.J., Bartosik, A., Meurer, M., Barry, J.D., Mardin, B.R., Kaufmann, A., Trautmann, S., Wachsmuth, M., Pereira, G., Huber, W., Schiebel, E., Knop, M., 2012. Tandem fluorescent protein timers for in vivo analysis of protein dynamics. Nat. Biotechnol. 30, 708–714.

Kim, Y.E., Hipp, M.S., Bracher, A., Hayer-Hartl, M., Ulrich Hartl, F., 2013. Molecular chaperone functions in protein folding and proteostasis. Annu. Rev. Biochem. 82, 323–355.

Kimata, Y., Oikawa, D., Shimizu, Y., Ishiwata-Kimata, Y., Kohno, K., 2004. A role for BiP as an adjustor for the endoplasmic reticulum stress-sensing protein Ire1. J. Cell Biol. 167, 445–456.

Kinzy, T.G., Ripmaster, T.L., Woolford, J.L., 1994. Multiple genes encode the translation elongation factor EF-1 gamma in Saccharomyces cerevisiae. Nucleic Acids Res. 22, 2703–2707.

Knop, M., Finger, A., Braun, T., Hellmuth, K., Wolf, D.H., 1996. Der1, a novel protein specifically required for endoplasmic reticulum degradation in yeast. EMBO J. 15, 753–763.

Kohlmann, S., Schäfer, A., Wolf, D.H., 2008. Ubiquitin ligase Hul5 is required for fragment-specific substrate degradation in endoplasmic reticulum-associated degradation. J. Biol. Chem. 283, 16374–16383.

Korennykh, A. V., Egea, P.F., Korostelev, A.A., Finer-Moore, J., Zhang, C., Shokat, K.M., Stroud, R.M., Walter, P., 2009. The unfolded protein response signals through high-order assembly of Ire1. Nature 457, 687–693.

Kravtsova-Ivantsiv, Y., Ciechanover, A., 2012. Non-canonical ubiquitin-based signals for proteasomal degradation. J. Cell Sci. 125, 539–548.

Krojer, T., Pangerl, K., Kurt, J., Sawa, J., Stingl, C., Mechtler, K., Huber, R., Ehrmann, M., Clausen, T., 2008a. Interplay of PDZ and protease domain of DegP ensures efficient elimination of misfolded proteins. Proc. Natl. Acad. Sci. U. S. A. 105, 7702–7707.

Krojer, T., Sawa, J., Schäfer, E., Saibil, H.R., Ehrmann, M., Clausen, T., 2008b. Structural basis for the regulated protease and chaperone function of DegP. Nature 453, 885–890. doi:10.1038/nature07004

Labbadia, J., Morimoto, R.I., 2015. The biology of proteostasis in aging and disease. Annu. Rev. Biochem. 84, 435–464.

Lee, K.P.K., Dey, M., Neculai, D., Cao, C., Dever, T.E., Sicheri, F., 2008. Structure of the dual enzyme Ire1 reveals the basis for catalysis and regulation in nonconventional RNA splicing. Cell 132, 89–100.

Lee, P., Cho, B.R., Joo, H.S., Hahn, J.S., 2008. Yeast Yak1 kinase, a bridge between PKA and stress-responsive transcription factors, Hsf1 and Msn2/Msn4. Mol. Microbiol. 70, 882–895.

Lee, P., Kim, M.S., Paik, S.M., Choi, S.H., Cho, B.R., Hahn, J.S., 2013. Rim15-dependent activation of Hsf1 and Msn2/4 transcription factors by direct phosphorylation in Saccharomyces cerevisiae. FEBS Lett. 587, 3648–3655.

Leggett, D.S., Hanna, J., Borodovsky, A., Crosas, B., Schmidt, M., Baker, R.T., Walz, T., Ploegh, H., Finley, D., 2002. Multiple associated proteins regulate proteasome structure and function. Mol. Cell 10, 495–507. doi:10.1016/S1097-2765(02)00638-X

Leppert, G., McDevitt, R., Falco, S.C., Van Dyk, T.K., Ficke, M.B., Golin, J., 1990. Cloning by gene amplification of two loci conferring multiple drug resistance in Saccharomyces. Genetics 125, 13–20.

Li, W., Srinivasula, S.M., Chai, J., Li, P., Wu, J.W., Zhang, Z., Alnemri, E.S., Shi, Y., 2002. Structural insights into the pro-apoptotic function of mitochondrial serine protease HtrA2/Omi. Nat. Struct. Biol. 9, 436–441. doi:10.1038/nsb795

Livneh, I., Cohen-Kaplan, V., Cohen-Rosenzweig, C., Avni, N., Ciechanover, A., 2016. The life cycle of the 26S proteasome: From birth, through regulation and function, and onto its death. Cell Res. 26, 869–885.

Loewith, R., Hall, M.N., 2011. Target of rapamycin (TOR) in nutrient signaling and growth control. Genetics 189, 1177–1201.

Martins, L.M., 2002. The serine protease Omi/HtrA2: A second mammalian protein with a Reaper-like function. Cell Death Differ. 9, 699–701.

Martins, L.M., Iaccarino, I., Tenev, T., Gschmeissner, S., Totty, N.F., Lemoine, N.R., Savopoulos, J., Gray, C.W., Creasy, C.L., Dingwall, C., Downward, J., 2002. The serine protease Omi/HtrA2

regulates apoptosis by binding XIAP through a Reaper-like motif. J. Biol. Chem. 277, 439–444.

Martins, L.M., Turk, B.E., Cowling, V., Borg, A., Jarrell, E.T., Cantley, L.C., Downward, J., 2003. Binding specificity and regulation of the serine protease and PDZ domains of HtrA2/Omi. J. Biol. Chem. 278, 49417–49427.

Matta-Camacho, E., Kozlov, G., Li, F.F., Gehring, K., 2010. Structural basis of substrate recognition and specificity in the N-end rule pathway. Nat. Struct. Mol. Biol. 17, 1182–1187.

Medicherla, B., Goldberg, A.L., 2008. Heat shock and oxygen radicals stimulate ubiquitin-dependent degradation mainly of newly synthesized proteins. J. Cell Biol. 182, 663–673. doi:10.1083/jcb.200803022

Merdanovic, M., Mamant, N., Meltzer, M., Poepsel, S., Auckenthaler, A., Melgaard, R., Hauske, P., Nagel-Steger, L., Clarke, A.R., Kaiser, M., Huber, R., Ehrmann, M., 2010. Determinants of structural and functional plasticity of a widely conserved protease chaperone complex. Nat. Struct. Mol. Biol. 17, 837–843. doi:10.1038/nsmb.1839

Metzger, M.B., Pruneda, J.N., Klevit, R.E., Weissman, A.M., 2014. RING-type E3 ligases: Master manipulators of E2 ubiquitin-conjugating enzymes and ubiquitination. Biochim. Biophys. Acta 1843, 47–60.

Miller, S.B., Ho, C.-T., Winkler, J., Khokhrina, M., Neuner, A., Mohamed, M.Y., Guilbride, D.L., Richter, K., Lisby, M., Schiebel, E., Mogk, A., Bukau, B., 2015. Compartment-specific aggregases direct distinct nuclear and cytoplasmic aggregate deposition. EMBO J. 34, 778–797. doi:10.15252/embj.201489524

Mogk, A., Bukau, B., Kampinga, H.H., 2018. Cellular handling of protein aggregates by disaggregation machines. Mol. Cell 69, 214–226.

Mori, K., Kawahara, T., Yoshida, H., Yanagi, H., Yura, T., 1996. Signalling from endoplasmic reticulum to nucleus: transcription factor with a basic-leucine zipper motif is required for the unfolded protein-response pathway. Genes to Cells 1, 803–817.

Murphy, J.P., Stepanova, E., Everley, R.A., Paulo, J.A., Gygi, S.P., 2015. Comprehensive temporal protein dynamics during the diauxic shift in Saccharomyces cerevisiae. Mol. Cell. Proteomics 14, 2454–2465.

Mutka, S.C., Walter, P., 2001. Multifaceted physiological response allows yeast to adapt to the loss of the signal recognition particle-dependent protein-targeting pathway. Mol. Biol. Cell 12, 577–588.

Nathan, D.F., Vos, M.H., Lindquist, S., 1997. In vivo functions of the Saccharomyces cerevisiae Hsp90 chaperone. Proc. Natl. Acad. Sci. U. S. A. 94, 12949–12956.

Nikawa, J.-I., Yamashita, S., 1992. IRE1 encodes a putative protein kinase containing a membrane-spanning domain and is required for inositol phototrophy in Saccharomyces cerevisiae. Mol. Microbiol. 6, 1441–1446.

Nillegoda, N.B., Theodoraki, M.A., Mandal, A.K., Mayo, K.J., Ren, H.Y., Sultana, R., Wu, K., Johnson, J., Cyr, D.M., Caplan, A.J., 2010. Ubr1 and Ubr2 function in a quality control pathway for degradation of unfolded cytosolic proteins. Mol. Biol. Cell 21, 2102–2116.

O'Rourke, S.M., Herskowitz, I., 2004. Unique and redundant roles for HOG MAPK pathway components as revealed by whole-genome expression analysis. Mol. Biol. Cell 15, 532–542.

Oertle, T., Klinger, M., Stuermer, C.A.O., Schwab, M.E., 2003. A reticular rhapsody: Phylogenic evolution and nomenclature of the RTN/Nogo gene family. FASEB J. 17, 1238–1247.

Padmanabhan, N., Fichtner, L., Dickmanns, A., Ficner, R., Schulz, J.B., Braus, G.H., 2009. The yeast HtrA orthologue Ynm3 is a protease with chaperone activity that aids survival under heat stress. Mol. Biol. Cell 20, 68–77.

Parag, H.A., Raboy, B., Kulka, R.G., 1987. Effect of heat shock on protein degradation in mammalian cells: involvement of the ubiquitin system. EMBO J. 6, 55–61.

Park, S.H., Kukushkin, Y., Gupta, R., Chen, T., Konagai, A., Hipp, M.S., Hayer-Hartl, M., Hartl, F.U., 2013. PolyQ proteins interfere with nuclear degradation of cytosolic proteins by sequestering the Sis1p chaperone. Cell 154, 134–145. doi:10.1016/j.cell.2013.06.003

REFERENCES

Pédelacq, J.D., Cabantous, S., Tran, T., Terwilliger, T.C., Waldo, G.S., 2006. Engineering and characterization of a superfolder green fluorescent protein. Nat. Biotechnol. 24, 79–88.

Perry, J.R., Basrai, M.A., Steiner, H.-Y., Naider, F., Becker, J.M., 1994. Isolation and characterization of a Saccharomyces cerevisiae peptide transport gene. Mol. Cell. Biol. 14, 104–115.

Pincus, D., Aranda-Diaz, A., Zuleta, I.A., Walter, P., El-Samad, H., 2014. Delayed Ras/PKA signaling augments the unfolded protein response. Proc. Natl. Acad. Sci. U. S. A. 11, 14800–14805.

Plun-Favreau, H., Klupsch, K., Moisoi, N., Gandhi, S., Kjaer, S., Frith, D., Harvey, K., Deas, E., Harvey, R.J., McDonald, N., Wood, N.W., Martins, M.L., Downward, J., 2007. The mitochondrial protease HtrA2 is regulated by Parkinson's disease-associated kinase PINK1. Nat. Cell Biol. 9, 1243–1252.

Prasad, R., Kawaguchi, S., Ng, D.T.W., 2010. A nucleus-based quality control mechanism for cytosolic proteins. Mol. Biol. Cell 21, 2117–2127.

Promlek, T., Ishiwata-Kimata, Y., Shido, M., Sakuramoto, M., Kohno, K., Kimata, Y., 2011. Membrane aberrancy and unfolded proteins activate the endoplasmic reticulum stress sensor Ire1 in different ways. Mol. Biol. Cell 22, 3520–3532.

Ramos, P.C., Höckendorff, J., Johnson, E.S., Varshavsky, A., Dohmen, R.J., 1998. Ump1p is required for proper maturation of the 20S proteasome and becomes its substrate upon completion of the assembly. Cell 92, 489–499.

Raychaudhuri, S., Loew, C., Körner, R., Pinkert, S., Theis, M., Hayer-Hartl, M., Buchholz, F., Hartl, F.U., 2014. Interplay of acetyltransferase EP300 and the proteasome system in regulating heat shock transcription factor 1. Cell 156, 975–985.

Rock, K.L., Gramm, C., Rothstein, L., Clark, K., Stein, R., Dick, L., Hwang, D., Goldberg, A.L., 1994. Inhibitors of the proteasome block the degradation of most cell proteins and the generation of peptides presented on MHC class I molecules. Cell 78, 761–771.

Ron, D., Walter, P., 2007. Signal integration in the endoplasmic reticulum unfolded protein response. Nat. Rev. Mol. Cell Biol. 8, 519–529.

Ruggiano, A., Foresti, O., Carvalho, P., 2014. Quality control: ER-associated degradation: protein quality control and beyond. J. Cell Biol. 204, 869–879.

Sato, B.K., Schulz, D., Do, P.H., Hampton, R.Y., 2009. Misfolded membrane proteins are specifically recognized by the transmembrane domain of the Hrd1p ubiquitin ligase. Mol. Cell 34, 212–222.

Scheffner, M., Nuber, U., Huibregtse, J.M., 1995. Protein ubiquitination involving an E1–E2–E3 enzyme ubiquitin thioester cascade. Nature 373, 81–83.

Schoebel, S., Mi, W., Stein, A., Ovchinnikov, S., Pavlovicz, R., DImaio, F., Baker, D., Chambers, M.G., Su, H., Li, D., Rapoport, T.A., Liao, M., 2017. Cryo-EM structure of the protein-conducting ERAD channel Hrd1 in complex with Hrd3. Nature 548, 352–355. doi:10.1038/nature23314

Schuck, S., Gallagher, C.M., Walter, P., 2014. ER-phagy mediates selective degradation of endoplasmic reticulum independently of the core autophagy machinery. J. Cell Sci. 127, 4078–4077.

Schuhmann, H., Mogg, U., Adamska, I., 2011. A new principle of oligomerization of plant DEG7 protease based on interactions of degenerated protease domains. Biochem. J. 435, 167–174. doi:10.1042/BJ20101613

Segal, E., Shapira, M., Regev, A., Pe'er, D., Botstein, D., Koller, D., Friedman, N., 2003. Module networks: Identifying regulatory modules and their condition-specific regulators from gene expression data. Nat. Genet. 34, 166–176.

Sehgal, S.N., Baker, H., Vézina, C., 1975. Rapamycin (AY-22,989), a new antifungal antibiotic. II. Fermentation, isolation and characterization. J. Antibiot. (Tokyo). 28, 727–732.

Shaner, N.C., Campbell, R.E., Steinbach, P.A., Giepmans, B.N.G., Palmer, A.E., Tsien, R.Y., 2004. Improved monomeric red, orange and yellow fluorescent proteins derived from Discosoma sp. red fluorescent protein. Nat. Biotechnol. 22, 1567–1572.

Shao, S., Von der Malsburg, K., Hegde, R.S., 2013. Listerin-dependent nascent protein ubiquitination relies on ribosome subunit dissociation. Mol. Cell 50, 637–648.

Shi, Y., Mosser, D.D., Morimoto, R.I., 1998. Molecular chaperones as HSF1-specific transcriptional

repressors. Genes Dev. 12, 654–666. doi:10.1101/gad.12.5.654

Sidrauski, C., Cox, J.S., Walter, P., 1996. tRNA ligase is required for regulated mRNA splicing in the unfolded protein response. Cell 87, 405–413.

Sidrauski, C., Walter, P., 1997. The transmembrane kinase Ire1p is a site-specific endonuclease that initiates mRNA splicing in the unfolded protein response. Cell 90, 1031–1039. doi:10.1016/S0092-8674(00)80369-4

Silke, J., Meier, P., 2013. Inhibitor of apoptosis (IAP) proteins–modulators of cell death and inflammation. Cold Spring Harb. Perspect. Biol. 1–19.

Sontag, E.M., Samant, R.S., Frydman, J., 2017. Mechanisms and functions of spatial protein quality control. Annu. Rev. Biochem. 86, 97–122.

Sontag, E.M., Vonk, W.I.M., Frydman, J., 2014. Sorting out the trash: The spatial nature of eukaryotic protein quality control. Curr. Opin. Cell Biol. 26, 139–146.

Sorger, P.K., Pelham, H.R.B., 1988. Yeast heat shock factor is an essential DNA-binding protein that exhibits. Cell 54, 855–864.

Specht, S., Miller, S.B.M., Mogk, A., Bukau, B., 2011. Hsp42 is required for sequestration of protein aggregates into deposition sites in Saccharomyces cerevisiae. J. Cell Biol. 195, 617–629.

Spiess, C., Beil, A., Ehrmann, M., 1999. A temperature-dependent switch from chaperone to protease in a widely conserved heat shock protein. Cell 97, 339–347.

Sprouffske, K., Wagner, A., 2016. Growthcurver: An R package for obtaining interpretable metrics from microbial growth curves. BMC Bioinformatics 17, 172.

Stanley, A.M., Carvalho, P., Rapoport, T., 2011. Recognition of an ERAD-L substrate analyzed by site-specific in vivo photocrosslinking. FEBS Lett. 585, 1281–1286.

Stolz, A., Besser, S., Hottmann, H., Wolf, D.H., 2013. Previously unknown role for the ubiquitin ligase Ubr1 in endoplasmic reticulum-associated protein degradation. Proc. Natl. Acad. Sci. U. S. A. 110, 15271–15276.

Summers, D.W., Wolfe, K.J., Ren, H.Y., Cyr, D.M., 2013. The Type II Hsp40 Sis1 cooperates with Hsp70 and the E3 ligase Ubr1 to promote degradation of terminally misfolded cytosolic protein. PLoS One 8, e52099.

Swanson, R., Locher, M., Hochstrasser, M., 2001. A conserved ubiquitin ligase of the nuclear envelope/endoplasmic reticulum that functions in both ER-associated and Matα2 repressor degradation. Genes Dev. 15, 2660–2674.

Takatsuki, A., Arima, K., Tamura, G., 1971. Tunicamycin, a new antibiotic: Isolation and characterization of tunicamycin. J. Antibiot. (Tokyo). 24, 215–223.

Tasaki, T., Sriram, S.M., Park, K.S., Kwon, Y.T., 2012. The N-end rule pathway. Annu. Rev. Biochem. 81, 261–289.

Tasaki, T., Zakrzewska, A., Dudgeon, D.D., Jiang, Y., Lazo, J.S., Kwon, Y.T., 2009. The substrate recognition domains of the N-end rule pathway. J. Biol. Chem. 284, 1884–1895. doi:10.1074/jbc.M803641200

Taxis, C., Knop, M., 2006. System of centromeric, episomal, and integrative vectors based on drug resistance markers for Saccharomyces cerevisiae. Biotechniques 40, 73–78.

Teichert, U., Mechler, B., Muller, H., Wolf, D.H., 1989. Lysosomal (vacuolar) proteinases of yeast are essential catalysts for protein degradation, differentiation, and cell survival. J. Biol. Chem. 264, 16037–16045.

Thevelein, J.M., De Winde, J.H., 1999. Novel sensing mechanisms and targets for the cAMP-protein kinase A pathway in the yeast Saccharomyces cerevisiae. Mol. Microbiol. 33, 904–918.

Toda, T., Cameron, S., Sass, P., Zoller, M., Wigler, M., 1987. Three different genes in S. cerevisiae encode the catalytic subunits of the cAMP-dependent protein kinase. Cell 50, 277–287. doi:10.1016/0092-8674(87)90223-6

Tong, A.H.Y., Boone, C., 2005. Synthetic genetic array analysis in Saccharomyces cerevisiae, in: Xiao,

W. (Ed.), Yeast Protocol. Methods in Molecular Biology, Vol. 313. Humana Press, Totowa, NJ, pp. 171–192.

Travers, K.J., Patil, C.K., Wodicka, L., Lockhart, D. avid J., Weissman, J.S., Walter, P., 2000. Functional and genomic analyses reveal an essential coordination between the unfolded protein response and ER-associated degradation. Cell 101, 249–258.

Truebestein, L., Tennstaedt, A., Mönig, T., Krojer, T., Canellas, F., Kaiser, M., Clausen, T., Ehrmann, M., 2011. Substrate-induced remodeling of the active site regulates human HTRA1 activity. Nat. Struct. Mol. Biol. 18, 386–388. doi:10.1038/nsmb.2013

Turner, G.C., Du, F., Varshavsky, A., 2000. Peptides accelerate their uptake by activating a ubiquitin-dependent proteolytic pathway. Nature 405, 579–583.

Vande Walle, L., Lamkanfi, M., Vandenabeele, P., 2008. The mitochondrial serine protease HtrA2/Omi: An overview. Cell Death Differ. 15, 453–460.

Vande Walle, L., Van Damme, P., Lamkanfi, M., Saelens, X., Vandekerckhove, J., Gevaert, K., Vandenabeele, P., 2007. Proteome-wide identification of HtrA2/Omi substrates. J. Proteome Res. 6, 1006–1015.

Varshavsky, A., 2012. The ubiquitin system, an immense realm. Annu. Rev. Biochem. 81, 167–176.

Varshavsky, A., 2011. The N-end rule pathway and regulation by proteolysis. Protein Sci. 20, 1298–1345.

Verghese, J., Abrams, J., Wang, Y., Morano, K.A., 2012. Biology of the heat shock response and protein chaperones: budding yeast (Saccharomyces cerevisiae) as a model system. Microbiol. Mol. Biol. Rev. 76, 115–158.

Verma, R., Oania, R., Fang, R., Smith, G.T., Deshaies, R.J., 2011. Cdc48/p97 mediates UV-dependent turnover of RNA Pol II. Mol. Cell 41, 82–92.

Vihervaara, A., Sistonen, L., 2014. HSF1 at a glance. J. Cell Sci. 127, 261–266.

Voeltz, G.K., Prinz, W.A., Shibata, Y., Rist, J.M., Rapoport, T.A., 2006. A class of membrane proteins shaping the tubular endoplasmic reticulum. Cell 124, 573–586.

Walsh, N.P., Alba, B.M., Bose, B., Gross, C.A., Sauer, R.T., 2003. OMP peptide signals initiate the envelope-stress response by activating DegS protease via relief of inhibition mediated by its PDZ domain. Cell 113, 61–71.

Walter, D., Wissing, S., Madeo, F., Fahrenkrog, B., 2006. The inhibitor-of-apoptosis protein Bir1p protects against apoptosis in S. cerevisiae and is a substrate for the yeast homologue of Omi/HtrA2. J. Cell Sci. 119, 1843–1851.

Walter, P., Ron, D., 2011. The unfolded protein response: from stress pathway to homeostatic regulation. Science (80-.). 334, 1081–1086.

Wang, G., Yang, J., Huibregtse, J.M., 1999. Functional domains of the Rsp5 ubiquitin-protein ligase. Mol. Cell. Biol. 19, 342–352.

Wang, L., Mao, X., Ju, D., Xie, Y., 2004. Rpn4 is a physiological substrate of the Ubr2 ubiquitin ligase. J. Biol. Chem. 279, 55218–55223.

Wiederrecht, G., Seto, D., Parker, C.S., 1988. Isolation of the gene encoding the S. cerevisiae heat shock transcription factor. Cell 54, 841–853. doi:10.1016/S0092-8674(88)91197-X

Wilken, C., Kitzing, K., Kurzbauer, R., Ehrmann, M., Clausen, T., 2004. Crystal structure of the DegS stress sensor: How a PDZ domain recognizes misfolded protein and activates a protease. Cell 117, 483–494. doi:10.1016/S0092-8674(04)00454-4

Wolf, D.H., Fink, G.R., 1975. Proteinase C (carboxypeptidase Y) mutant of yeast. J. Bacteriol. 123, 1150–1156.

Xia, Z., Webster, A., Du, F., Piatkov, K., Ghislain, M., Varshavsky, A., 2008. Substrate-binding sites of UBR1, the ubiquitin ligase of the N-end rule pathway. J. Biol. Chem. 283, 24011–24028.

Yamamoto, A., Mizukami, Y., Sakurai, H., 2005. Identification of a novel class of target genes and a novel type of binding sequence of heat shock transcription factor in Saccharomyces cerevisiae. J.

Biol. Chem. 280, 11911–11919.

Yau, R., Rape, M., 2016. The increasing complexity of the ubiquitin code. Nat. Cell Biol. 18, 579–586.

Ye, Y., Meyer, H.H., Rapoport, T.A., 2001. The AAA ATPase Cdc48/p97 and its partners transport proteins from the ER into the cytosol. Nature 414, 652–656.

Zhang, H., Baehrecke, E.H., 2015. Eaten alive: novel insights into autophagy from multicellular model systems. Trends Cell Biol. 25, 376–387.

Zhang, L., Wang, X., Fan, F., Wang, H.W., Wang, J., Li, X., Sui, S.F., 2017. Cryo-EM structure of Nma111p, a unique HtrA protease composed of two protease domains and four PDZ domains. Cell Res. 27, 582–585. doi:10.1038/cr.2017.5

Zhang, Y., Nijbroek, G., Sullivan, M.L., McCracken, A.A., Watkins, S.C., Michaelis, S., Brodsky, J.L., 2001. Hsp70 molecular chaperone facilitates endoplasmic reticulum-associated protein degradation of cystic fibrosis transmembrane conductance regulator in yeast. Mol. Biol. Cell 12, 1303–1314.

Zheng, N., Shabek, N., 2017. Ubiquitin ligases: structure, function, and regulation. Annu. Rev. Biochem. 129–157.

ACKNOWLEDGEMENTS